UNIVERSITA' DEGLI STUDI DI PARMA

Dottorato di Ricerca in Fisiopatologia Sistemica

Ciclo XXVII

Inositol 1,4,5-Trisphosphate Receptors and Electromechanical Coupling in Cardiomyocytes

Recettori dell'Inositolo Trifosfato e Proprieta' Elettromeccaniche dei Cardiomiociti

Coordinatore:
Chiar.mo Prof. Enrico Maria Silini

Tutor:
Chiar.mo Prof. Federico Quaini

Dottorando:
Dott. Sergio Signore

Contents

Abstract

The role of inositol 1,4,5-trisphosphate receptors (IP3Rs) in mediating Ca^{2+} mobilization in the adult heart is poorly understood. Moreover, whether these Ca^{2+} release channels are present and operative in human ventricular cardiomyocytes remains to be defined. IP3Rs may be activated after Gαq-protein–coupled receptor stimulation, affecting Ca^{2+} cycling, enhancing myocyte performance, and potentially favoring the occurrence of arrhythmic events. For this purpose, IP3R function was determined in left ventricular myocytes obtained from human hearts, and this analysis was integrated with assays in mouse myocytes to identify the mechanisms by which IP3Rs influence the electric and mechanical properties of the myocardium. We identified that IP3Rs are expressed and operative in human left ventricular myocytes. After Gαq-protein–coupled receptor activation, Ca^{2+} mobilized from the sarcoplasmic reticulum via IP3Rs contributes to the decrease in resting membrane potential, prolongation of the action potential, and occurrence of early afterdepolarizations. Ca^{2+} transient amplitude and cell shortening are enhanced, and extrasystolic and dysregulated Ca^{2+} elevations and contractions become apparent. These alterations in the electromechanical behavior of human cardiomyocytes are coupled with increased isometric twitch of the ventricular myocardium and arrhythmic events, suggesting that Gαq-protein–coupled receptor activation provides inotropic reserve, which is hampered by electric instability and contractile abnormalities. Additionally, our findings support the notion that increases in Ca^{2+} load by IP3Rs promote Ca^{2+} extrusion by forward-mode Na^{+}/Ca^{2+} exchange, an important mechanism of arrhythmic events. In conclusion, the Gαq-protein/coupled receptor/IP3R axis modulates the electromechanical properties of the human myocardium and its propensity to develop arrhythmias.

Keywords: cardiomyocytes, cardiac, electromechanical coupling, arrhythmias, calcium, inositol 1,4,5-trisphosphate receptors.

List of Abbreviations

2-APB, 2-aminoethyl diphenylborinate

AP, action potential

ATP, adenosine 5′-triphosphate

DAG, diacylglycerol

EAD, early after depolarization

ER, endoplasmic reticulum

ET-1, endothelin-1

GPCR, Gαq-protein-coupled receptor

IP3, inositol 1,4,5-triphosphate

IP3R, inositol 1,4,5-triphosphate receptor

LV, left ventricle

NCX, Na^{+}/Ca^{2+} exchanger;

PKC, protein kinase C

RMP, resting membrane potential

RyR, ryanodine receptor

SERCA, sarco-endoplasmic Ca^{2+} pump

SR, sarcoplasmic reticulum

XeC, xestospongin-C

Introduction

The heart supplies blood to the whole body and this function is accomplished by the organized contraction of cardiac muscle cells. The mechanical activity is initiated by the electrical excitation of the myocardium, which acts as a functional syncytium in propagating membrane depolarization in cardiomyocytes (Joyner et al. 1983). The depolarization during the action potential (AP) leads to Ca^{2+} entry via voltage-activated L-type Ca^{2+} channel (Figure 1). This Ca^{2+} in turns triggers the translocation of this cation from the sarcoplasmic reticulum (SR) to the cytoplasm, a process termed Ca^{2+} induced-Ca^{2+} released (CICR, Fabiato, 1983). The resulting elevation in cytosolic Ca^{2+} (Ca^{2+} transient) promotes cross-bridge formation of the myofilament leading myocyte contraction (Bers, 2002). Subsequently, cytosolic [Ca^{2+}] declines due to the re-uptake into the SR via the Ca^{2+}-ATPase (SERCA) and its extrusion via Na^{+}/Ca^{2+} exchanger (NCX). This reduction allows Ca^{2+} to dissociate from the myofilaments and relaxation to occur (Bers, 2014).

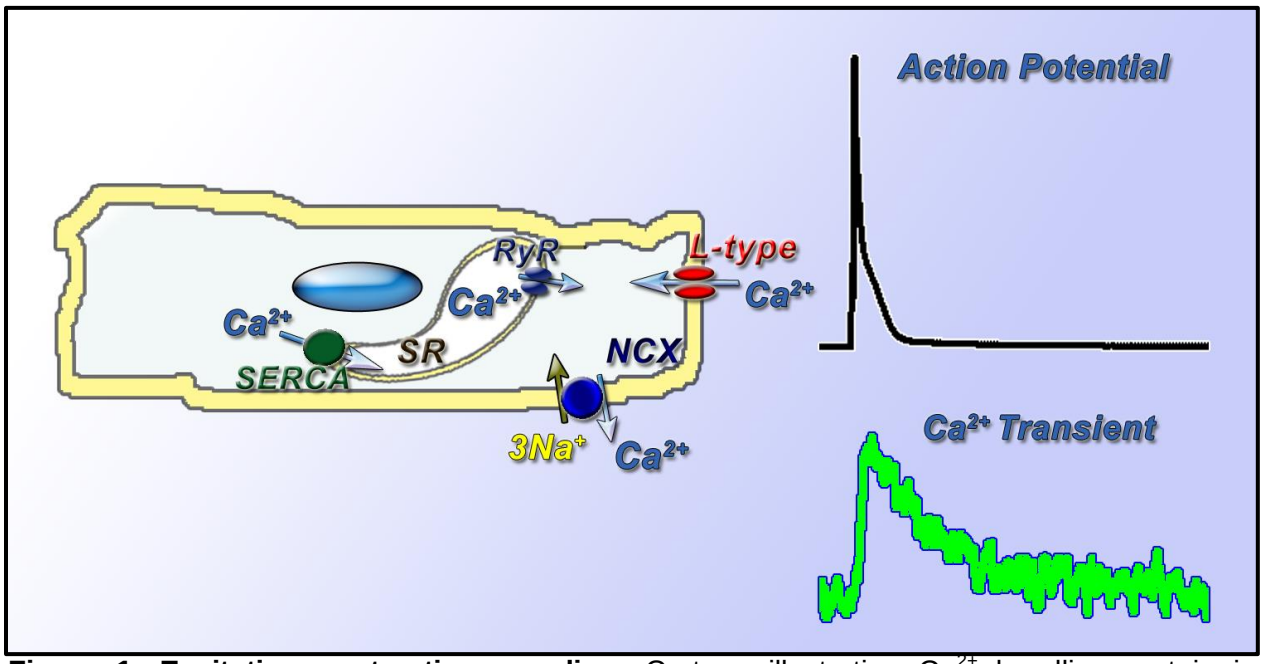

Figure 1. Excitation contraction coupling. Cartoon illustrating Ca^{2+} handling protein in cardiomyocytes. On right side, an action potential and corresponding Ca^{2+} transient obtained from a mouse left ventricular myocyte are reported (courtesy of Dr. Rota).

The repolarization phase of the AP is a critical determinant of the kinetics of Ca^{2+} entry since it controls the pattern of Ca^{2+} influx via L-type channels (I_{CaL}) and NCX, in a time and voltage dependent manner (Rota et al. 2007; Signore et al. 2013). Thus, transmembrane Ca^{2+} fluxes and CICR modulate the temporal dynamic of $[Ca^{2+}]_i$, providing an important link between electrical activity, on the one hand, and myocyte and myocardial contractility and relaxation, on the other.

In the heart, myocytes located in different anatomical regions present typical AP characteristics due to the differential expression of a variety of voltage-gated ion channels. The AP profile of left ventricular (LV) myocytes is composed of five phases (Figure 2): the rapid depolarization phase (phase 0, the upstroke) driven by the influx of Na^+ ions via fast activating/inactivating channels (I_{Na}); the early repolarization phase (phase 1), mediated by fast activation of the transient outward K^+ currents (I_{to} and the ultra-rapid I_{Kur}); the plateau phase (phase 2), which is maintained by the balance of inward currents (I_{CaL} and late Na^+ current, I_{NaL}), outward K^+ currents (delayed rectifier, I_{Kr} and I_{Ks}) and NCX; the late repolarization phase (phase 3) is mediated by continuous K^+ efflux by delayed rectifier and inward rectifier (I_{K1}) currents. Phase 4 is the resting membrane potential, which is maintained by inward rectifier K^+ conductance, together with NCX and the Na/K-ATPase. Phase 4 corresponds to cellular diastole.

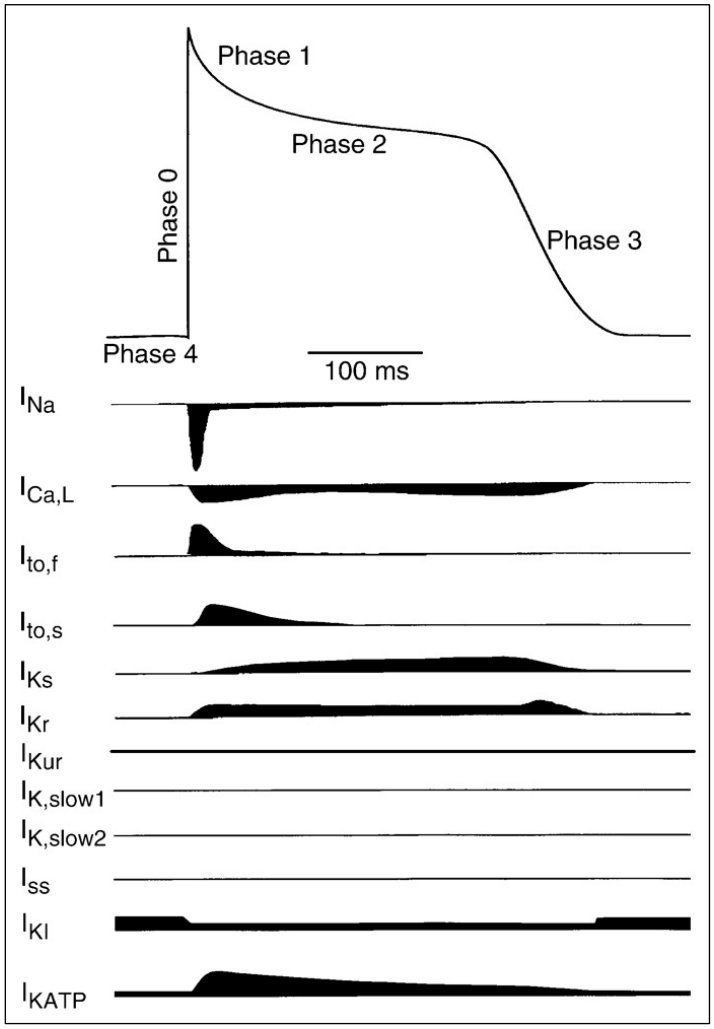

Figure 2. Action potential waveform and underlying ionic currents in adult ventricular myocyte. Adapted from Nerbonne & Kass, 2005.

Myocytes located in pacemaker regions are characterized by the ability to generate a progressive membrane depolarization during diastole, which smoothly transition into phase 1, mainly mediated by Ca^{2+} influx. Although mechanisms related to diastolic depolarization are not fully agreed upon, ion channels and Ca^{2+} released from the SR constitute, respectively, “membrane clock” and “calcium clock” responsible for the depolarization of sino-atrial nodal cells (Zaniboni et al. 2014; Maltsev & Lakatta, 2007). Important factors in determining the automaticity of pacemaker cells are represented by the lack of I_{K1} and by the presence of the funny current I_f, the latter allowing pacemaker cells to have a diastolic potential less negative with respect to the surrounding atrial myocytes.

The electrophysiological characteristics of cardiomyocytes are species-dependent (Figure 4). Cells from large mammals and humans present long APs with prominent plateau. In contrast, small rodents have a short AP lacking the plateau phase. These properties are caused by the different expression and conductance of the various ion channels, resulting in dissimilar ionic current profile (Figure 4). Although the mechanism of excitation contraction (EC)-coupling is comparable in myocytes from large and small mammals, differences in the kinetics of Ca^{2+} transients are observed (see current results). Despite these factors, cells from human and rodent hearts present large similarities and, under pathological conditions, undergo comparable electromechanical adaptations. Typically, AP prolongation occurs in the failing human heart, a condition that is reiterated in experimental rodent models (Houser et al. 2000; Piacentino et al. 2003; Steadman et al. 2011).

Ca^{2+} is a ubiquitous intracellular signal that regulates different cellular functions, and has a central role in the physiology of the heart (Berridge et al. 2000). In human cardiac progenitor cells (hCPCs) Ca^{2+} release from the endoplasmic reticulum via inositol 1,4,5-triphosphate receptors (IP3Rs) promotes spontaneous Ca^{2+} oscillations. These events modulate cell cycle progression and the fate of hCPCs (Ferreira-Martins et al. 2009). Additionally, alterations of Ca^{2+} signals via IP3Rs controls apoptosis and commitment of differentiating embryonic stem cells (Liang et al. 2010). Although limited data in rodents and rabbits suggest that IP3Rs are expressed in left ventricular (LV) myocytes (Domeier et al. 2008; Harzheim et al. 2009), whether the presence of IP3Rs in primitive cells is preserved in the derived LV myocyte progeny playing a role in Ca^{2+} homeostasis remains to be defined.

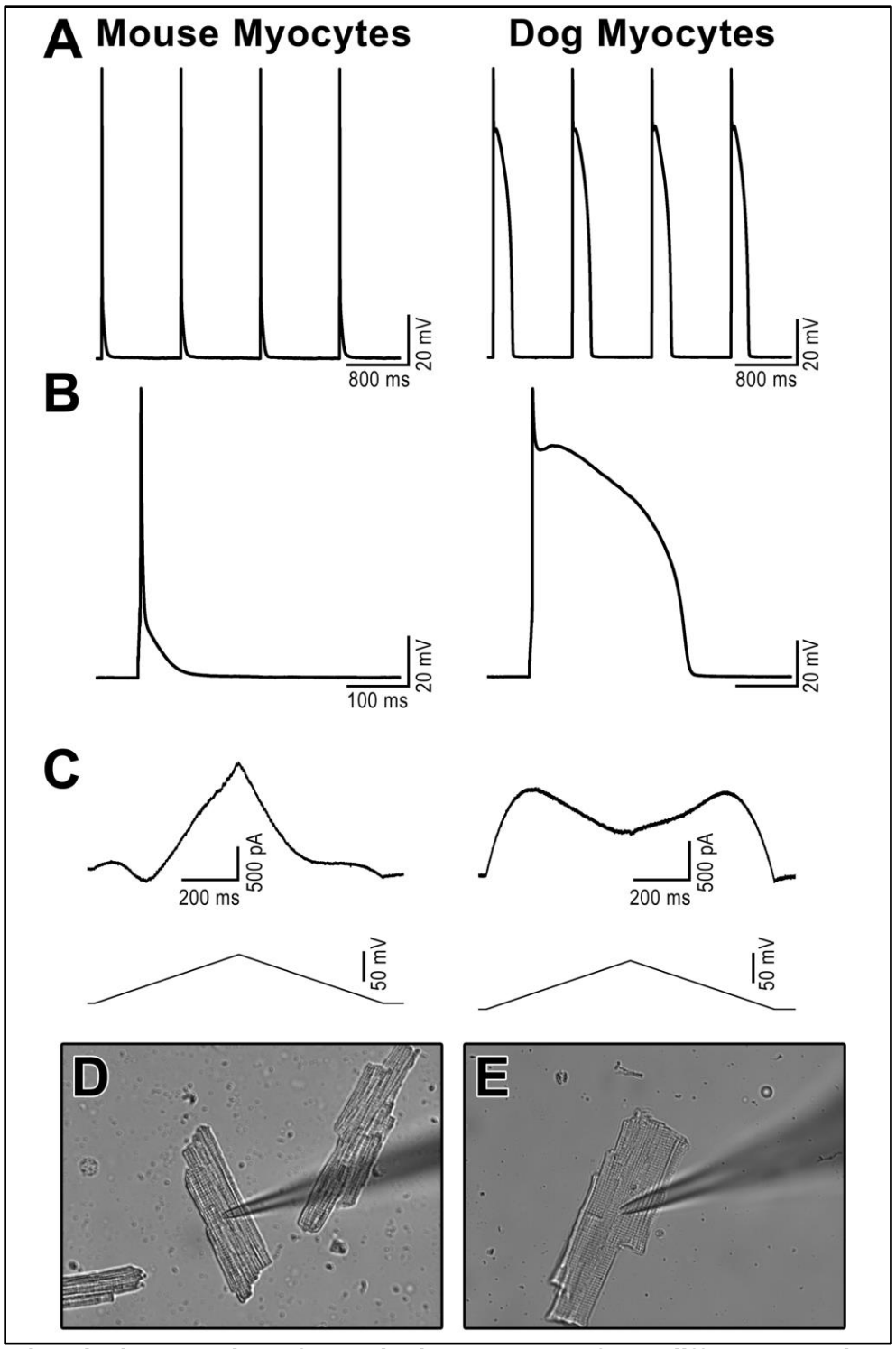

Figure 3. Electrical properties of ventricular myocytes from different species. A, Action potentials recorded by patch-clamp in a mouse and dog cardiomyocytes. **B,** Action potential are shown at higher temporal resolution. **C,** A voltage-clamp command in the form of depolarizing and repolarizing ramps identifies differences in the ionic current profile in myocytes obtained from the two species. **D,** Micrographs illustrating mouse and dog LV myocytes analyzed by patch-clamp (Signore and Rota, unpublished data).

Impaired IP3R-Ca^{2+} signaling and alterations of the calcineurin-NFAT pathway lead to developmental defects and abrogate cardiac hypertrophy induced by isoproterenol or angiotensin II (Nakayama et al. 2010; Uchida et al. 2010). Moreover, initial observations raise the possibility that enhanced IP3R activity may increase Ca^{2+} transient amplitude, the incidence of extra-systolic Ca^{2+} elevations and the propensity for arrhythmias (Harzheim et al. 2009).

Dysfunctional RyRs result in spontaneous Ca^{2+} release or enhanced Ca^{2+} leak, pathologies found in inherited and acquired arrhythmogenic diseases (Houser, 2000; Wehrens et al. 2005; Knollmann et al. 2006; ter Keurs & Boyden, 2007; Herron et al. 2010), strengthening the notion that defects in Ca^{2+} homeostasis impact on the electrical properties of the heart.

Thus, the hypothesis may be raised that abnormalities in Ca^{2+} transients in the presence of Gαq-protein-coupled receptors (GPCR) agonists may involve IP3R-mediated Ca^{2+} mobilization, cytoplasmic Ca^{2+} overload, perturbations in transmembrane potential, and/or sensitization of RyRs, leading to elementary release of Ca^{2+} and electrical instability.

Ca^{2+} mobilized by IP3Rs relies on intracellular levels of IP3, which is produced by phospholipase C (PLC). GPCR agonists promote PLC function that generates IP3 and diacylglycerol (DAG). IP3 stimulates IP3Rs and Ca^{2+} translocation from intracellular stores (Ferreira-Martins et al. 2009; Berridge et al. 2000; Ferreira-Martins et al. 2012), whereas DAG activates transient receptor potential channels (TRPCs) (Hardie, 2007), and protein kinase C (PKC) isoforms, phosphorylating a wide spectrum of ion channels and contractile proteins (Steinberg et al. 1995; Braz et al. 2004; Mohácsi et al. 2004). Additionally, GPCR ligands may initiate PLC-independent signaling mechanisms, modulating transmembrane ionic fluxes (Mohácsi et al. 2004; Vassort et al. 2001). Thus, whether IP3Rs contribute to the functional consequences of GPCR stimulation in cardiomyocytes remains to be elucidated.

Based on this premise, we have investigated the role of IP3Rs in human LV myocytes obtained from normal donor hearts not used from transplantation. This analysis in human cells was complemented with a number of assays in mouse myocytes to define the role of IP3Rs in Ca^{2+} mobilization, electrical activity, arrhythmic events, and myocyte contractile behavior following GPCR stimulation.

Materials and Methods

Human Hearts and Myocyte Isolation

In this study we employed donor hearts not used for transplantation and explanted failing hearts (Table 1). Donor and failing human hearts were shipped in cold cardioplegia solution, and were processed immediately upon receipt.

Table 1: Human Samples

	Gender	N	Age
Human donor hearts	Male	14	43.6 ± 5.9
	Female	20	48.8 ± 5.2
Control human hearts (autopsies)	Male	2	62.3 ± 3.4
	Female	1	
Explanted end-stage failing hearts	Male	8	49.0 ± 6.9
	Female	7	53.0 ± 3.8

Myocardial samples, obtained at autopsy from patients who died from causes other than cardiovascular diseases, were fixed in formalin and used as controls for the quantitative evaluation of myocyte apoptosis by the terminal deoxynucleotidyl transferase assay. As previously performed in our laboratory (Goichberg et al. 2011) large LV myocardial samples were used; a branch of the left main coronary artery was cannulated and the distal arteries were ligated. Initially, the tissue was perfused with a solution containing (mmol/L): NaCl 126, KCl 4.4, $MgCl_2$ 5, HEPES 5, glucose 22, taurine 20, creatine 5, Na pyruvate 5, NaH_2PO_4 5, and 2,3-butanedione monoxime 10 (pH 7.4, adjusted with NaOH). A constant temperature of 37°C was maintained, and the buffer was gassed with 85% O_2 and 15% N_2. After ~10 minutes, 0.015 mmol/L $CaCl_2$, 274 units/ml collagenase (type 2, Worthington Biochemical Corp), and 0.57 units/ml protease (type XIV, Sigma) were added to the perfusate for enzymatic dissociation of the tissue. At completion of digestion, the myocardium was cut in small pieces, subjected to repeated pipetting to obtain a single cell preparation and re-suspended in Ca^{2+} 0.015 mmol/L

solution. Aliquots of cell suspensions were centrifuged for 5 minutes at 20*g*, and myocytes were frozen for biochemical assays.

Mouse Hearts and Myocyte Isolation

Female C57Bl/6 mice at ~3 months of age were used in this study. Animals were maintained in accordance with the Guide for Care and Use of Laboratory Animals, and all animal experiments were approved by the local animal care committee (Institutional Animal Care and Use Committees, IACUC). Mice were anesthetized with pentobarbital (50 mg/kg body weight, i.p.), the heart was excised and cannulated for retrograde perfusion through the aorta. A protocol similar to that described for the isolation of human cells was utilized here as well (Rota et al. 2005; Rota et al. 2007; Signore et al. 2013). Isolated myocytes were suspended in Ca^{2+} 0.1 mmol/L solution. For myocyte isolation, a protocol similar to that described above was employed (Rota et al. 2005; Rota et al. 2007). Antibodies for FACS analysis, and primers for PCR studies are listed in (Table 2) and (Table 3).

Table 2: List of Antibodies

Antigen	Antibody	Manufacturer
sarcomeric *α*-actinin	mouse monoclonal	Sigma
α-smooth muscle actin	mouse monoclonal	Sigma
von Willebrand factor	sheep polyclonal	AbD Serotec
PECAM-1	goat polyclonal	R&D Systems
procollagen 1*α*	goat polyclonal	Santa Cruz

Table 3: List of Primers

Gene	Primers
Human IP3R type-1	F: 5'- GAAGAGCACATCAAGGAAGAACAC -3'
	R: 5'- TGCTGACCAATGACATGGCT -3'
Human IP3R type-2	F: 5'- TAGTCCTGGTGAAAGTTAAAGACCC -3'
	R: 5'- CAGACTCATGGTCGATTCCAACT -3'
Human IP3R type-3	F: 5'- TGTACTTCATTGTGCTGGTCCG -3'
	R: 5'- CGAATCTCATTCTGCTCCCC -3'
Mouse IP3R type-1	F: 5'- GAGAGTTACGTGGCAGAGATGATC -3'
	R: 5'- GGCCAGAAAGATTGGTGACC -3'
Mouse IP3R type-2	F: 5'- TGTGGCATTACCTGTACTTCATCG -3'
	R: 5'- TCCGGATCTCATTTTGCTCAC -3'
Mouse IP3R type-3	F: 5'- CTGGAGCATAACATGTGGAACTACC -3'
	R: 5'- TGCAGGATGCGGATCTCATT -3'

Cell Shortening and Ca^{2+} Transient Measurements in Isolated Myocytes

Isolated LV myocytes were placed in a bath located on the stage of Axiovert (Zeiss), IX51 and IX71 (Olympus) inverted microscopes for measurements of contractility, Ca^{2+} transients and patch-clamp studies (Rota et al. 2005; Rota & Vassalle, 2003). Experiments were performed at room temperature.

Cells were bathed continuously with a Tyrode solution containing (mmol/L): NaCl 140, KCl 5.4, $MgCl_2$ 1, HEPES 5, Glucose 5.5 and $CaCl_2$ 1.0 (pH 7.4, adjusted with NaOH). Measurements were performed in field-stimulated cells by using IonOptix fluorescence and contractility systems (IonOptix) and by video edge detection (Crescent Electronics). Contractions were elicited by rectangular depolarizing pulses, 2 ms in duration, and twice-diastolic threshold in intensity, by platinum electrodes (Rota et al. 2007). Cell shortening was measured by edge-track detection system (Rota et al. 2005; Rota et al. 2007). Changes in mean sarcomere length were computed

by determining the mean frequency of sarcomere spacing by fast Fourier transform, and then frequency data were converted to length. Ca^{2+} transients were measured by epifluorescence after loading the myocytes with 10 μml/L Fluo-3 AM (Invitrogen). Excitation length was 480 nm with emission collected at 535 nm using a 40x oil objective. Fluo-3 signals were expressed as normalized fluorescence (F/F_0). Following treatment with IP3R modulators, some human myocytes were excluded from the analysis if prolonged contraction could not be discriminated from after-contraction during relaxation. Since in some experiments the effects of IP3R stimulation on myocyte contractility and cytoplasmic Ca^{2+} levels were measured simultaneously, the impact of the fluorescent Ca^{2+} sensitive dye on cell contraction was studied. When myocytes were loaded with Fluo-3, sarcomere shortening was significantly decreased with respect to non-loaded cells (Figure 4). Thus, the weak contractile activity of myocytes throught the current study have to be evaluated in light of this specific experimental condition employed.

Figure 4. Cell contractility and Ca^{2+} indicator Fluo-4. Sarcomere shortening in myocytes not loaded or following loading with the Ca^{2+} sensitive dye Fluo-4. Quantitative data are shown as mean±SEM. *P<0.05 versus Non-loaded Myocytes.

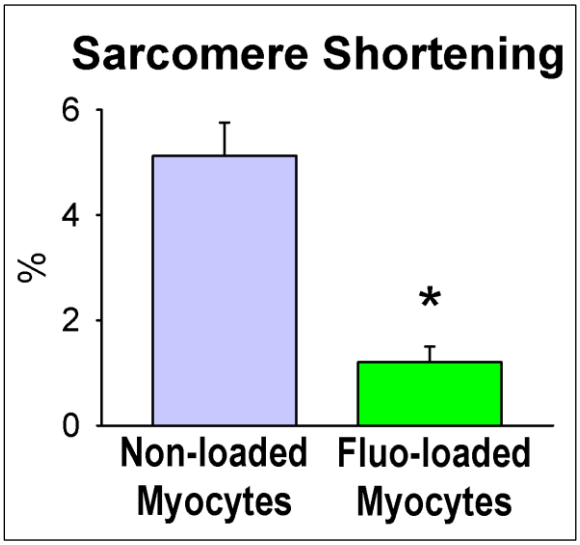

Modulators of IP3R function included Gαq-protein coupled receptor agonists endothelin-1 (100 nmol/L, Sigma), ATP (10 μmol/L, Sigma), angiotensin II (50 nmol/L, Sigma), phenylephrine hydrochloride (10 μmol/L, Sigma) (Gambassi et al. 1998; Pieske et al. 1999; Remus et al. 2006; Domeier et al. 2008; Gergs et al. 2008; Gonzalez et al. 2008; Higazi et al. 2009; Ferreira-Martins et al. 2009; Harzheim et al. 2009; Nakayama et al. 2010; Ferreira-Martins et al. 2012). Additionally, thimerosal (10 μmol/L, Sigma) was utilized to enhance the affinity of IP3Rs to IP3 (Ferreira-Martins et al. 2009; Ferreira-Martins et al. 2012; Bootman et al. 1992) IP3R function

was inhibited by exposing myocytes to xestospongin-C (2 μmol/L, Sigma) or 2-APB (2-aminoethyl diphenylborinate, 10 μmol/L, Sigma); phospholipase-C activity was attenuated with U-73122 (2 μmol/L, Sigma) (Domeier et al. 2008; Higazi et al. 2009; Ferreira-Martins et al. 2009; Harzheim et al. 2009; Ferreira-Martins et al. 2012). PKC function was inhibited with chelerythrine (2 μmol/L, Sigma) (Dobson et al. 2008). RyR channels were blocked with ryanodine (10 μmol/L, MP Biomedicals) (Ferreira-Martins et al. 2009; Nett & Vassalle, 2003).

Patch-Clamp Studies

Data were acquired by means of the whole-cell patch-clamp technique in voltage and current-clamp modes using Multiclamp 700A and 700B amplifiers (Molecular Devices). Electrical signals were digitized using 250 kHz 16-bit resolution A/D converters (Digidata 1322 and 1440A, Molecular Devices) and recorded using pCLAMP 9.0 and 10 software (Molecular Devices) with low-pass filtering at 2 kHz (Rota et al. 2005; Rota et al. 2007; Rota et al. 2007; Ferreira-Martins et al. 2009; Rota & Vassalle, 2003).

For measurements of the action potential (AP), current-clamp mode was employed. Cells were stimulated with current pulses 1.5 times threshold. Myocytes were bathed with Tyrode solution as described above. The composition of the pipette solution was (mmol/L): NaCl 10, KCl 113, $MgCl_2$ 0.5, K_2-ATP 5, glucose 5.5, HEPES 10 (pH 7.2 with KOH). The pipettes were pulled by means of a vertical (PB-7, Narishige) or horizontal (P-1000, Sutter Instrument) glass microelectrode pullers; when filled with intracellular solution pipettes had a resistance of 1-2 MΩ. In Fluo-3 loaded myocytes, the fluorescence signal intensity was collected using a photomultiplier, and a photon to voltage converter (IonOptix) connected to the patch-clamp A/D converter (Rota et al. 2007).

For electrophysiological and mechanical studies only rod-shaped myocytes exhibiting cross striations, and showing no spontaneous contractions or contractures were selected; cells were used within 12 hours following organ acquisition.

IP3 dialysis in myocytes was achieved by whole-cell configuration patch-clamp, or by microinjection technique (FemtoJet, Eppendorf AG) in patch-clamped cells by dissolving 50 μmol/L D-myo-Inositol 1,4,5-triphosphate potassium salt (Sigma) in the pipette solution (Ferreira-Martins et al. 2009; Hoesch et al. 2004).

For $[Ca^{2+}]_i$ buffered conditions (Song et al. 1998), the pipette solution contained 10 mmol/L EGTA and 5 mmol/L $CaCl_2$, which results in ~150 nmol/L free $[Ca]_i$, calculated using Maxchelator program (http://www.stanford.edu/~cpatton/maxc.html). Membrane capacitance (C_m) was measured in voltage-clamp mode using a 5 mV voltage step and pCLAMP software algorithm (Rota et al. 2005; Rota et al. 2007; Rota et al. 2007; Ferreira-Martins et al. 2009; Rota & Vassalle, 2003). For action potential clamp (AP-clamp) assays, a set of AP waveforms were utilized as voltage-clamp commands in myocytes loaded with Fluo-3 AM (Rota et al. 2007). The 2 solutions were similar to those utilized in current-clamp experiments. In the experiments in which RyRs were blocked, myocytes were initially incubated with 10 μmol/L ryanodine and then superfused with the same solution. To deplete Ca^{2+} from the SR, cells were incubated with 10 μmol/L thapsigargin and 10 mmol/L caffeine (Sigma), and subsequently superfused and dialyzed with 5 μmol/L thapsigargin (Zaniboni et al. 1998; Zima et al. 2010) In these studies, myocytes were monitored for the absence of Ca^{2+} transients and/or cell shortening. Treatment with IP3R agonist was performed after the acquisition of baseline data.

In excitation-contraction coupling (ECC) gain studies, Ca^{2+} current and Ca^{2+} transients were measured simultaneously in voltage-clamped myocytes (Rota et al. 2007). Cells were loaded with Fluo-3 AM and bathed with a modified Tyrode solution in which KCl was replaced with CsCl and 2 mmol/L 4-aminopyridine was added. The composition of the pipette solution was (mmol/L): NaCl 10, CsCl 113, $MgCl_2$ 0.5, Tris-ATP 5, glucose 5.5, HEPES 10 and tetraethylammonium chloride 20 (pH 7.2 with CsOH). Cells were depolarized for 300 ms from holding potential (V_h) -40 mV to a family of test potentials ranging from -30 to +70 mV. Each voltage-clamp was preceded by a train of 4 conditioning pulses (100 ms, 1Hz) from -40 to 0 mV (Rota et al. 2007).

Contraction in patch-clamped myocytes was evaluated using ImageJ by reslice of the cell profile collected by videoclips and a CCD camera (Retiga EXi Fast 1394, QImaging).

The nickel sensitive current was determined as follows: myocytes were bathed with a modified Tyrode solution in which KCl was replaced with CsCl; 10 μmol/L ryanodine and 4 μmol/L nicardipine were then added (Ozdemir et al. 2008). Pipette solution was identical to that used in ECC gain measurements. Following a 200 ms depolarization from -40 mV to +80 mV, a hyperpolarizing ramp 2 sec in duration was applied to reach -120 mV. The voltage-clamp

protocol was utilized in the absence and presence of 2.5 mmol/L $NiCl_2$ in myocytes exposed to Tyrode, ATP, ET-1, or dialyzed by D-myo-IP3 salt. The nickel sensitive current was calculated as the difference between currents in the presence and absence of nickel.

To establish the time course of Ca^{2+} transients evoked by depolarizing steps and by caffeine, myocytes were bathed with Tyrode solution under voltage-clamp. Ca^{2+} transients were elicited by voltage steps 50 ms in duration from V_h -70 mV to 0 mV, at 0.2 Hz. Every 2-4 min, a 20 mmo/L caffeine spritz 0.5 sec in duration was delivered using a microinjector (FemtoJet, Eppendorf AG). Cells were studied in the absence or presence of ATP or ET-1. Analysis of Ca^{2+} transients was not extended to portion of recordings in which large inward currents (~>1 nA), potentially reflecting store-operated Ca^{2+} entry, were observed.

In Vivo AAV9-shRNA-IP3R2-EGFP Vector Delivery

To compromise IP3R type-2 expression in myocytes, an AAV9 vector carrying transgenic small hairpin-RNA targeting IP3R type-2 and EGFP (AAV9shRNA-IP3R2-EGFP, Vector Biolabs) was administered in twelve mice by intraventricular injections of 80 μl of solution containing the vector at titer of 8.8x10 (Gonzalez et al. 2008) VG/ml resuspended in PBS. Administration was performed in anesthetized mice (1.5% isoflurane) using a 32G needle Hamilton syringe. Mice were sacrificed 3 weeks after.

Cardiomyocytes obtained from mice treated with AAV9-shRNA-IP3R2-EGFP vector were loaded with the Ca^{2+} indicator Rhod-2 (10 μmol/L; Invitrogen) (Ferreira-Martins et al. 2009; Ferreira-Martins et al. 2012). Excitation length was 545 nm with emission collected at 605 nm using a 40x objective. Rhod-2 signals obtained from EGFP-positive and EGFP-negative myocytes were expressed as normalized fluorescence (F/F_0), where F_0 is the diastolic fluorescent level subtracted by the background signal measured in the region adjacent to the cell. To establish whether the amplitude of Ca^{2+} transients was affected by the type of fluorescent Ca^{2+} indicator employed, mouse myocytes were loaded with Rhod-2, Fluo-4 (5 μmol/L; Invitrogen), or a combination of the two dyes. Rhod-2 originated stronger diastolic, systolic, and background fluorescent signal, with respect to Fluo-4 (Figure 5A). However, kinetics of Ca^{2+} raise and decay were comparable, as shown by the normalized Ca^{2+} transient traces (Figure 5B). Importantly, when Ca^{2+} transient amplitude was expressed as ratio with

respect to diastolic Ca^{2+} level (F/F_0), Fluo-4 originated larger transient amplitude (Figure 5C). Importantly, previous work from our laboratory documented that EGFP does not interfere with detection of Rhod-2, by emission spectra analysis and intracellular Ca^{2+} measurements (Ferreira-Martins et al. 2009).

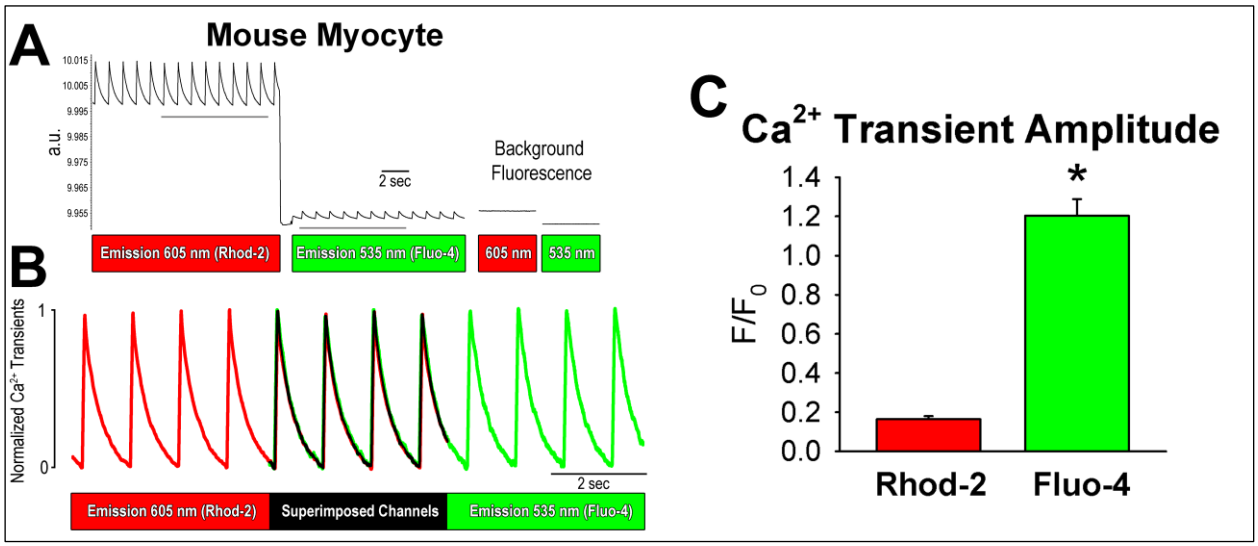

Figure 5. Ca^{2+} indicators and Ca^{2+} transients in mouse myocytes. A, Ca^{2+} transient (black-traces) in a myocyte loaded with the Ca^{2+} sensitive dyes Rhod-2 and Fluo-4; Ca^{2+} transient was collected using the red fluorescent channel (emission wavelength 605 nm), and the green fluorescent channel (emission wavelength 535 nm). Background fluorescence was obtained in the region adjacent to the cell. Gray lines indicate portions of the recording reported in panel B. **B**, Ca^{2+} transients obtained with the red and green fluorescent channels are normalized by their amplitude and partly superimposed. **C**, Quantitative data for cells loaded with Rhod-2 or Fluo-4 are shown as mean±SEM *P<0.05 versus Rhod-2.

Quantitative RT-PCR

Total RNA from isolated human and mouse LV myocytes, and mouse LV myocardium was extracted utilizing TRIZOL reagent (Invitrogen). cDNA was obtained from 1 μg total RNA in a 20 μl reaction containing Reverse Transcription buffer (Applied Biosystems), 4 mmol/L each of dNTP together with 50 U of MultiScribe reverse transcriptase (Applied Biosystems), 20 U of RNase inhibitor (Applied Biosystems) and 5 μmol/L of oligo-$(dT)_{15}$ primer. This mixture was

incubated at 37°C for 2 h. Subsequently, real-time RT-PCR was performed with primers designed using the Vector NTI Advance 11 (Invitrogen) software (Rota et al. 2007; Gonzalez et al. 2008). Sequences of primers are reported in (Table 3). The 7300 Real Time PCR system (Applied Biosystems) was employed for quantitative RT-PCR. In each case, 1 μl of cDNA was combined with Power SYBR Green Master Mix (Applied Biosystems) in a 20 μl reaction. Cycling conditions were as follow: 95°C for 10 min followed by 40 cycles of amplification (95°C denaturation for 15 sec, 60°C annealing and extension for 1 min). The melting curve was then obtained. To avoid the influence of genomic contamination, forward and reverse primers for each gene were located in different exons. PCR products were run on 2% agarose/1x TBE gel to confirm the specificity of the reaction. Total RNA extracted from human and mouse brain (Clontech) was employed as controls.

Western Blotting

Whole cell protein extracts from cell pellets of isolated human or mouse myocytes were prepared using RIPA buffer (Sigma), supplemented with a cocktail of protease inhibitors (Roche) and phosphatase inhibitors (Sigma). Equivalent of 50 μg of proteins were separated on 4 to 20% SDS-PAGE, transferred onto PVDF membrane, blocked with 5% BSA and exposed to the following primary antibodies: rabbit polyclonal IP3R type-2 (Cell Signaling), rabbit polyclonal IP3R type I/II/III (Santa Cruz Biotechnology), mouse GAPDH (Millipore) followed by horseradish peroxidase-conjugated secondary antibodies (Cell Signaling Technology and Jackson ImmunoResearch Laboratories), and developed using Pierce SuperSignal West Femto Maximum Sensitivity Chemiluminescent Substrate (Fisher Scientific). IP3R expression was normalized by GAPDH.

Two-Photon Microscopy

Myocytes were loaded with 10 μmol/L Fluo-3 AM (Invitrogen) and placed on the stage of a two-photon microscope (BX51WI Olympus microscope coupled with a Bio-Rad Radiance 2100MP system). Cells were bathed with a Tyrode solution, and field stimulated using platinum electrodes. Fluo-3 was excited at 900-960 nm wavelength with mode-locked Ti:sapphire femtosecond laser (Tsunami, Spectra-Physics), and the emission signal was collected at 535

nm. Images were acquired in line scan mode with a 2 ms sampling rate (Ferreira-Martins et al. 2009).

Isometric Force in Human Trabeculae Carneae

Thin LV trabeculae were dissected from the LV wall and mounted in a horizontal tissue bath (Steiert, Hugo Sachs Elektronik-Harvard Apparatus) connected to a force transducer (F10, Harvard Apparatus). Muscles were superfused with Krebs–Henseleit buffer (KHB; Sigma), containing in mmol/L: 118 NaCl, 4.7 KCl, 11 glucose, 1.2 $MgSO_4$, 1.2 KH_2PO_4, 1.8 $CaCl_2$ and 25 $NaHCO_3$ gassed with 95% O_2/5% CO_2 (pH 7.4) at 37°C. Tissue was stimulated by two platinum electrodes using field stimulation from an isolated stimulator output (frequency 0.5 Hz; impulse duration 2 ms; intensity 1.5-fold threshold). Each muscle was stretched to the length at which force of contraction was maximal. The developed tension was measured isometrically with the force transducer attached to a Bridge Amp (ADInstruments) and a 4 kHz A/D converter (Power Lab 4/30, ADInstruments). Contractile signal was recorded using LabChart 7 Pro software (ADInstruments). Muscle preparations were allowed to equilibrate for at least 60 min. The effect of ATP (100 μmol/L), endothelin-1 (100 nmol/L), and isoproterenol (100 nmol/L, Sigma) on developed tension, is expressed as fold change with respect to baseline values obtained in the absence of these agonists.

Ex-vivo Electrical Properties of Human and Mouse Myocardium

Human LV samples and mouse hearts were perfused, respectively, through a large branch of the left coronary artery and the aorta in a Langendorff apparatus at a constant pressure of 80 mm Hg with KHB solution (Goichberg et al. 2011). The temperature was maintained at 37°C by immersing the myocardial tissue in a water-heated glassware reservoir (Radnoti), containing preheated KHB. Human myocardium and mouse hearts were stimulated with a 2 ms square pulse at two-times its threshold level (4 channels stimulator, BMS 414, Crescent Electronics), using a mini-coaxial electrode (Harvard Apparatus). Myocardial electrical activity was monitored employing a two-lead mini ECG system (Harvard Apparatus) in which electrodes were placed on the endocardial and epicardial aspects of the human LV sample, or on the right atrium and apex of the mouse heart. Monophasic action potentials (MAPs) were recorded using a micro

MAP-Tip electrode (Harvard Apparatus) (Goichberg et al. 2011). ECG and MAP signals were amplified (Animal Bio Amp, ADInstruments), digitized using a 4 kHz A/D converter (Power Lab 8/30, ADInstruments) and recorded using LabChart 7 Pro software (ADInstruments) with low and high-pass filtering at 1 kHz and 0.3 Hz, respectively. A protocol of programmed electrical stimulation (PES) was used to assess the propensity of mouse hearts to develop ventricular arrhythmias (Goichberg et al. 2011; Roell et al. 2007). PES consisted of a train of pacing stimuli (S1) applied at 150 ms cycle length, with an extra stimulus (S2) inserted every eighth beat. The S1-S2 interval was progressively reduced until the S2 stimulus either failed to generate an action potential or induced arrhythmic events. The appearance of ventricular tachycardia (3 or more consecutive ectopic beats characterized by atria-ventricular dissociation) and/or ventricular fibrillation was established (Goichberg et al. 2011). ATP (20 μmol/L), ET-1 (100 nmol/L), and thimerosal (20 μmol/L) were used to promote IP3R function. In a subset of experiments, 10 μmol/L glibenclamide was employed to block I_{KATP}, a repolarizing current activated under ischemic conditions (Pandit et al. 2011).

Data Analysis

The magnitude of sampling employed in each measurement is listed in Appendix. Data are presented as mean±SEM. Independent samples were compared using ANOVA analysis with Bonferroni correction or Fisher's exact tests, as appropriate for continuous or categorical responses. The normality and homogeneity of variance of the data were checked first to meet the assumptions of ANOVA. Paired observations were evaluated with Wilcoxon signed-rank sum test or paired *t*-test as appropriate. For data with multiple measurements (myocytes) from the same donor (mouse/patient), linear mixed-effects models with patient/mouse as random effect, main effects for treatment group were applied to examine and compare response changes. The compound symmetry covariance matrix was specified to account for dependency among observations. Differences in mean changes between assessments were compared between groups and within each group by LSMEANS statement. Throughout, a $P<0.05$ was considered statistical significance and all tests were two sided with a type I error of 0.05. The statistical analyses were performed using SAS version 9.3 (SAS Institute) (Berenson et al. 1988).

Results

Human Hearts

Human cardiomyocytes were obtained from the LV of 34 donor hearts declined from transplantation; 14 males and 20 females, with an average age of 44±4 years (Table 1). In donor hearts, foci of replacement fibrosis and areas of diffuse interstitial fibrosis were not detected histologically. Myocyte apoptosis was comparable in three randomly selected donor hearts and age-matched control hearts obtained at autopsy from patients who died from causes other than cardiovascular diseases (Figure 6). Thus, myocyte survival in donor hearts was not affected by the preservation protocol, which involved cardioplegic solution. End-stage failure in explanted hearts was of ischemic (n=6) and non-ischemic (n=9) origin.

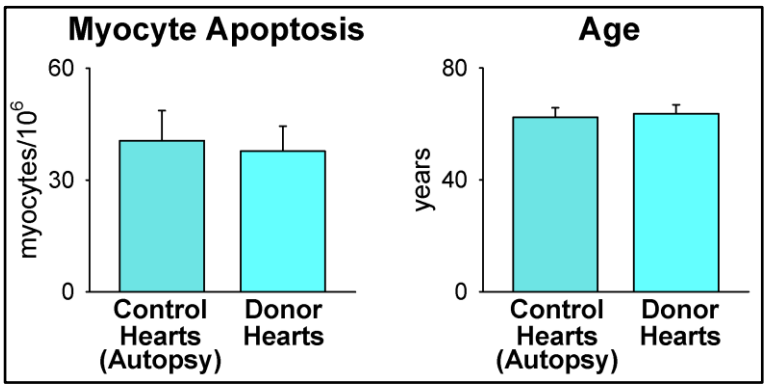

Figure 6. Myocyte death. Myocyte apoptosis measured by TdT-labeling in control hearts obtained from 3 randomly selected donor hearts not used for transplantation and 3 age-matched control hearts collected at autopsy. Results are shown as mean±SEM.

IP3Rs, Ca^{2+} Transients, and Human Myocyte Contractility

Ca^{2+} release from the ER via IP3Rs originates cytosolic Ca^{2+} oscillations in human cardiac progenitor (Ferreira et al. 2009), raising the possibility that these channels are preserved and functional in adult cardiomyocytes. Thus, we established whether IP3Rs are expressed in human LV myocytes and whether their function modulates Ca^{2+} cycling and contractility in this cell compartment. This analysis was integrated with assays in mouse cells. Molecular studies were conducted in isolated myocyte preparations with minimal levels of contamination from fibroblasts, endothelial cells and smooth muscle cells, as established by immunocytochemistry and FACS analysis (Figure 8). Transcripts for the three IP3R subtypes were identified by qRT-PCR in human LV myocytes (Figure 8A and Figure 9). The expression of IP3R type-2 was also confirmed by Western blotting (Figure 8B). Similarly, the presence of IP3Rs in mouse LV myocytes was documented by both methodologies (Figure 10 and Figure 11).

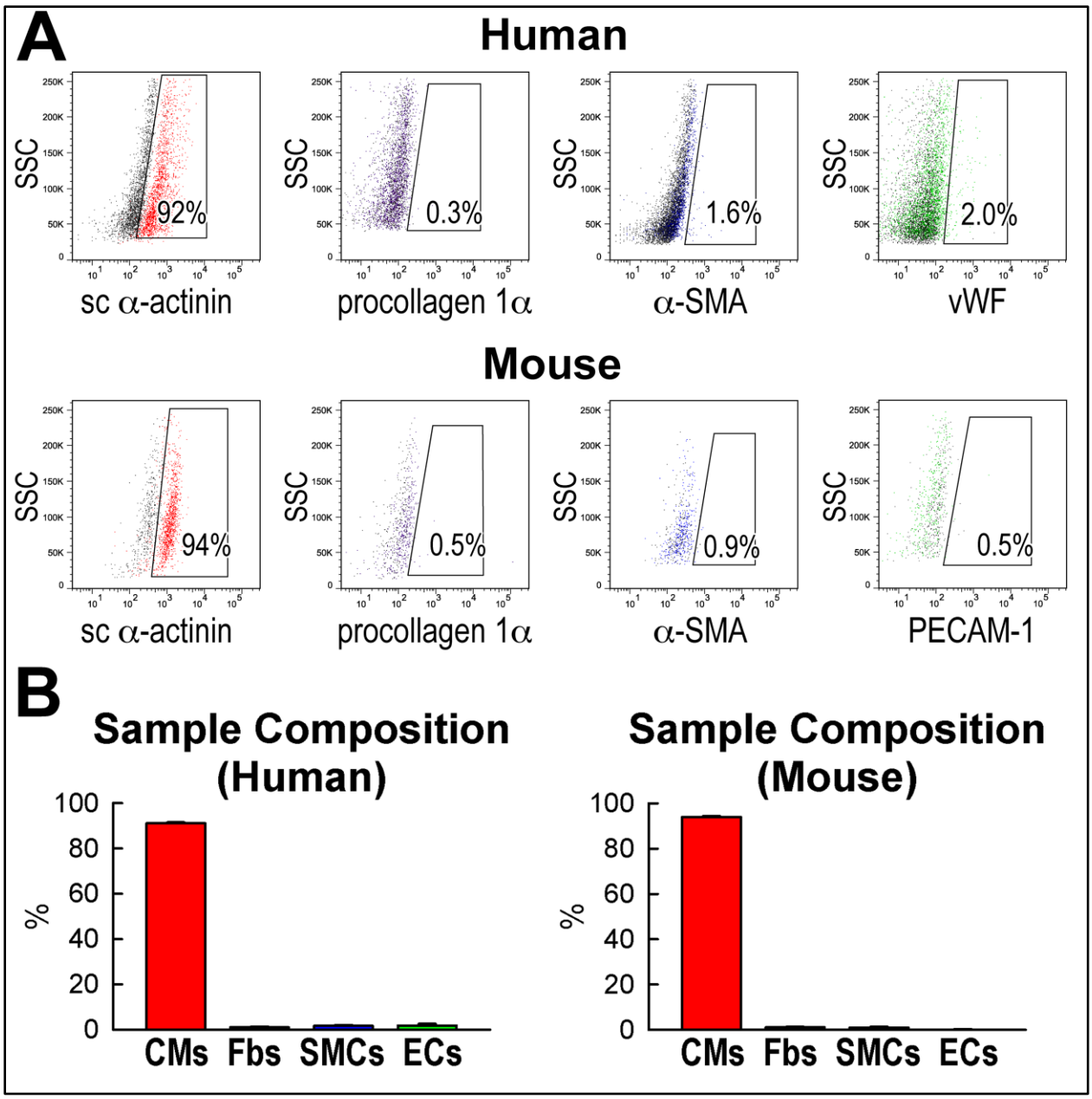

Figure 7. Human and mouse cardiac cells. A, Myocytes, fibroblasts, smooth muscle cells and endothelial cells were identified by *α*-sarcomeric actinin (sc α-actinin, red dots), procollagen-1*α* (purple dots), *α*-smooth muscle actin (*α*-SMA, blue dots), and von Willebrand factor (vWF, human; green dots) or PECAM-1 (mouse, green dots), respectively. Black dots correspond to negative control. **B,** Fraction of cardiomyocytes (CMs), fibroblasts (Fbs), smooth muscle cells (SMCs), and endothelial cells (ECs) in human and mouse myocyte preparations. Results are shown as mean±SEM.

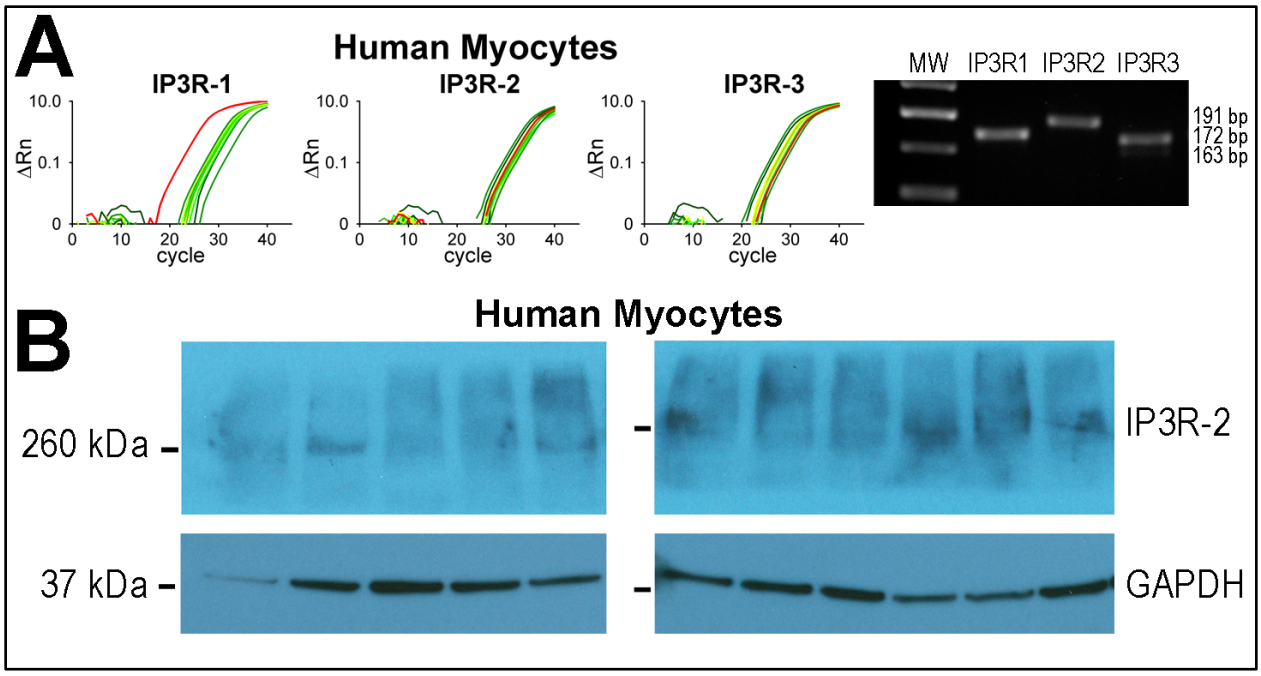

Figure 8. IP3Rs in human cardiomyocytes. A, qRT-PCR show transcripts for the three IP3R subtypes in human LV myocytes. Representative curves and PCR products are shown together with the mRNA obtained from the human brain, that was used as positive control (red curves). The PCR products had the expected molecular weight. Human *β*2-microglobulin: housekeeping gene (for sequences see Figure 9). **B,** Expression of IP3R protein by Western blotting in human LV myocytes with IP3R-2 and pan-IP3R antibodies, respectively. GAPDH: loading condition.

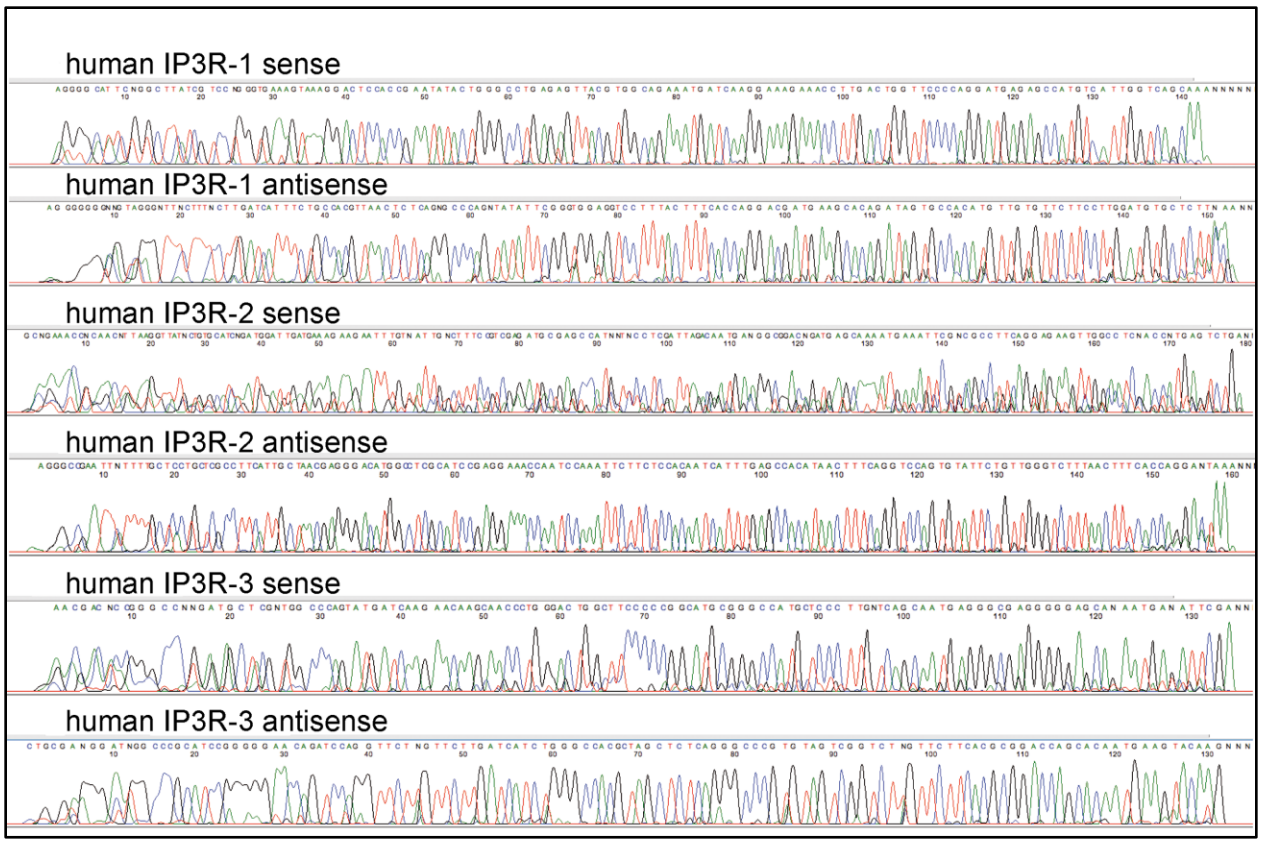

Figure 9. Sequences of human transcripts. Nucleotide sequences were obtained in a sense and anti-sense direction to confirm the specificity of the amplified PCR products for human genes.

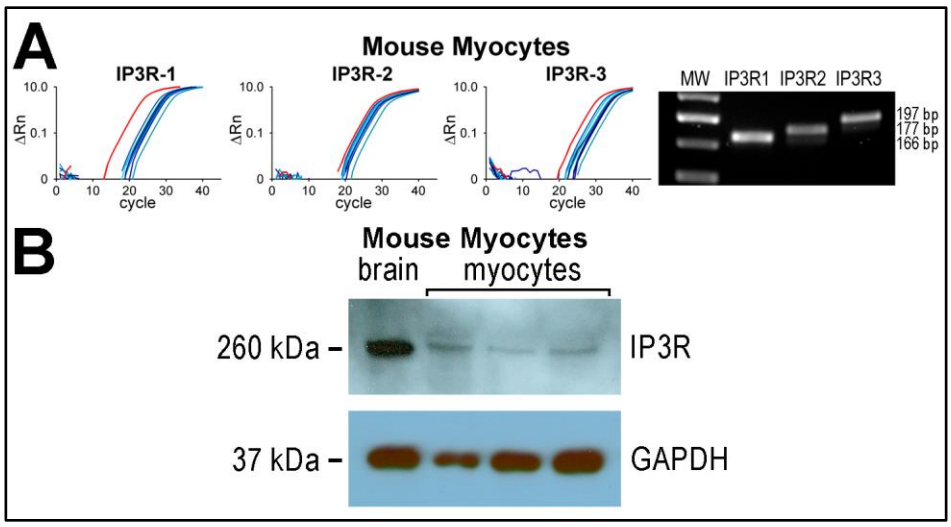

Figure 10. IP3Rs in mouse cardiomyocytes. A, qRT-PCR show transcripts for the three IP3R subtypes in mouse LV myocytes. Representative curves and PCR products are shown together with the mRNA obtained from the mouse brain, that was used as positive control (red curves). The PCR products had the expected molecular weight. MW: molecular weight. For sequences see Figure 11. **B,** Expression of IP3R protein by Western blotting in mouse LV myocytes with IP3R-2 and pan-IP3R antibodies, respectively. GAPDH: loading condition.

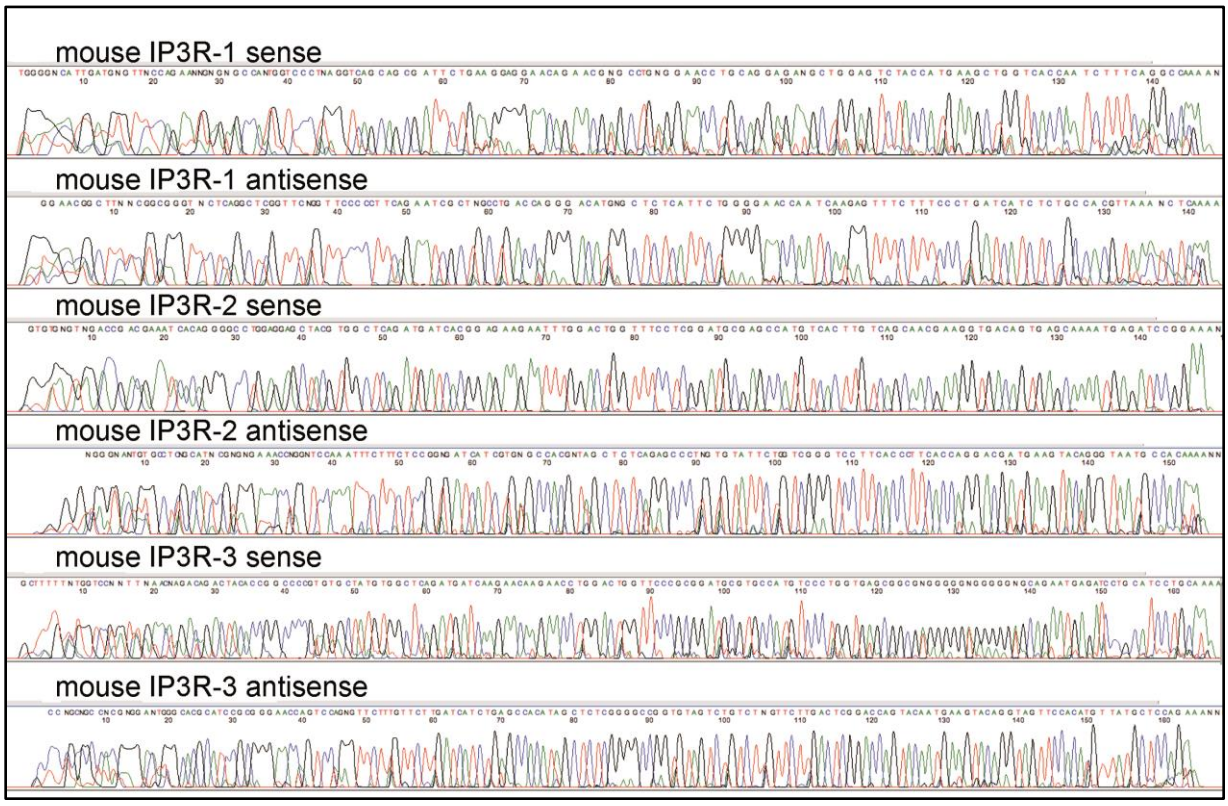

Figure 11. Sequences of mouse transcripts. Nucleotide sequences were obtained in a sense and anti-sense direction to confirm the specificity of the amplified PCR products for mouse genes.

The effect of IP3R activation on Ca^{2+} cycling and contractility of human LV myocytes was investigated by stimulating GPCRs with adenosine 5′-triphosphate (ATP) and endothelin-1 (ET-1), which both enhance the activity of PLC, and the synthesis of IP3 and DAG (Ferreira-Martins et al. 2009; Domeier et al. 2008; Harzheim et al. 2009; Nakayama et al. 2010; Ferreira-Martins et al. 2012; Pieske et al. 1999; Remus et al. 2006; Gergs et al. 2008). ATP increased myocyte contractility, and this response was attenuated with the unspecific IP3R blocker 2-APB (Figure 12A). The enhanced cell performance mediated by GPCR activation was coupled with an increase in Ca^{2+} transient amplitude (Figure 12B). Inhibition of IP3Rs with the selective blocker xestospongin-C (XeC) did not modify baseline myocyte mechanics, but abrogated the changes mediated by GPCR stimulation (Figure 12C).

The increase in contractility with these agonists led to episodes of after-contractions during relaxation in 27% of human cardiomyocytes; however, spontaneous and sustained Ca^{2+} elevations were observed rarely (Figure 13A-13C).

The effects of GPCR activation on cardiomyocytes were equally present in myocardial trabeculae dissected from the LV wall. ATP and ET-1 enhanced isometric developed tension, which was abolished by IP3R antagonists 2-APB and XeC (Figure 14). Thus, IP3R inhibition in human cardiomyocytes and myocardium attenuates the positive inotropic action of GPCR stimulation.

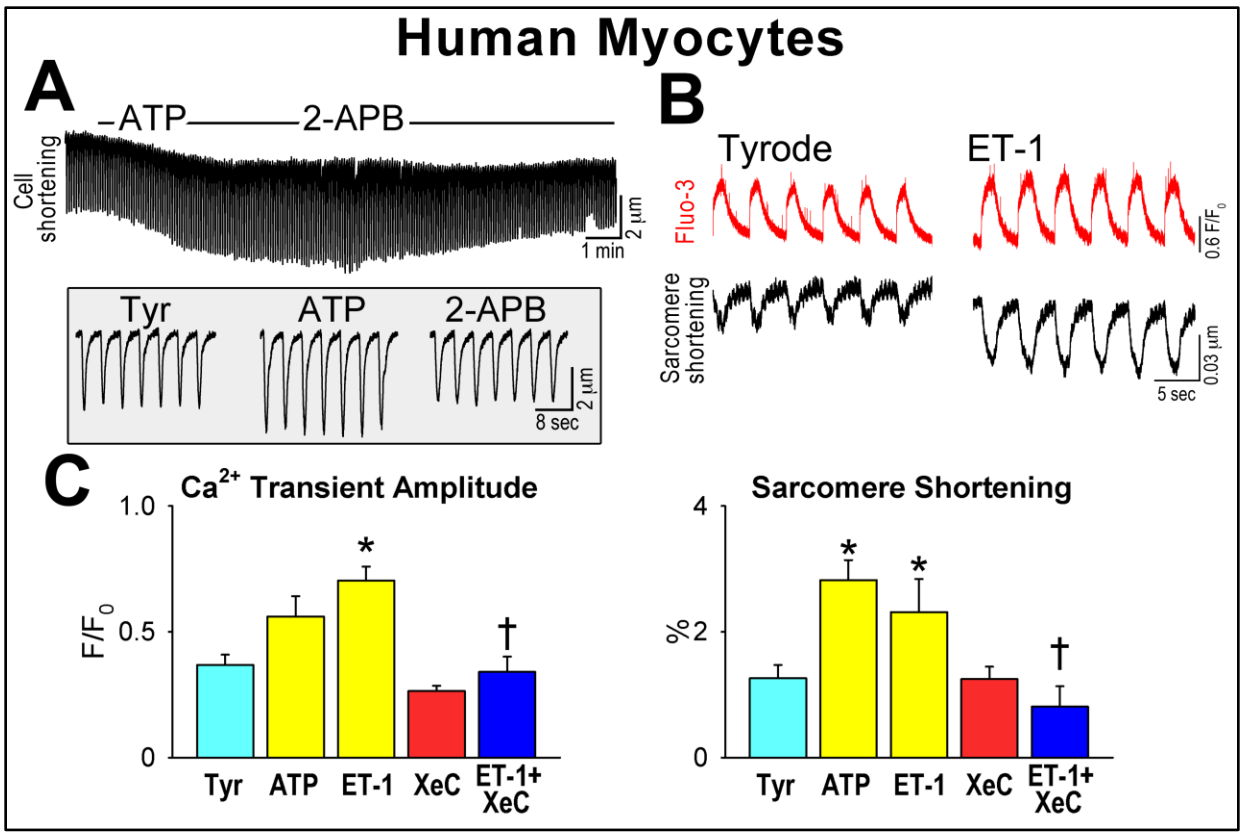

Figure 12. IP3Rs, Ca^{2+} cycling, and contractility in human cardiomyocytes. A, Sarcomere shortening in a field stimulated human cardiomyocyte, exposed first to ATP (10 *µ*mol/L) and then to the IP3R blocker 2-APB (10 *µ*mol/L). Higher time resolution traces are shown in the inset. **B,** Ca^{2+} transients (red-traces) and sarcomere shortening (black-traces) in a field stimulated cardiomyocyte before (Tyrode) and after exposure to ET-1 (100 nmol/L). **C,** Quantitative data for Fluo-loaded cells are shown as mean±SEM. Tyr: Tyrode; XeC: xestospongin-C (2 *µ*mol/L). **P*<0.05 versus Tyr, †*P*<0.05 versus ET-1.

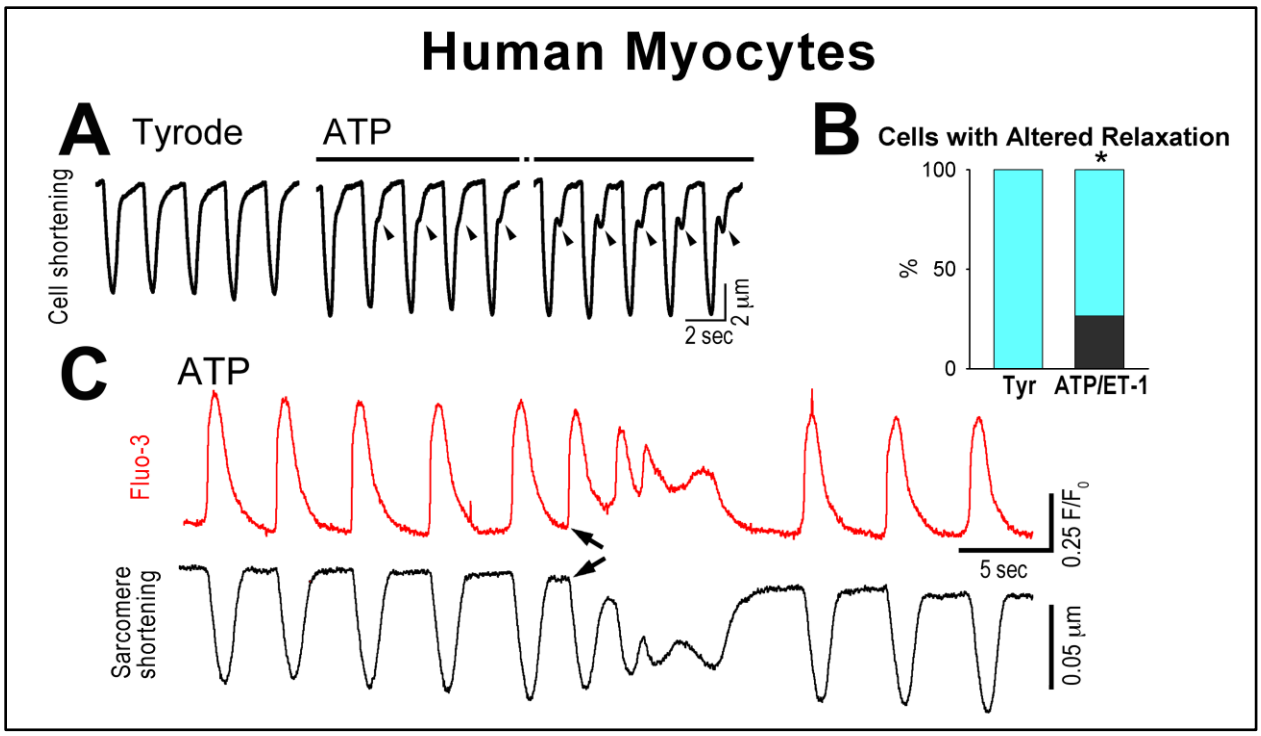

Figure 13. IP3Rs, Ca^{2+} cycling, and contractility in human cardiomyocytes. A. After-contractions (arrowheads) in a LV myocyte exposed to ATP. **B,** Fraction of myocytes, 27%, with impaired relaxation (black portion of the bar). **P*<0.05 versus Tyr. **C,** Ca^{2+} transients (red-traces) and sarcomere shortening (black-traces) in field stimulated cardiomyocyte exposed to ATP. An ectopic (arrows) and sustained Ca^{2+} elevation coupled with prolonged contraction is shown.

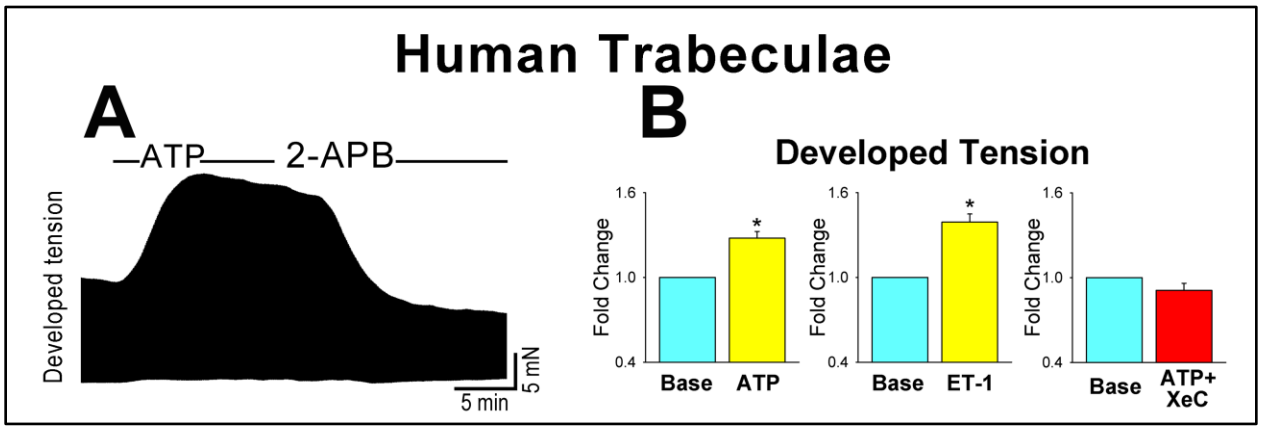

Figure 14. IP3Rs, Ca^{2+} cycling, and contractility in human cardiomyocytes. A, Isometric tension in human LV trabeculae exposed to ATP (100 μmol/L) and then to the IP3R blocker 2-APB. **B,** Quantitative data are shown as mean±SEM. Base: baseline in the presence of Krebs-Henseleit buffer. **P*<0.05 versus Base.

GPCRs and Electrical Instability

To establish whether the electrical properties of human cardiomyocytes were influenced by activation of GPCRs, membrane potential and $[Ca^{2+}]_i$ were measured simultaneously in current-clamped cells loaded with the Ca^{2+} indicator Fluo-3. In human cardiomyocytes, ATP and ET-1 decreased resting membrane potential (RMP), prolonged the action potential (AP), and promoted the occurrence of early after-depolarizations (EADs), together with an increase in Ca^{2+} transient amplitude and extra-systolic Ca^{2+} elevations. Comparable responses were observed with the IP3R agonist, thimerosal (Figure 15).

Importantly, ATP and ET-1 had similar effects on the intact myocardium. Human samples were perfused in a Langendorff apparatus, and transmural pseudo-ECG and monophasic action potentials (MAPs) were recorded. GPCR agonists ET-1 and ATP delayed the electrical recovery and prolonged MAPs (Figure 16A, and 16B), mimicking the observations at the myocyte level.

Moreover, tachycardia and premature ventricular contractions occurred (Figure 16C). To exclude the contribution of ischemia, potentially introduced during the preservation of the organ, measurements were obtained in the presence of K_{ATP} channel blockade, since these channels are activated by hypoxia. Inhibition of K_{ATP} channels had no consequences on MAPs (Figure 17), indicating that the electrical manifestations dictated by GPCR stimulation were independent from myocardial ischemia. Thus, GPCR stimulation prolongs the AP and promotes the electrical instability of cardiomyocytes and the myocardium.

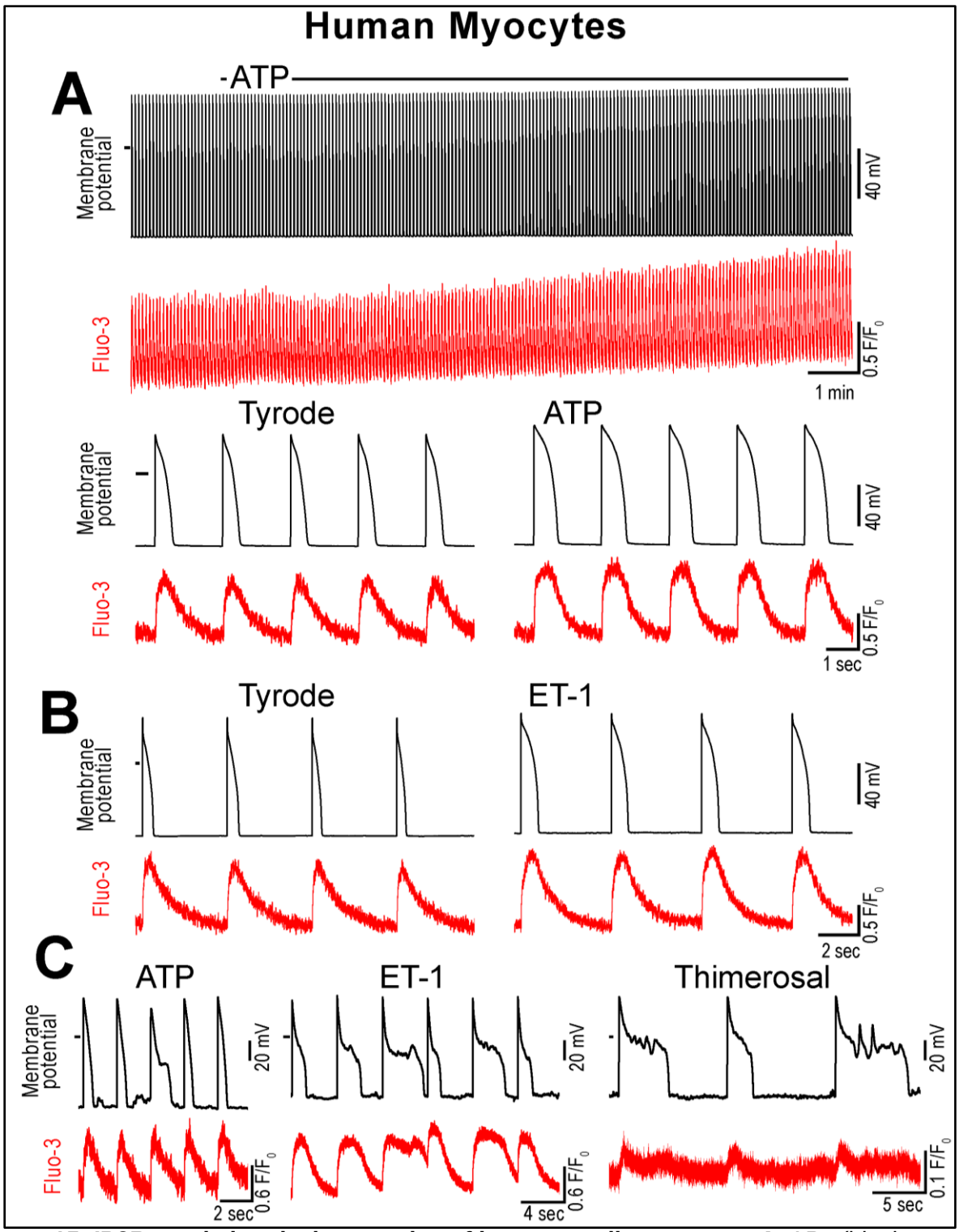

Figure 15. IP3Rs and electrical properties of human cardiomyocytes. **A,** APs (black-traces) and Ca^{2+} transients (red-traces) in a human myocyte exposed to ATP. In the lower panel, traces are shown at higher time resolution. **B,** AP (black-traces) and Ca^{2+} transients (red-traces) in a human myocyte before and after ET-1 exposure. **C,** EADs (black-traces) and Ca^{2+} transients (red-traces) of human myocytes with ATP, ET-1, and the IP3R-agonist, thimerosal (10 μmol/L).

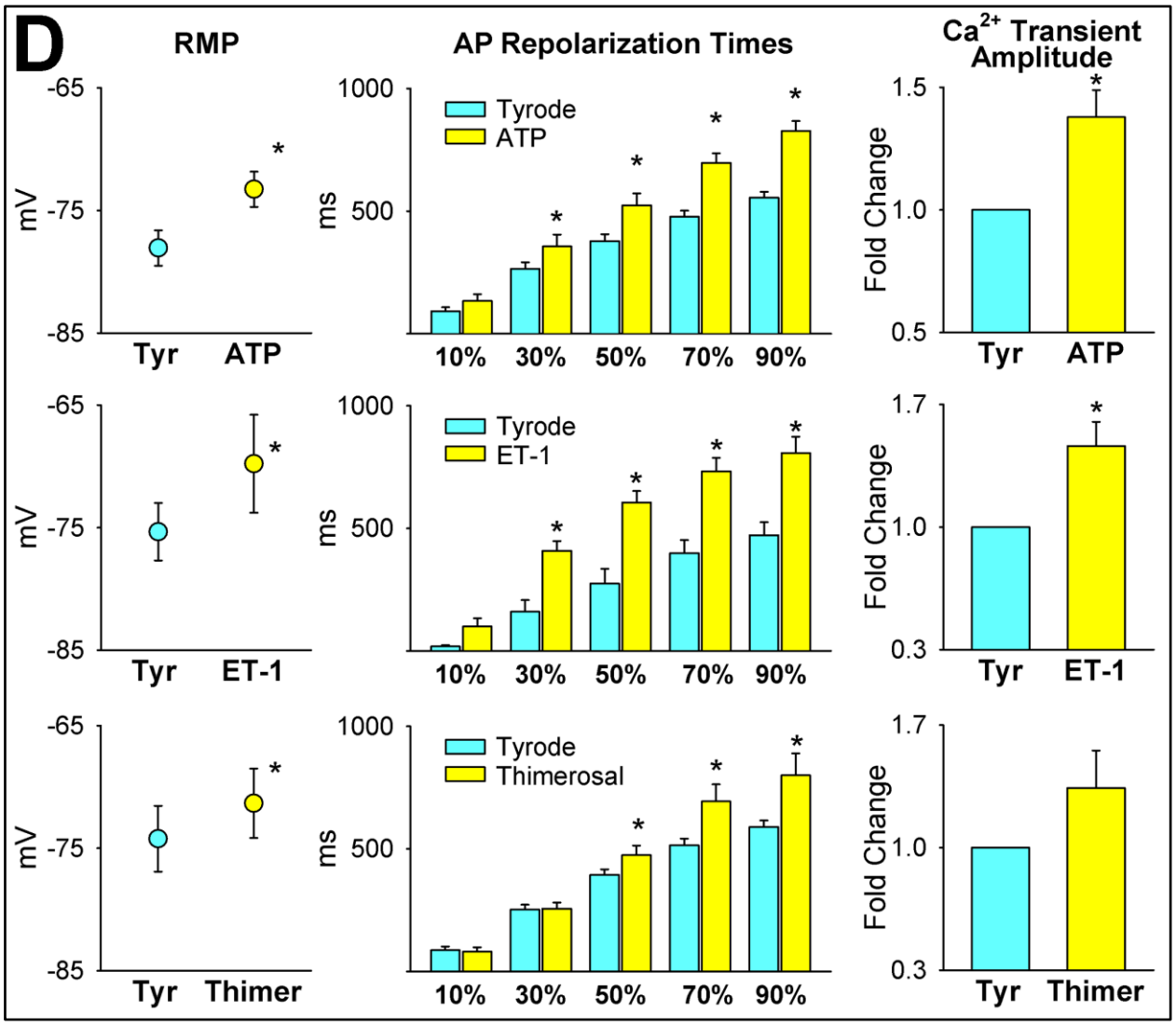

Figure 15. IP3Rs and electrical properties of human cardiomyocytes (continued). D, Quantitative data are shown as mean±SEM. **P*<0.05 versus Tyr**.**

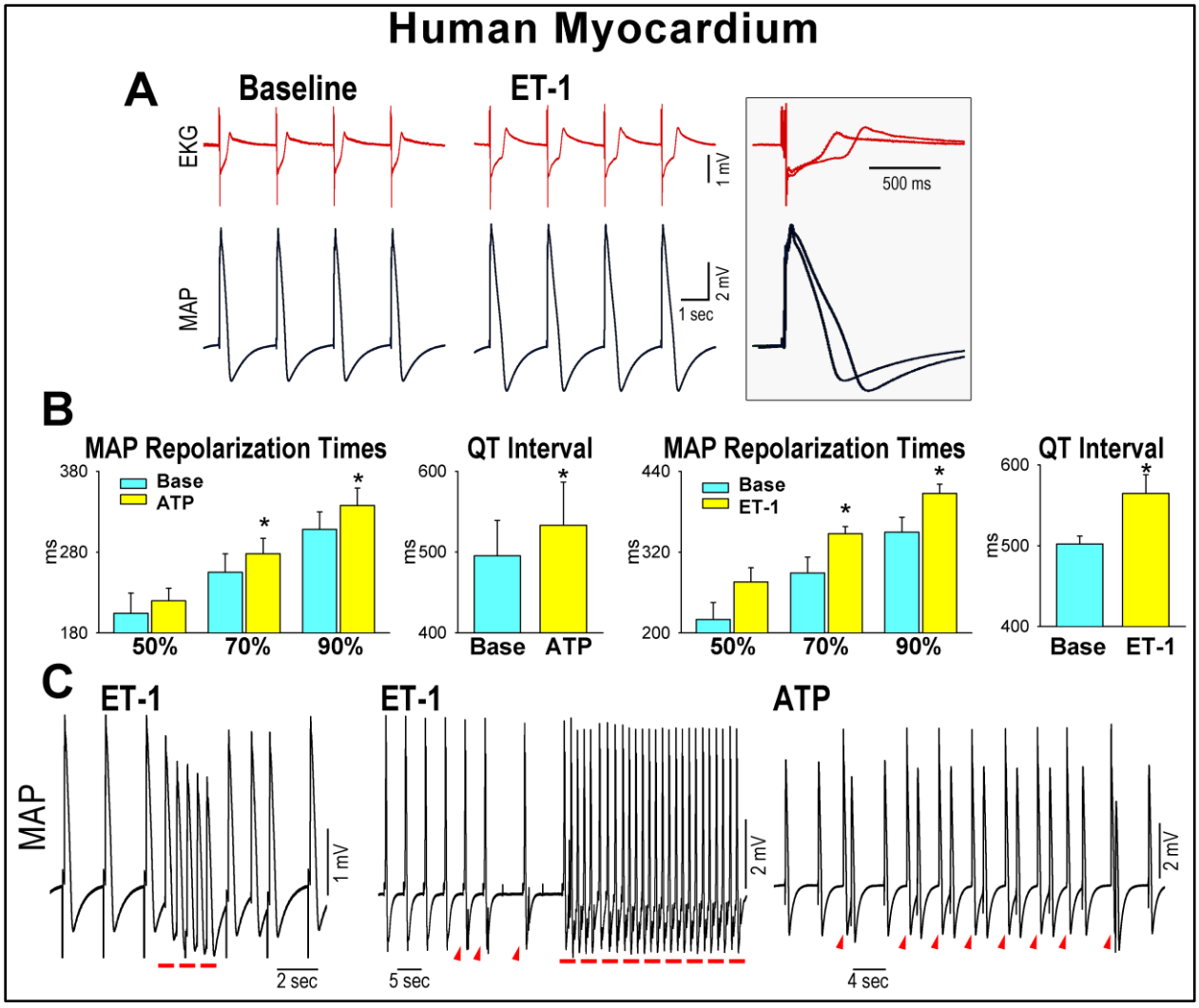

Figure 16. IP3Rs and electrical properties of human myocardium. A, ET-1 prolongs the electrical activation (pseudo-ECG, red-traces) and the AP (black-traces) of paced human myocardium. **B,** Quantitative data are shown as mean±SEM. Base: Krebs-Henseleit buffer. **P*<0.05 versus Base. **C,** Premature-ventricular-contractions (PVCs; red-arrowheads) and triggered-activity (red-dashed-lines) in human myocardium with ET-1 and ATP (20 μmol/L).

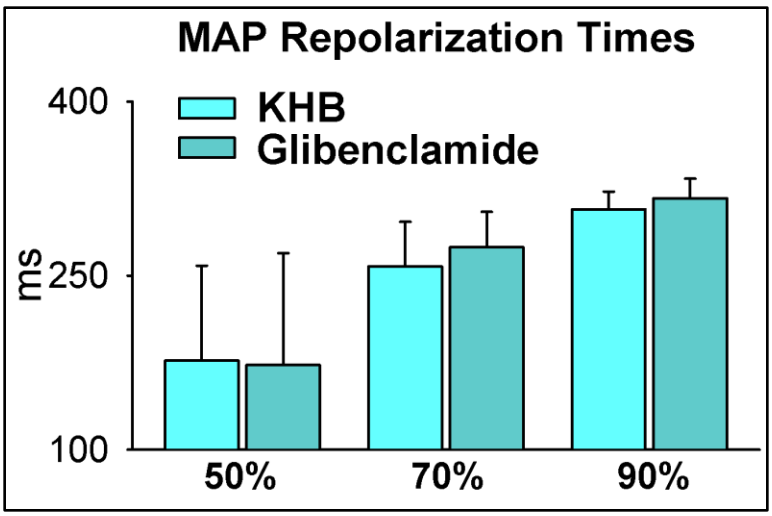

Figure 17. Monophasic action potentials and I_{KATP} activation. Quantitative data for human LV tissue perfused in a Langendorff system indicate the minimal effects of the I_{KATP} blocker glibenclamide (10 μmol/L) on repolarization time. Data are shown as mean±SEM. Base: Krebs-Henseleit buffer.

GPCR Simulation in the Failing Human Heart

Contractile reserve is severely reduced in heart failure (HF), and the GPCR/IP3R axis may represent an important signaling pathway modulating the inotropic state of the diseased myocardium. Thus, explanted failing hearts were studied (Table 1). By Western blotting, IP3R-2 expression was significantly increased in failing LV myocytes (Figure 18A). Importantly, stimulation of GPCRs with ATP in failing LV myocytes led to a reduction in RMP and prolongation of the AP (Figure 18B). Similarly, measurements of cell shortening in one failing LV cardiomyocyte revealed that this GPCR/IP3R activation increased contractility, elicited premature contraction and altered relaxation (Figure 18C).

The effects of GPCR stimulation on the myocardium were evaluated in an isometric system. In comparison with donor human hearts, the inotropic response of LV trabeculae to the β-adrenergic agonist isoproterenol was significantly attenuated in failing hearts (Figure 19A). In contrast, GPCR stimulation promoted an increase in developed tension in the diseased myocardium mimicking the findings obtained in healthy hearts (Figure 14 and Figure 19B). Thus, the inotropic reserve is decreased in the failing heart muscle, while the GPCR/IP3R axis remains operative.

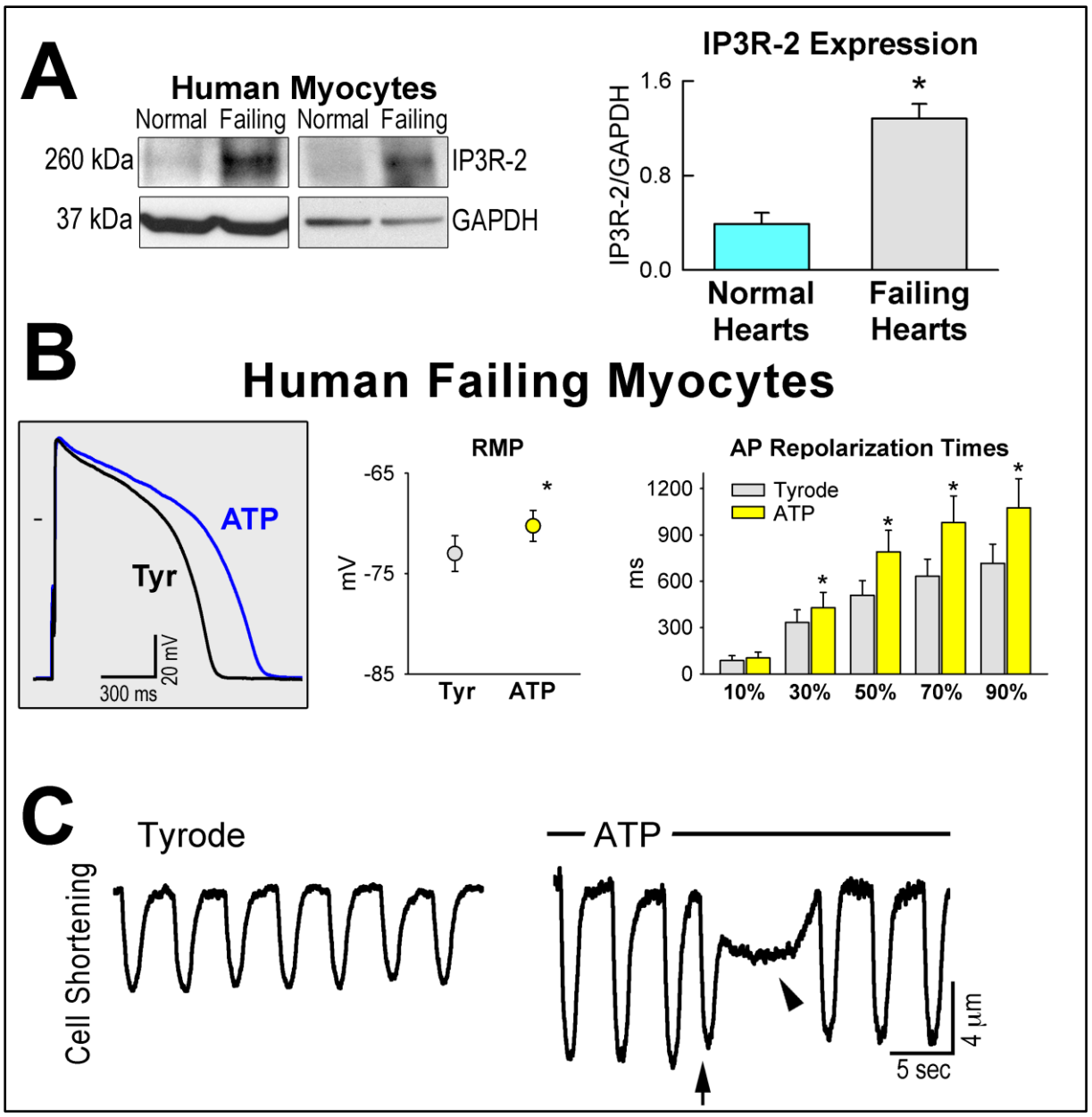

Figure 18. IP3Rs and GPCR activation in the failing human myocardium. A, Expression of IP3R-2 protein by Western blotting in normal and failing human LV myocytes. GAPDH: loading condition. Quantitative data are shown as mean±SEM. **P*<0.05 versus Normal Hearts. **B,** APs of a failing human myocyte before (black-trace, Tyr) and after (blue trace) exposure to ATP. Quantitative data are shown as mean±SEM. Tyr: Tyrode; **P*<0.05 versus Tyr, using paired *t*-test. **C,** Cell shortening in a field stimulated human failing cardiomyocyte, before and following exposure to ATP. Arrow and arrowhead point to a premature contraction and altered relaxation, respectively.

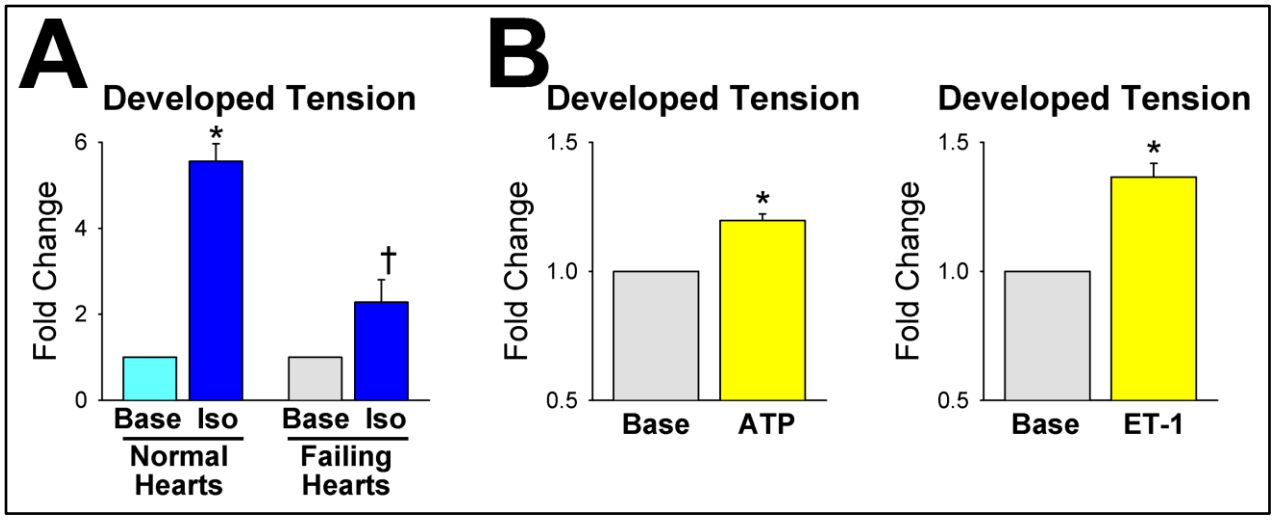

Figure 19. Contractile reserve of the failing human myocardium. A and **B,** Quantitative data for isometrically twitching human LV trabeculae. Data are shown as mean±SEM. Iso: isoproterenol (100 nmol/L); Base: baseline in the presence of Krebs-Henseleit buffer. **P*<0.05 versus Base, †*P*<0.05 versus Normal Heart in the presence of Iso.

IP3Rs and Mouse Cardiomyocytes

To define the role of IP3Rs in myocyte contractility following GPCR activation, a loss of function assay was introduced in LV mouse cardiomyocytes. Initial studies were performed to demonstrate that GPCRs agonists induce in mouse cardiomyocytes responses similar to those seen in human cells. ATP, ET-1, angiotensin II or phenylephrine stimulation led to an increase in Ca^{2+} transient amplitude and myocyte contractility. Diastolic Ca^{2+} was also elevated. Extra-systolic Ca^{2+} and sustained Ca^{2+} increases were apparent, resulting in after-contractions and prolonged contractures, respectively (Figure 20). Increased IP3R affinity by thimerosal led to comparable results. In contrast, IP3R blockade (XeC) or inhibition of IP3 synthesis (U-73122) abolished the effects of GPCR stimulation (Figure 20D-20F).

By employing two-photon microscopy working in line-scan mode, it was possible to demonstrate that extra-systolic Ca^{2+} and sustained increases in peak Ca^{2+} were distributed synchronously in the myocyte cytoplasm; this pattern of Ca^{2+} changes excludes that local releases of Ca^{2+} from the SR, or Ca^{2+} waves were involved in the process (Figure 21).

ATP and ET-1 may stimulate other effector pathways involving phosholipase-C (PLC), which activates PKC isoforms, resulting in the phosphorylation of ion channels and contractile proteins (Steinberg et al.1995; Braz et al. 2004; Mohácsi et al. 2004). To establish whether this

mechanism was implicated in myocyte performance, studies in mouse LV myocytes were conducted in the presence of the PKC inhibitor chelerythrine (Dobson et al. 2008). Chelerythrine failed to abrogate the inotropic response triggered by ATP and ET-1 (Figure 22) suggesting that PKC-independent pathways play a critical role in mediating the impact of GPCR stimulation in myocytes.

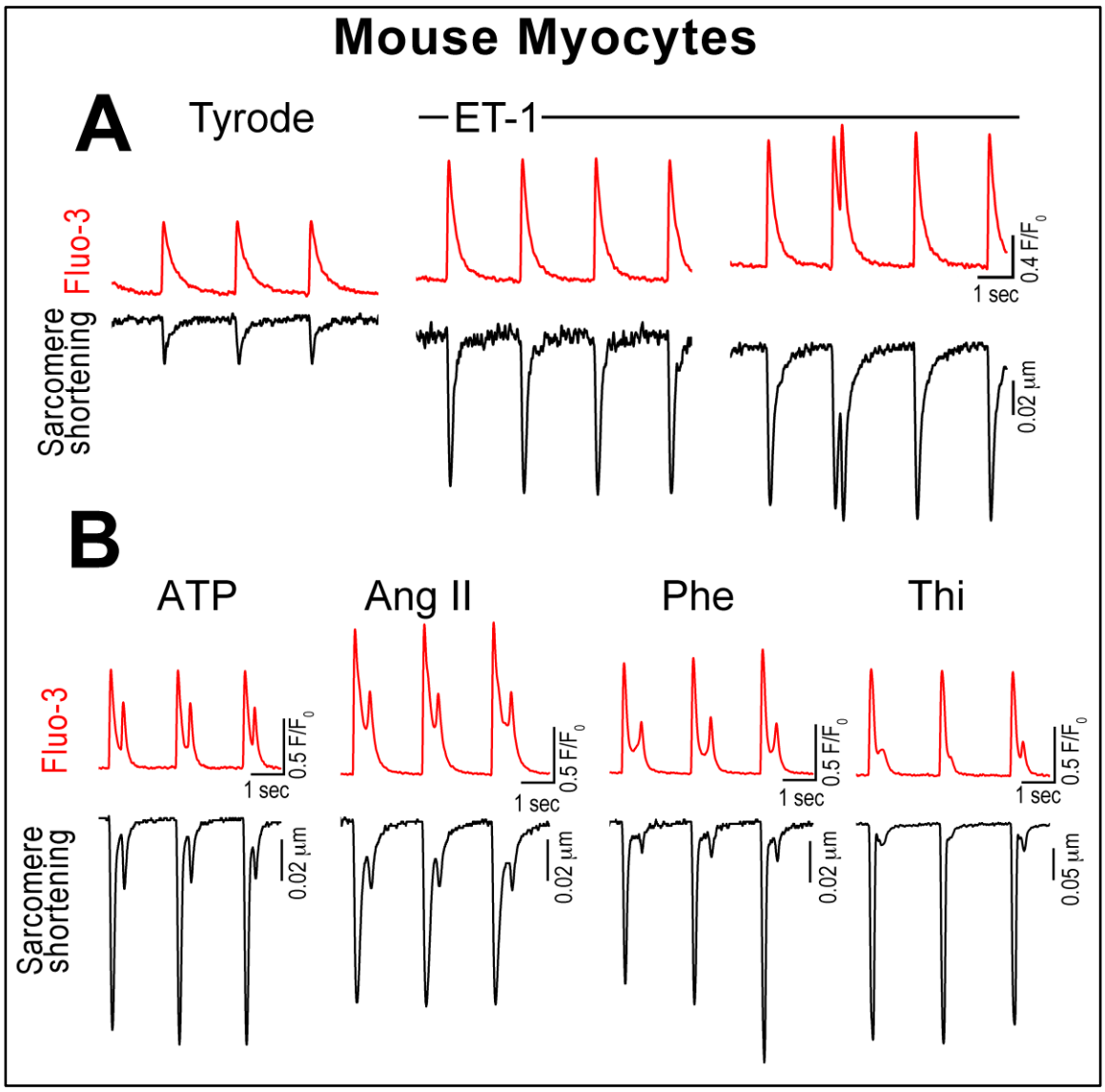

Figure 20. IP3Rs, Ca^{2+} transients and contractility in mouse myocytes. A, Ca^{2+} transients (red-traces), sarcomere shortening (black-traces), extra-systolic Ca^{2+} elevations and after-contraction in a field stimulated myocyte in the presence of ET-1. **B,** Effects of ATP (10 μmol/L), angiotensin II (Ang II, 50 nmol/L), phenylephrine (Phe, 10 μmol/L), and thimerosal (Thi, 10 μmol/L) on extra-systolic Ca^{2+} elevations (red-traces) and after-contractions (black-traces) in myocytes.

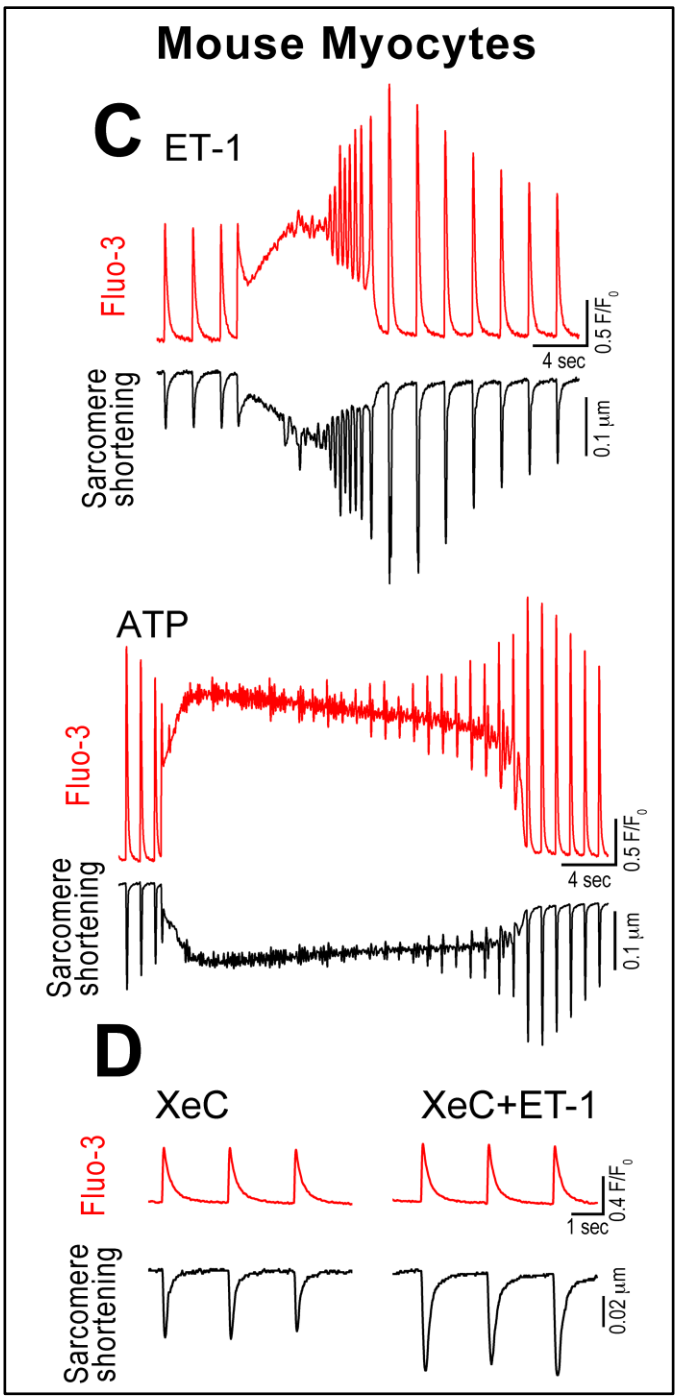

Figure 20. IP3Rs, Ca^{2+} transients and contractility in mouse myocytes (continued). C, ET-1 and ATP induce spontaneous sustained Ca^{2+} elevations and contracture in myocytes. **D,** IP3R blockade with xestospongin-C (XeC, 2 μmol/L) prevents largely the effects of ET-1 on Ca^{2+} transients (red-traces) and myocyte contractility (black-traces).

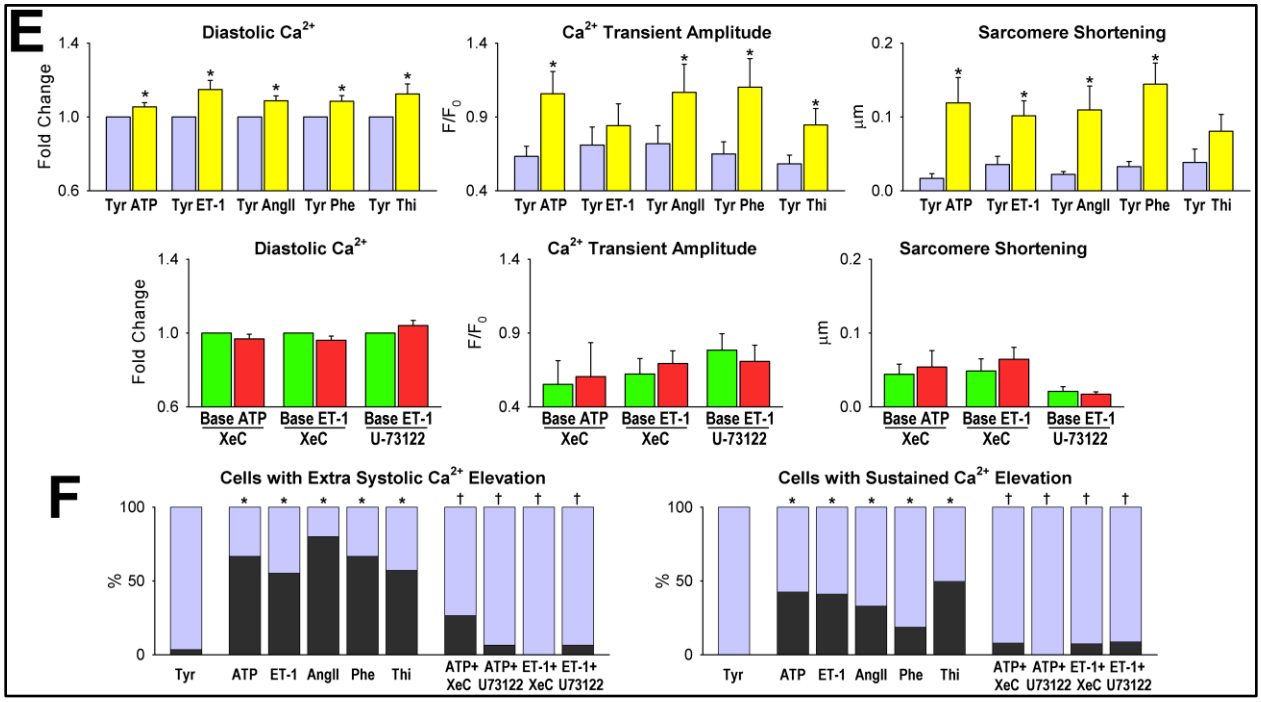

Figure 20. IP3Rs, Ca^{2+} transients and contractility in mouse myocytes (continued). E, Quantitative data are shown as mean±SEM **P*<0.05 versus Tyr. Tyr: Tyrode; Base: baseline prior to IP3R stimulation. **F,** Fraction of myocytes with extra-systolic and sustained Ca^{2+} elevations (black portion of the bars). **P*<0.05 vs. Tyr, †*P*<0.05 versus ATP or ET-1.

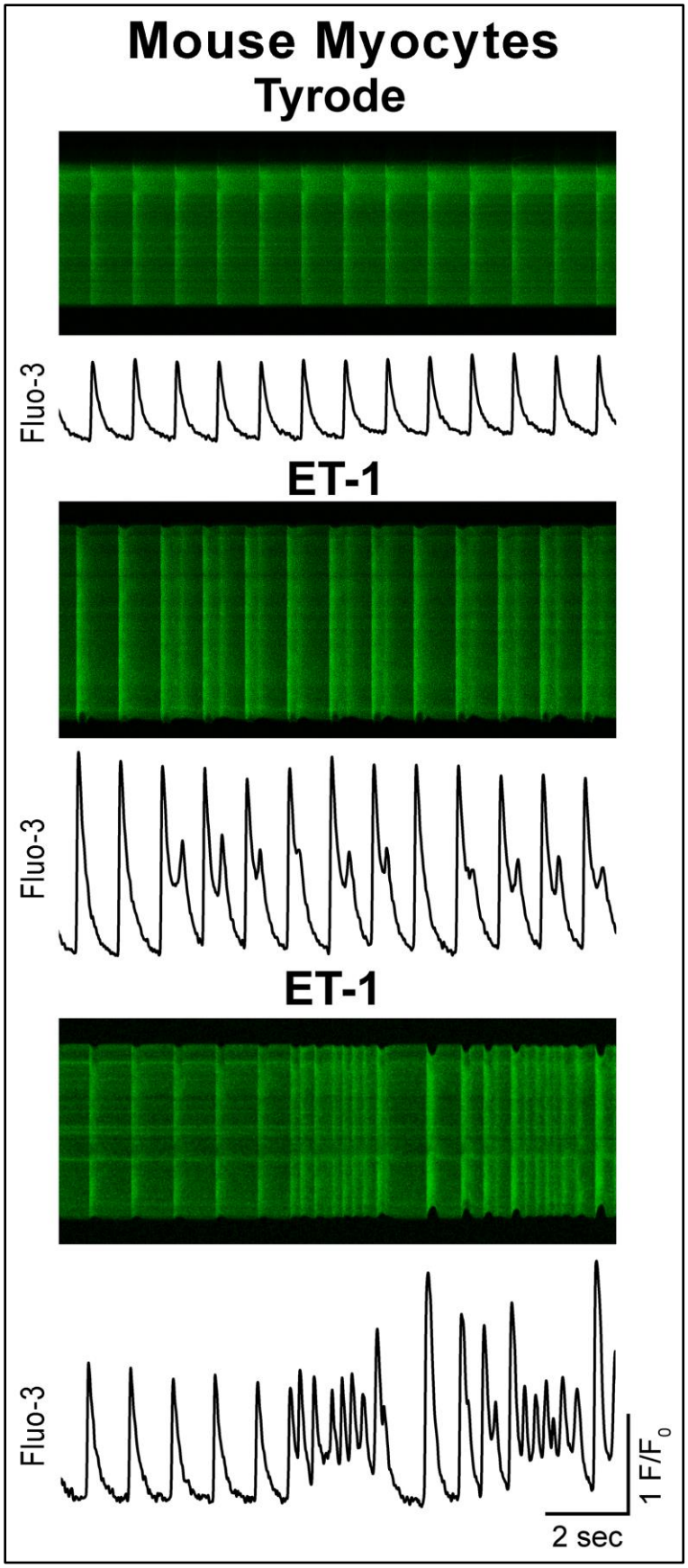

Figure 21. Ca^{2+} changes in mouse myocytes. Normal Ca^{2+} transients (upper), extra-systolic (center), and sustained Ca^{2+} elevations (lower) are distributed uniformly throughout the length of stimulated myocytes. Line scan images were acquired by two-photon microscopy in myocytes loaded with Fluo-3 (green). Traces from the line-scan mode are shown below each image.

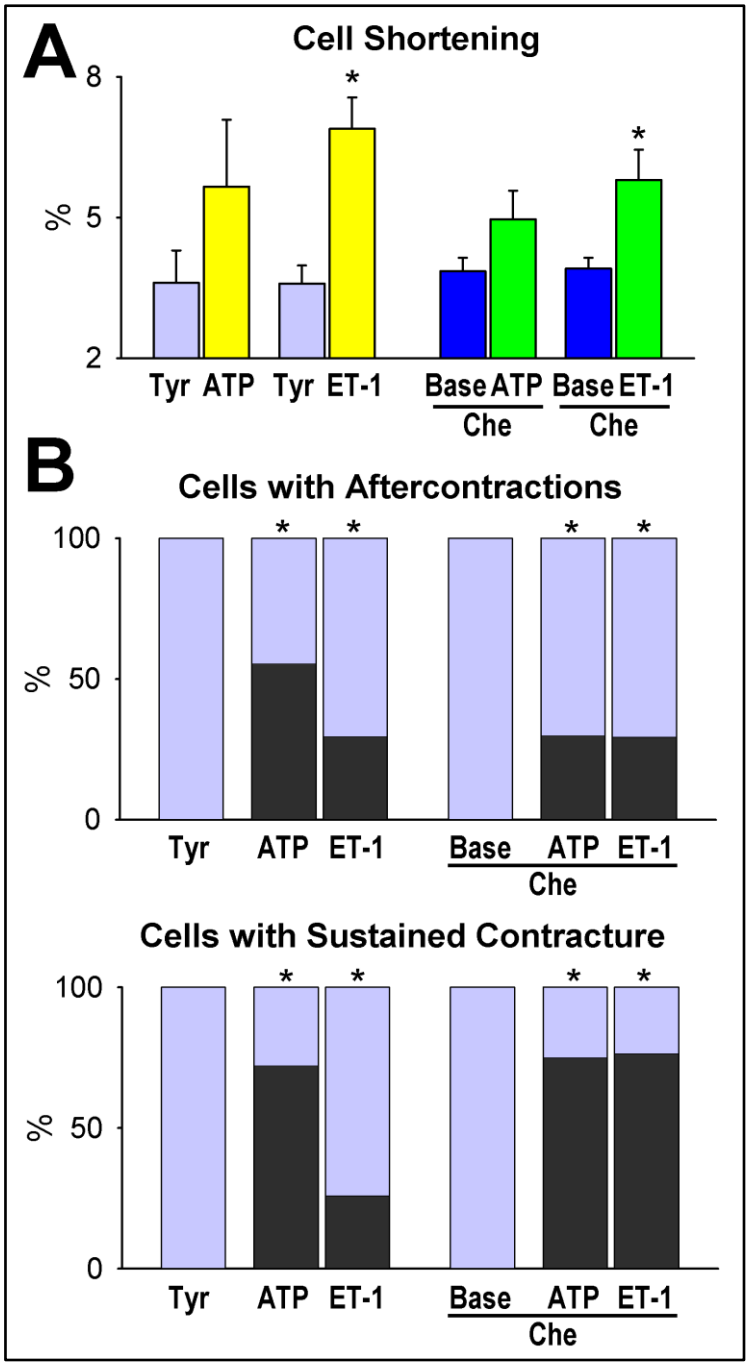

Figure 22. Inhibition of PKC does not abrogate the effects of GPCR activation on mouse myocytes. A, Quantitative data are shown as mean±SEM **P*<0.05 versus Tyr or Base. Tyr: Tyrode; Base: baseline prior to IP3R stimulation; Che, chelerythrine (2 *μ*mol/L). **B,** Fraction of myocytes with after-contractions and sustained contractures (black portion of the bars). **P*<0.05 versus Tyr or Base.

Based on this information, which strengthened the human results, the consequences of downregulation of IP3R type-2 on Ca^{2+} cycling in myocytes was tested using a small hairpin-RNA (sh-RNA) assay. An adeno-associated AAV9 vector carrying EGFP and sh-RNA targeting IP3R type-2 (shRNA-IP3R2-EGFP) was injected intravenously in mice (Figure 23). Three weeks later, EGFP-positive and EGFP-negative LV myocytes were isolated (Figure 24) and loaded with the Ca^{2+} indicator Rhod-2. Ca^{2+} transient was measured in field stimulated cells, in the absence and presence of ATP or ET-1. GPCRs activation failed to increase Ca^{2+} transients in EGFP-positive mouse myocytes. Similarly, extra-systolic and sustained Ca^{2+} elevations were not detected. Conversely, these responses were preserved in EGFP-negative cells (Figure 26).

Electrophysiologically, the effects of GPCR stimulation in mouse myocytes were similar to those observed in human cells. Activation of GPCR function with ATP or ET-1, or enhanced IP3R affinity by thimerosal decreased RMP, prolonged the AP, and increased the frequency of EADs in mouse myocytes. Ca^{2+} transient amplitude increased, and extra-systolic Ca^{2+} elevations were apparent (Figure 26). Similarly, spontaneous sustained depolarization to the plateau and long-lasting $[Ca^{2+}]_i$ increases were detected (Figure 27). Importantly, direct activation of IP3Rs by dialysis with IP3 in the myocyte cytoplasm had effects comparable to those seen with GPCR agonists or thimerosal (Figure 28). IP3R blockade, in the absence of GPCR agonists, did not alter the AP, Ca^{2+} transients and myocyte contractility (Figure 29). Conversely, IP3R inhibition reversed the effects of ET-1 and ATP on cardiomyocytes (Figure 30).

Electrical abnormalities similar to those observed in isolated myocytes were detected in the perfused mouse heart under conditions favoring IP3R function; the arrhythmic events triggered by regular pacing and programmed electrical stimulation were markedly enhanced (Figure 31).

Thus, IP3Rs mediate partly the effects of GPCR stimulation on Ca^{2+} cycling and the electrical and mechanical properties of adult human and mouse cardiomyocytes.

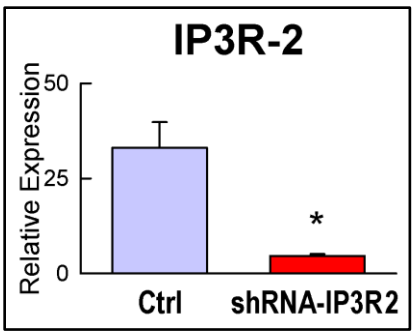

Figure 23. Downregulation of IP3Rs. Transcripts for IP3R type-2 are downregulated in the LV myocardium of mice injected with an adeno-associated AAV9 vector carrying EGFP and small hairpin-RNA targeting IP3R type-2 (shRNA-IP3R2).

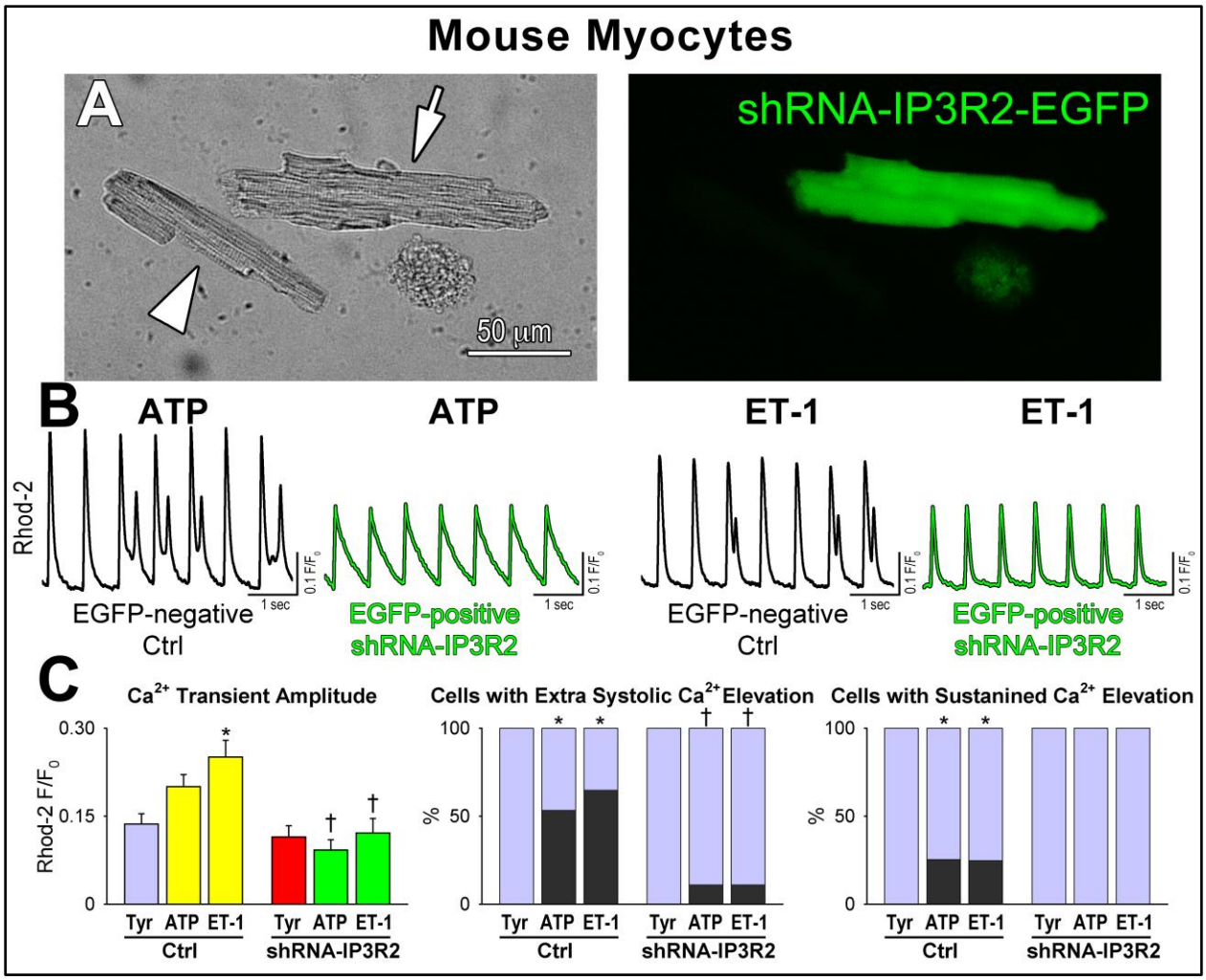

Figure 24. Downregulation of IP3Rs, Ca^{2+} transients, and extra-systolic Ca^{2+} elevations. A, Left panel: EGFP-negative myocyte (arrowheads) and EGFP-positive myocyte (arrows); the EGFP-positive myocyte is shown again by native EGFP fluorescence in the right panel. These myocytes were collected from a mouse heart treated with AAV9 vector carrying EGFP and shRNA targeting IP3R-2. **B,** Ca^{2+} transients in EGFP-negative (black-traces) and EGFP-positive myocytes (green-traces) in the presence of ATP and ET-1. **C,** Fraction of myocytes with extra-systolic and sustained Ca^{2+} elevation (black portion of the bars). Quantitative data are shown as mean±SEM. *P<0.05 versus Tyr. †P<0.05 versus EGFP-negative myocytes.

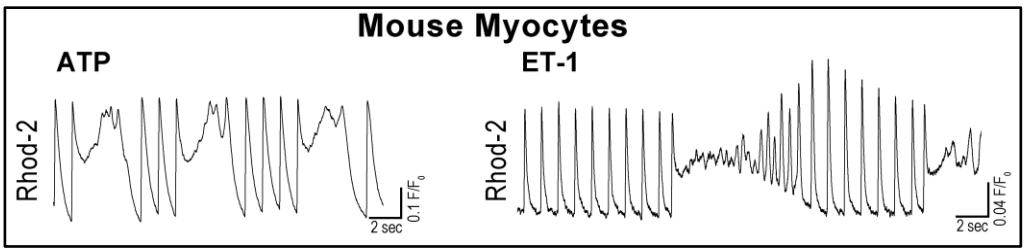

Figure 25. GPCR activation and Ca^{2+} transient in mouse myocytes. ATP and ET-1 induce sustained elevations of Ca^{2+} in EGFP-negative mouse myocytes with preserved expression of IP3R type 2. Cells were obtained from the LV myocardium of mice injected with an adeno-associated AAV9 vector carrying EGFP and small hairpin-RNA targeting IP3R type-2 (shRNA-IP3R2); myocytes were loaded with the Ca^{2+} sensitive dye Rhod-2.

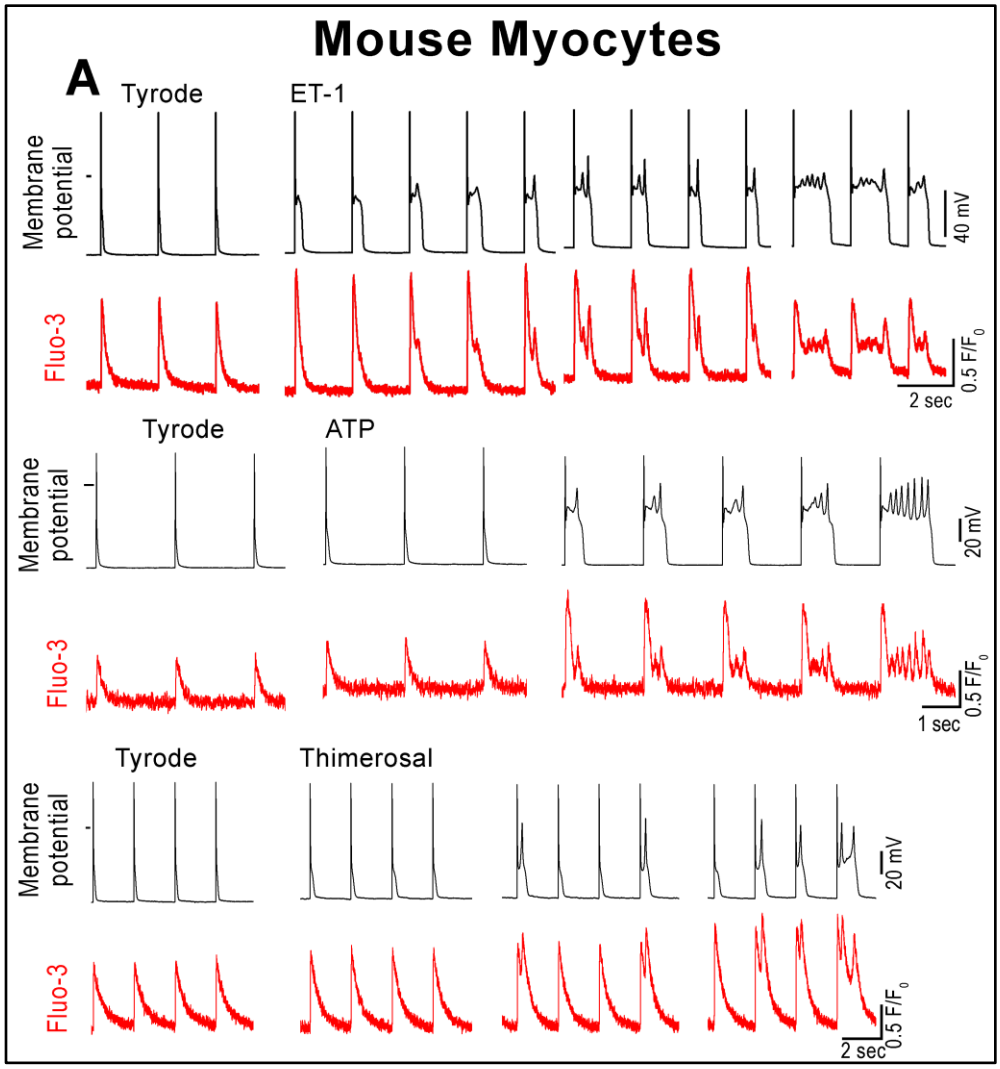

Figure 26. IP3R activation in mouse myocytes. A, Transmembrane potential (black-traces) and Ca^{2+} transients (red-traces) in current-clamped myocytes before and after exposure to ET-1 (upper traces), ATP (middle traces), and thimerosal (lower traces). IP3R stimulation results in prolongation of the AP and in EADs, which are coupled with increased Ca^{2+} transient and extra-systolic Ca^{2+} elevations.

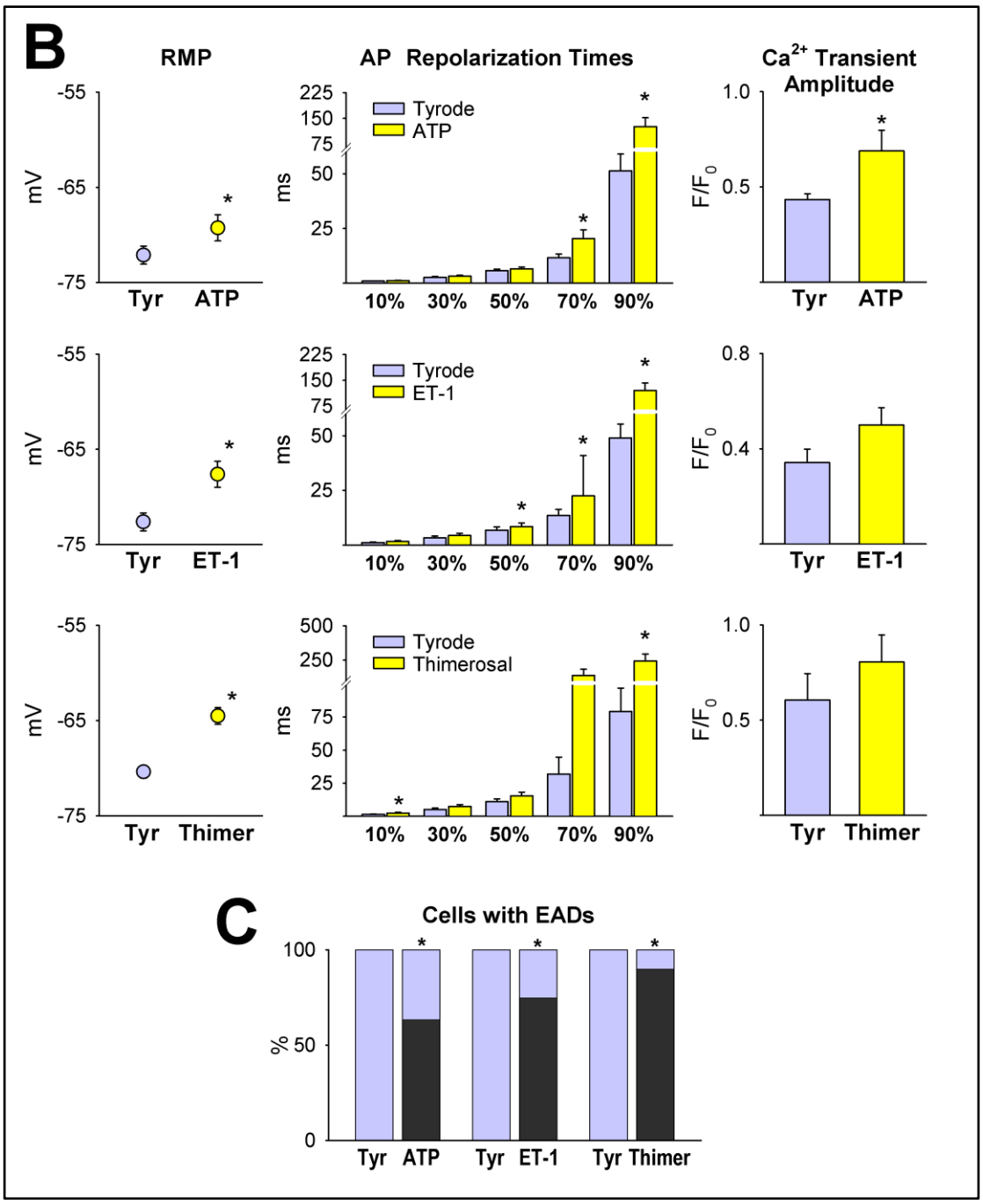

Figure 26. IP3R activation in mouse myocytes (continued). B, Quantitative data are shown as mean±SEM. **P*<0.05 versus Tyr. **C,** Fraction of myocytes with EADs (black portion of the bars). **P*<0.05 versus Tyr.

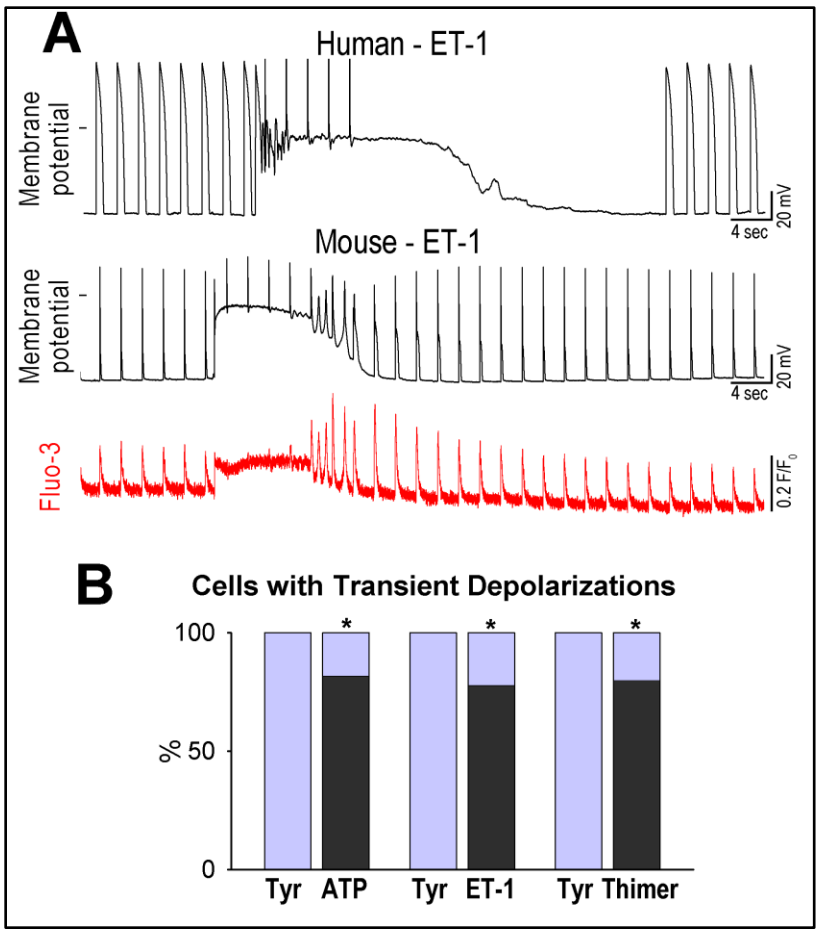

Figure 27. GPCR activation and myocyte function. A, Sustained membrane depolarization of the AP in human (upper black-trace) and mouse (lower black-trace) cardiomyocytes with ET-1 is associated with intracellular Ca^{2+} elevations (lower red trace). **B,** Fraction of mouse myocytes with sustained depolarizations (black portion of the bars). **P*<0.05 versus Tyr.

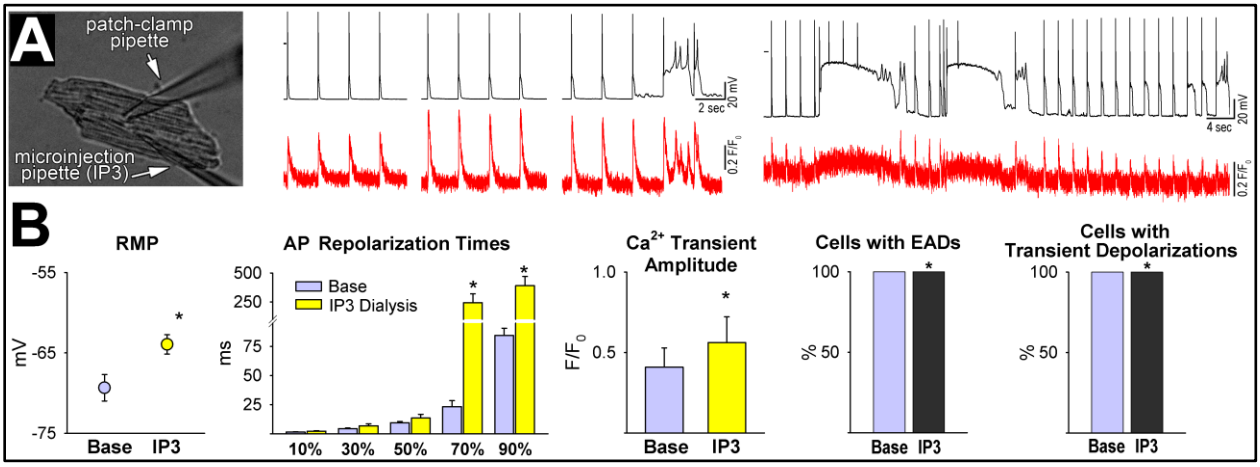

Figure 28. Downregulation of IP3Rs, Ca^{2+} transients, and extra-systolic Ca^{2+} elevations. A, Electrical (black-traces) and Ca^{2+} transient (red-traces) properties of myocytes dialyzed with IP3 (50 μmol/L, phase-contrast micrograph). **B,** Quantitative data are shown as mean±SEM. *P<0.05 versus Base, using paired *t*-test.

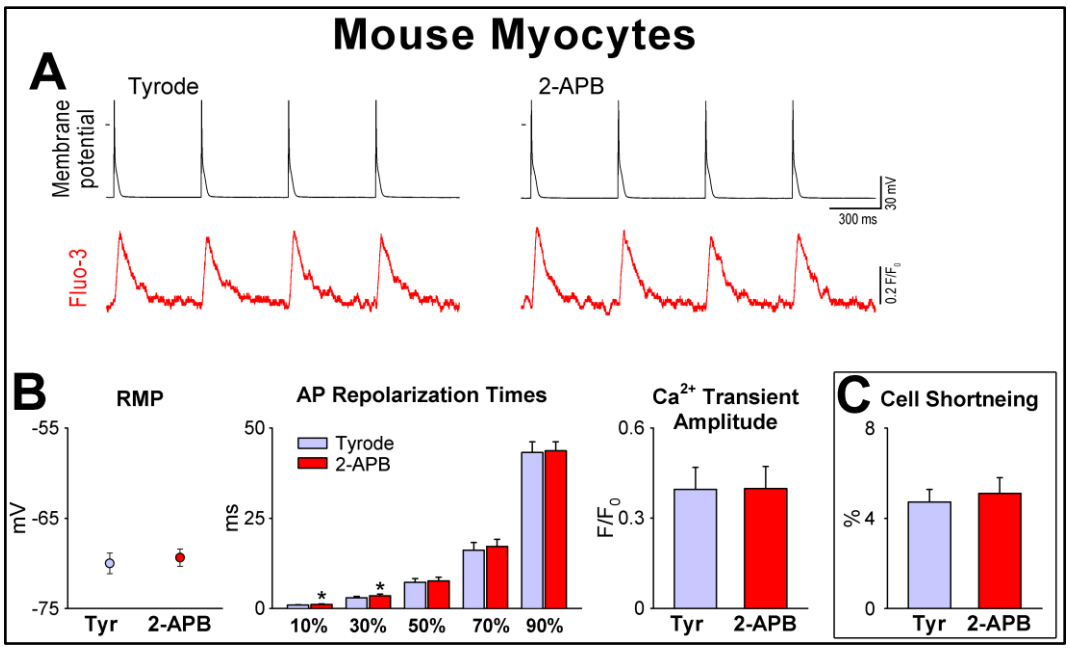

Figure 29. IP3R blockade in mouse myocytes. A, Electrical (black-traces) and Ca^{2+} transient (red-traces) properties of a mouse myocyte before and after blockade of IP3Rs with 2-APB (10 μmol/L). **B** and **C,** Quantitative data are shown as mean±SEM. **P*<0.05 versus Tyr.

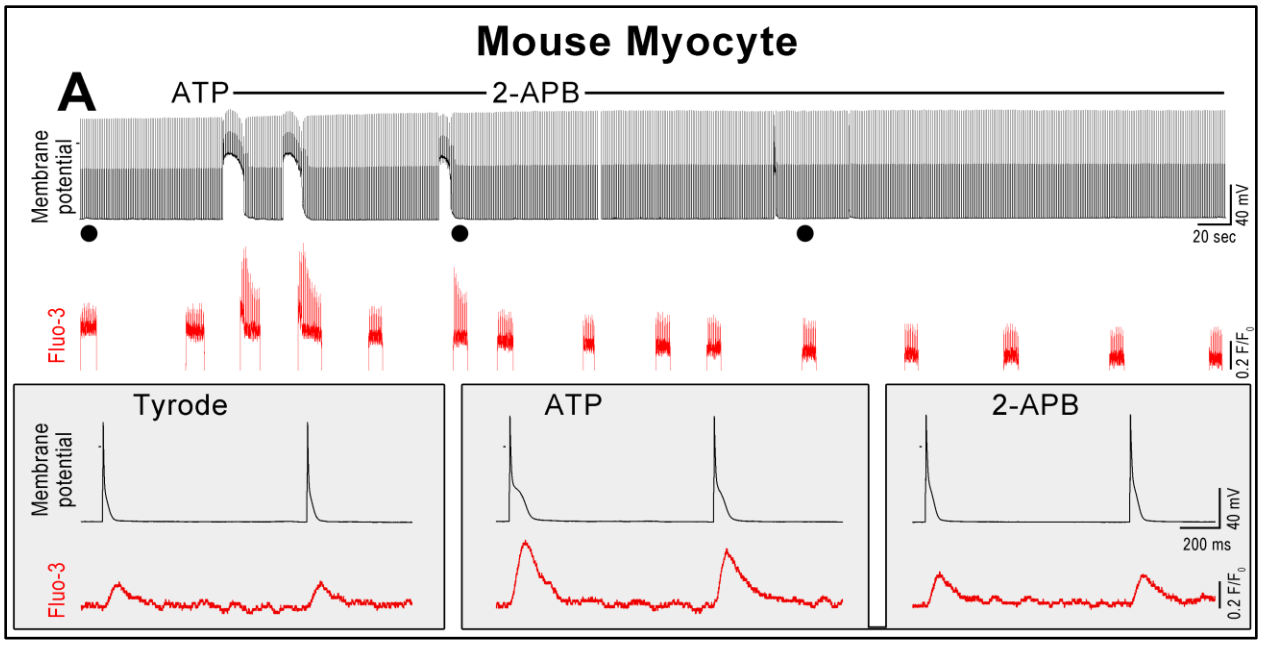

Figure 30. Effects of activation and blockade of IP3Rs on mouse myocytes. A, Transmembrane potential (black-traces) and Ca^{2+} transients (red-traces) in a mouse myocyte exposed to ATP and then to the IP3R blocker 2-APB. Prolonged APs and sustained depolarizations coupled with the increase in Ca^{2+} transient amplitude are induced by ATP and are reversed by 2-APB. Circles indicate portions of the traces shown at higher time resolution in the inset.

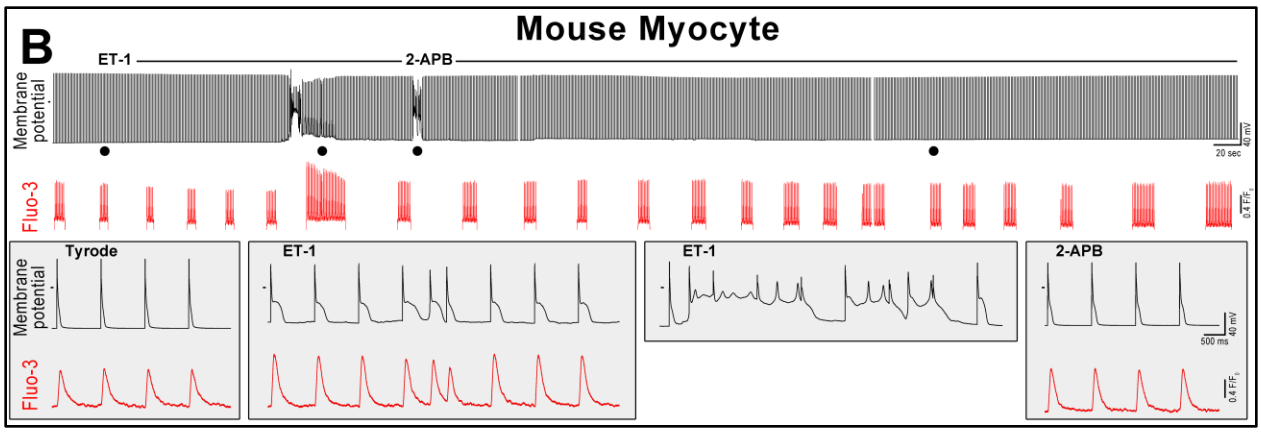

Figure 30. Effects of activation and blockade of IP3Rs on mouse myocytes (continued). B, Transmembrane potential (black-traces) and Ca^{2+} transients (red-traces) in a mouse myocyte exposed to ET-1 and then to the IP3R blocker 2-APB. ET-1 prolonged the AP, and induced spontaneous depolarization and EADs coupled with increased Ca^{2+} transient amplitude; these effects were reversed by 2-APB. Circles indicate portions of the traces shown at higher time resolution in the inset.

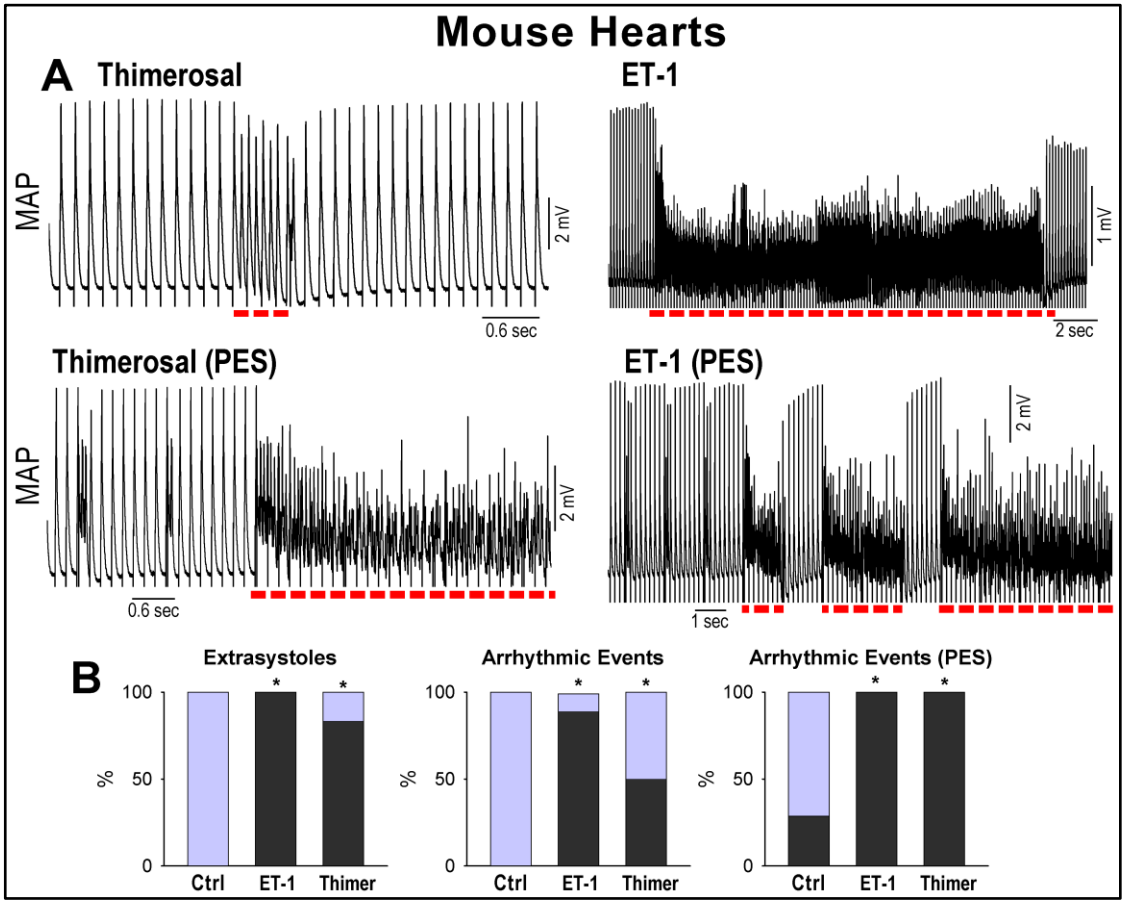

Figure 31. IP3Rs alter the electrical activity of the mouse heart. A, IP3R activation and arrhythmia (red-dashed-lines) of the mouse heart with pacing (upper-traces), or programmed electrical stimulation (PES; lower-traces). **B,** Fraction of mouse hearts showing arrhythmic episodes (black portion of the bars). Ctrl: Krebs-Henseleit buffer. **P*<0.05 versus Ctrl.

GPCR stimulation and Ca^{2+} Release from RyRs

The increase in Ca^{2+} transient amplitude and extra-systolic Ca^{2+} elevations induced by GPCR agonists in myocytes may result from the prolongation of the AP and altered repolarization phase. Alternatively, Ca^{2+} mobilized by IP3Rs may sensitize RyRs, enhancing excitation contraction-coupling gain and promoting spontaneous Ca^{2+} releases, which, in turn, may affect myocyte electrical properties (Harzheim et al. 2009).

To establish the role of the AP profile on the properties of Ca^{2+} transients following GPCR stimulation, AP-clamp studies were performed (Sah et al. 2001, Rota et al. 2007). AP waveforms were recorded in Tyrode solution (Ctrl-APs) or with GPCR agonists (GPCR-APs). Subsequently, these AP waveforms were employed as voltage-clamp commands, while monitoring intracellular Ca^{2+} in myocytes loaded with the Ca^{2+} indicator Fluo-3. Despite GPCR stimulation, Ctrl-APs were characterized by physiological Ca^{2+} transients with no extra-systolic Ca^{2+} elevations (n=23/23) (Figure 32-33). Conversely, GPCR-APs showed increased Ca^{2+} transients in the presence (n=27/27) or absence (n=8/8) of GPCR agonists (Figure 32-34). These experiments under voltage-clamp indicate that the alterations in Ca^{2+} transients observed following GPCR stimulation are secondary to changes in AP profile.

To test whether RyRs were sensitized by GPCR activation, Fluo-3 loaded myocytes were exposed to a family of depolarizing steps in voltage-clamp mode to progressively activate L-type Ca^{2+} current (I_{CaL}) and release of Ca^{2+} from RyRs (Gomez et al. 2001, Pott et al. 2005, Rota et al. 2007). I_{CaL}, Ca^{2+} transient amplitude, and the ability of Ca^{2+} influx to induce RyR-Ca^{2+} release (excitation contraction-coupling gain) did not change with activation of GPCRs (Figure 35).

These results tend to exclude the possibility that the release of Ca^{2+} following activation of IP3Rs enhances the sensitivity of RyRs.

To establish whether RyRs contribute to the changes in the electrical properties of myocytes after GPCR stimulation, these Ca^{2+} channels were blocked by ryanodine (Nett & Vassalle, 2003; Ferreira-Martins et al. 2009) and the effects of ATP were studied. Under this condition, Ca^{2+} transients and myocyte shortening were inhibited (Figure 36); however, RMP decreased, the AP was prolonged, and arrhythmic events occurred (Figure 37).

These findings suggest that RyRs are not implicated in the electrical instability of cardiomyocytes mediate by GCPR activation.

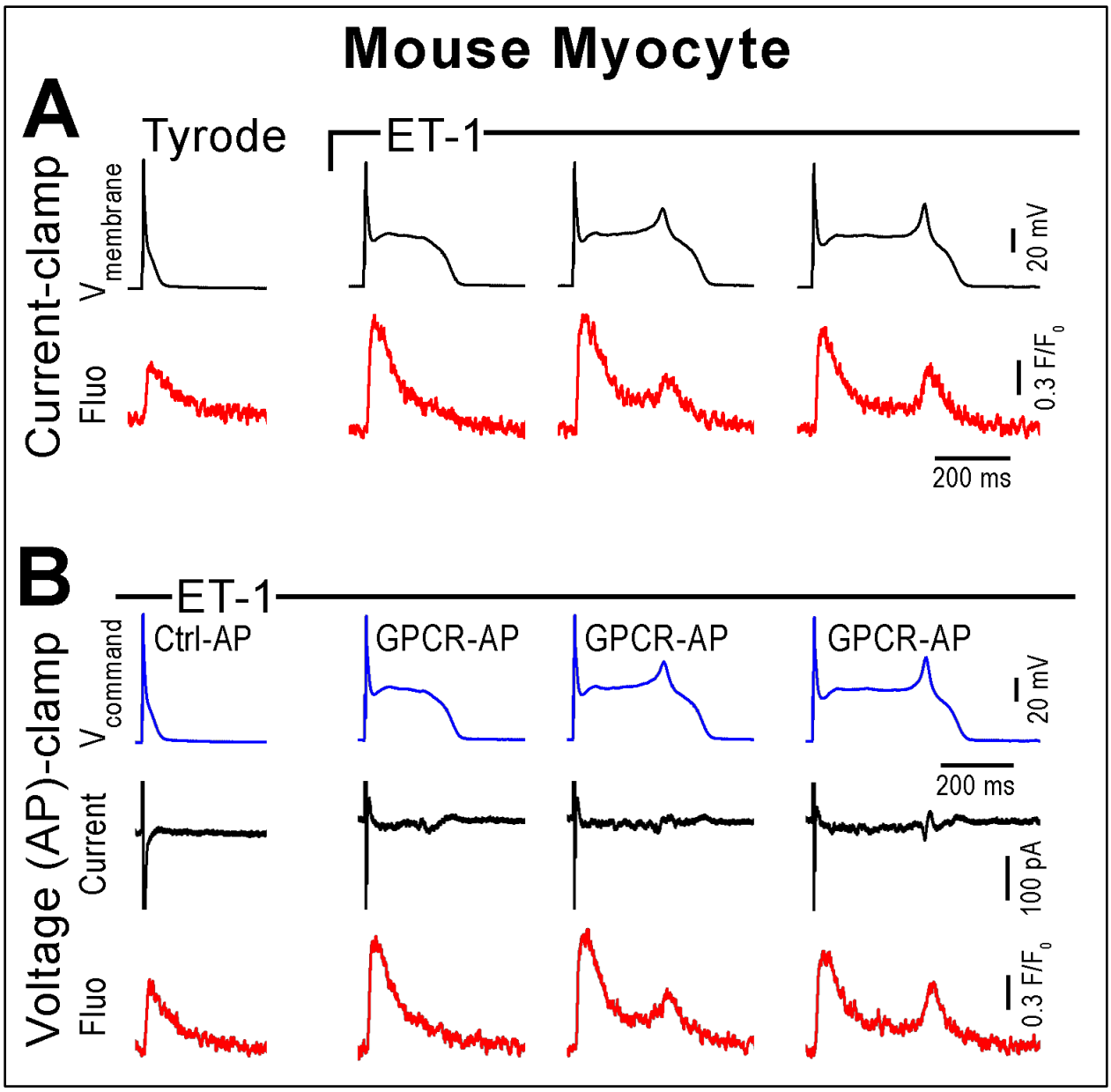

Figure 32. The profile of the AP conditions the effects of GPCR activation on Ca^{2+} transients, and IP3R activation does not alter ryanodine receptor function. A and **B,** APs ($V_{membrane}$: membrane potential, black-traces) and Ca^{2+} transients (Fluo-3, red-traces) in a mouse cardiomyocyte exposed to ET-1. APs with variable profiles were recorded in current-clamp mode (**A**) before (Ctrl-AP) and after activation of GPCRs (GPCR-AP) and used as voltage-clamp commands ($V_{command}$, blue-traces) (**B**); Ca^{2+} transients (red-traces) and membrane currents (black-traces) are shown.

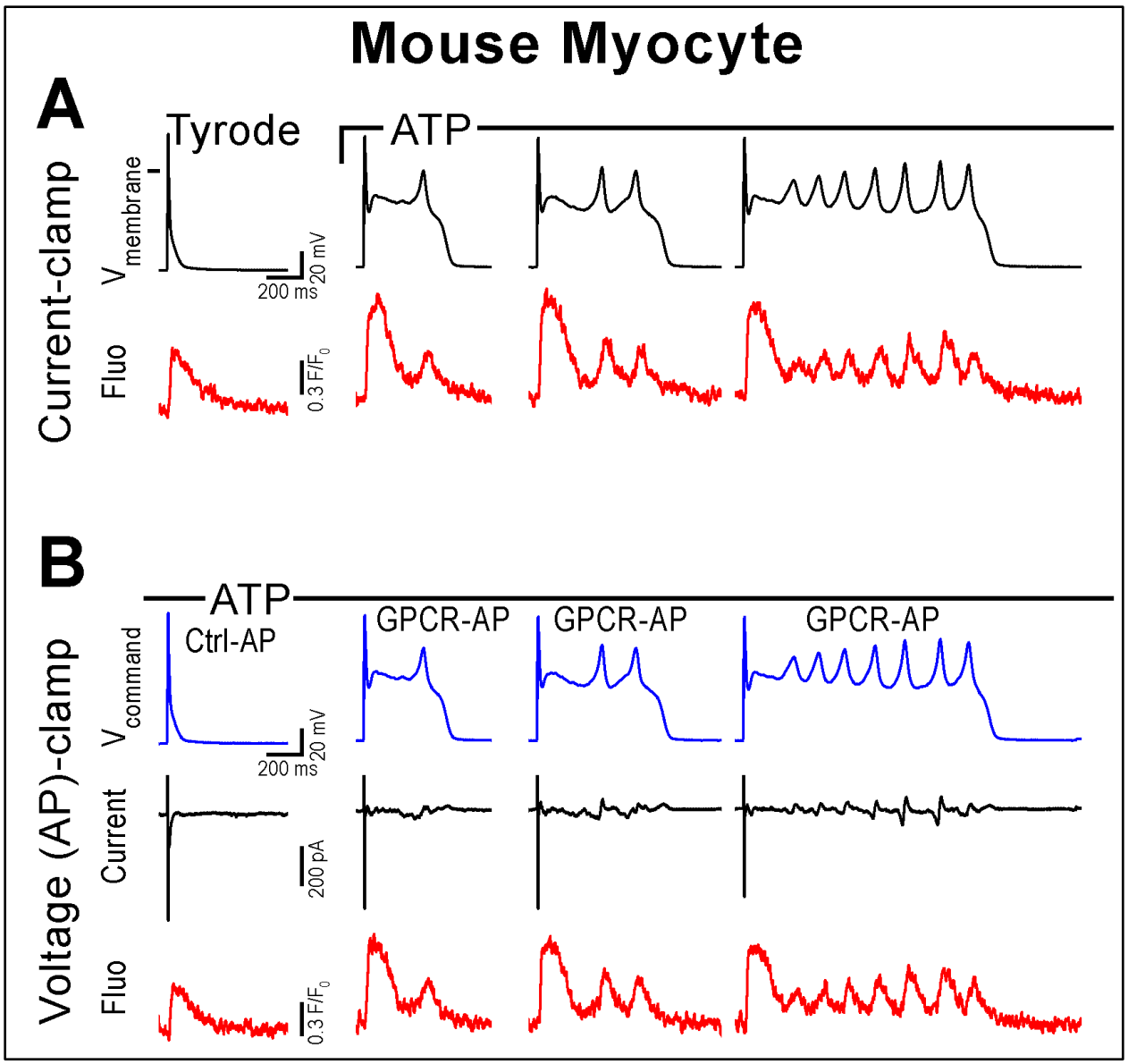

Figure 33. The profile of the AP conditions the effects of GPCR activation on Ca^{2+} transients. A and **B,** APs ($V_{membrane}$: membrane potential, black-traces) and Ca^{2+} transients (Fluo-3, red-traces) in a mouse cardiomyocyte exposed to ATP. APs with variable profiles were recorded in current-clamp mode (**A**) before (Ctrl-AP) and after activation of GPCRs (GPCR-AP) and used as voltage-clamp commands ($V_{command}$, blue-traces) (**B**); Ca^{2+} transients (red-traces) and membrane currents (black-traces) are shown.

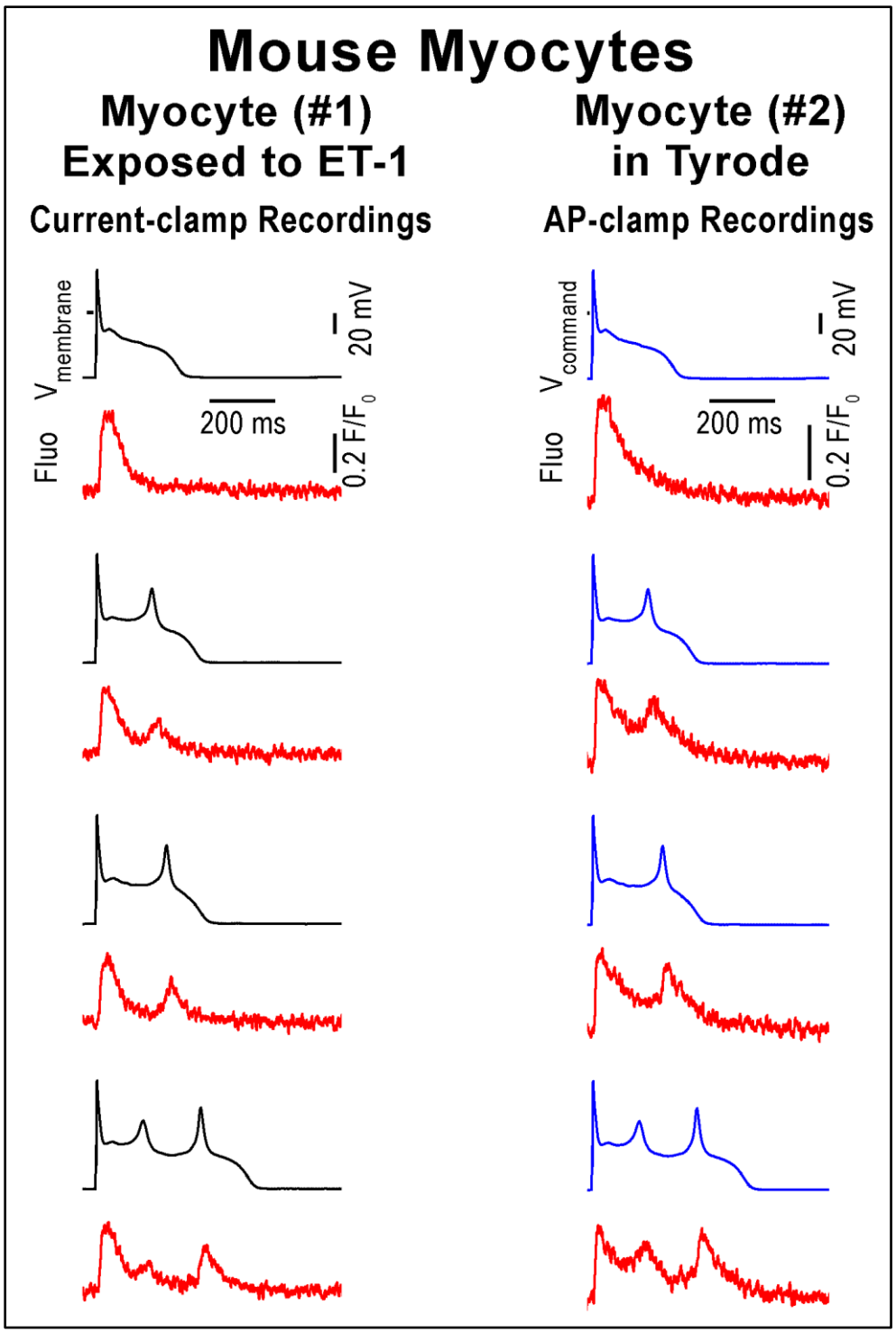

Figure 34. The profile of the AP conditions the effects of GPCR activation on Ca^{2+} transients. APs (black-traces) and Ca^{2+} transients (red-traces) in a myocyte exposed to ET-1 (left); the recorded APs were employed as IP3R-APs command (blue-traces) in a myocyte (right) kept in Tyrode solution.

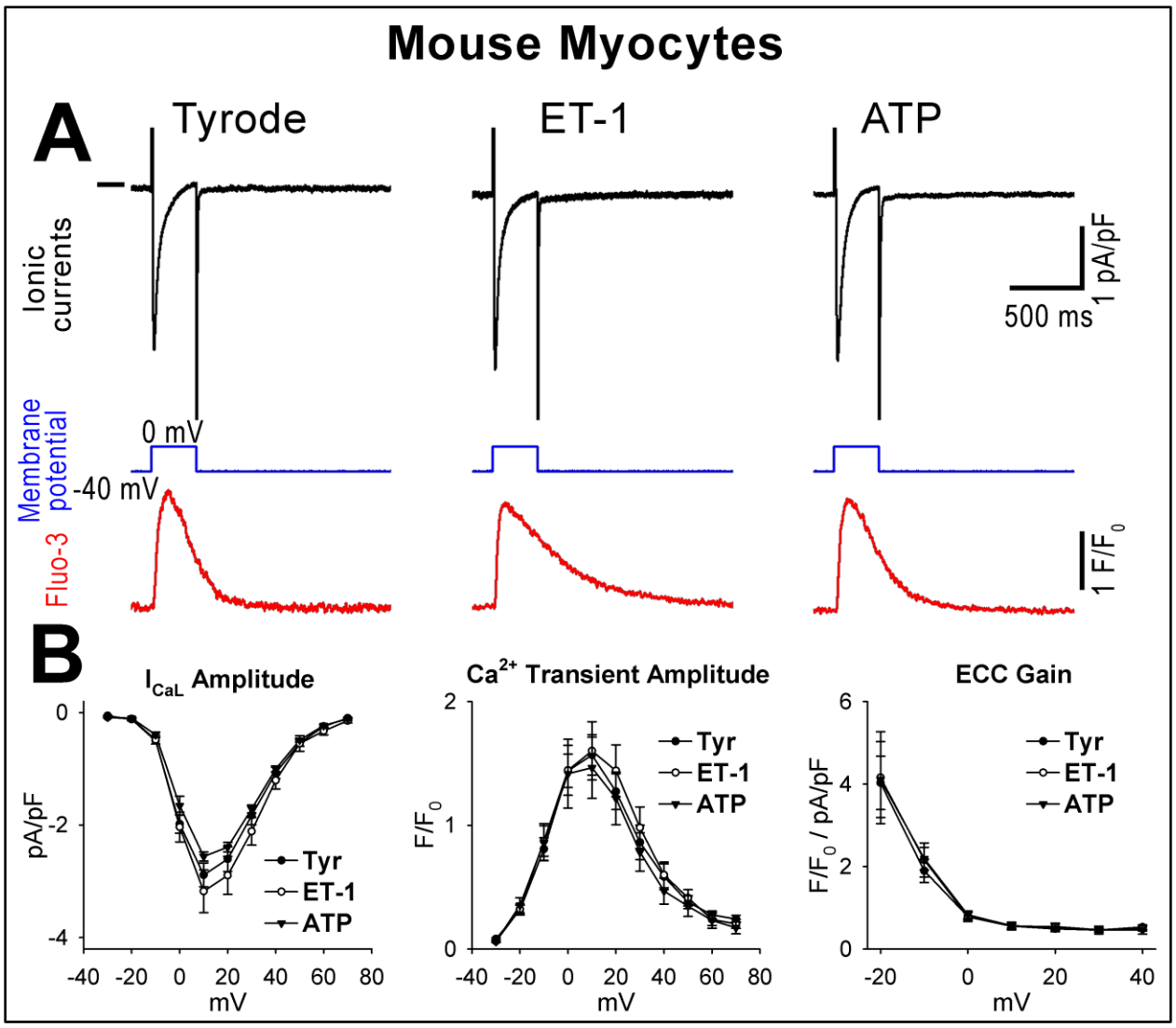

Figure 35. The effects of GPCR activation on Ca^{2+} transients, and IP3R activation does not alter ryanodine receptor function. **A,** I_{CaL} (black-traces) and Ca^{2+} transients (red-traces) elicited by depolarizing steps (blue-traces) by patch-clamp in the presence of ET-1 and ATP. **B,** Voltage relations for I_{CaL}, Ca^{2+} transient amplitude and ECC gain in Tyr and after IP3R stimulation.

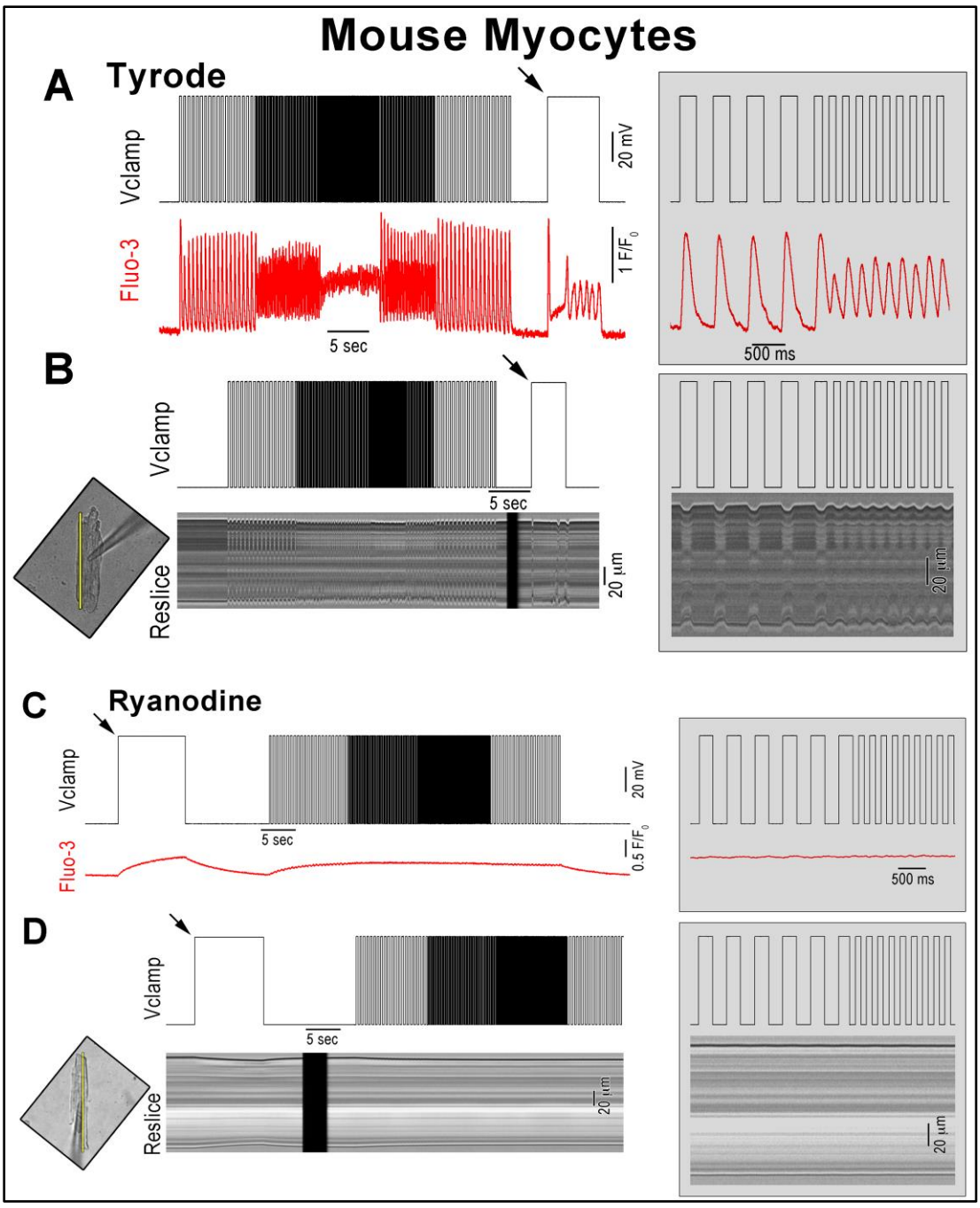

Figure 36. Effects of RyR blockade on Ca^{2+} cycling and contractility of mouse myocytes. **A** and **B**, Depolarizing steps in voltage-clamp mode (**A** and **B,** black traces) elicit Ca^{2+} transients (**A,** red traces) and cell shortening (**B,** reslice image) in a mouse myocyte in Tyrode solution. Long-lasting depolarizations to 0 mV (black traces, arrows) lead to Ca^{2+} elevations (**A**) and localized contractions in the form of waves (**B**). Higher time resolution traces and images are shown in the right panels. **C** and **D**, In the presence of ryanodine (10 μmol/L), depolarizing steps in voltage-clamp mode do not induce Ca^{2+} transients (**C,** red traces) and contractions (**D,** reslice image). Long-lasting depolarizations to 0 mV (arrows, black traces) generate small increases in intracellular Ca^{2+} (**C**) in the absence of waves of contraction (**D,** reslice image). Higher time resolution traces and images are shown in the right panels.

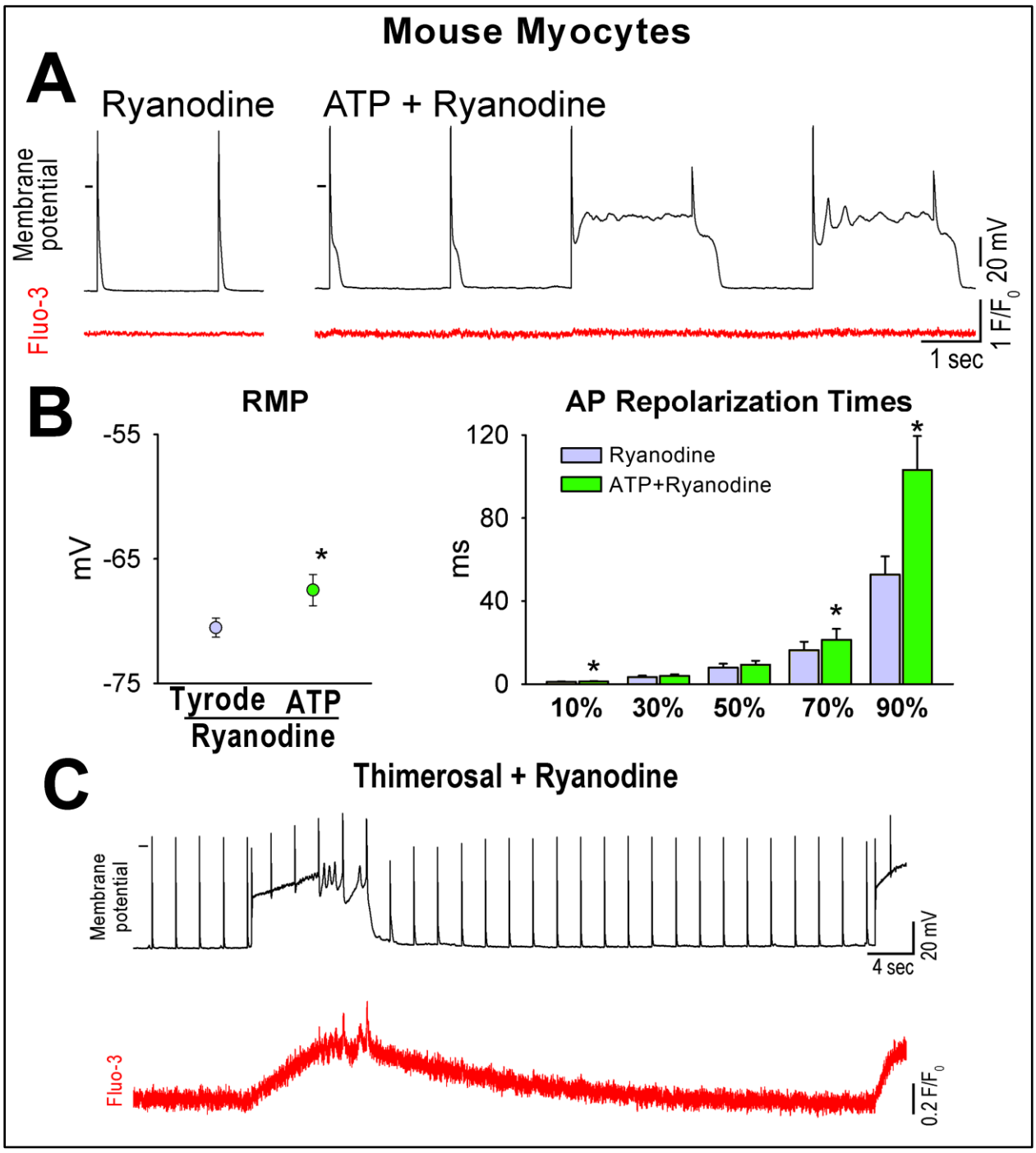

Figure 37. The effects of GPCR activation on Ca^{2+} transients, and IP3R activation does not alter ryanodine receptor function. A, Transmebrane potential (black traces) and cytosolic $[Ca^{2+}]_i$ (red traces) in myocytes exposed to ryanodine before and after ATP stimulation. **B,** Effects of IP3R activation on the AP following blockade of RyRs (ryanodine, 10 μmol/L). Quantitative data are shown as mean±SEM. **P*<0.05 versus ryanodine alone. **C,** IP3R activation and arrhythmic events. Transmembrane potential (black-trace) and cytosolic Ca^{2+} (red-trace) in a current-clamped mouse myocyte exposed to thimerosal in the presence of ryanodine. Blockade of RyRs did not prevent spontaneous sustained depolarizations.

IP3Rs and Electrical Properties Following GPCR Stimulation

Although GPCR stimulation prolongs the AP favoring an increase in Ca^{2+} transients, the mechanism(s) involved in the changes of the electrical activity of cardiomyocytes have not been defined as yet. Based on the fact that (a) IP3 dialysis or (b) enhanced IP3R affinity to IP3 recapitulate the effects of GPCR stimulation, and that (c) IP3R downregulation or (d) IP3R inhibition attenuate the effects of ATP and ET-1, the possibility was raised that mobilization of Ca^{2+} from the SR by IP3Rs contributes to the altered electrical properties of myocytes in the presence of GPCR agonists. Ca^{2+} translocation from the SR may enhance cytosolic Ca^{2+} load, which may promote Ca^{2+} extrusion via forward mode NCX; this process may contribute to the depolarization of the RMP, and the delayed repolarization phase of the AP (Spencer & Sham, 2003; Armoundas et al. 2003).

To test this hypothesis, voltage-clamp studies were performed in myocytes loaded with Fluo-3. IP3R function led to elevations in diastolic Ca^{2+} that were followed by sustained and transient inward currents. Importantly, the increase in diastolic Ca^{2+} developed slowly over a period of several seconds, potentially reflecting IP3R-mediated Ca^{2+} release (Figure 38A). The changes in resting Ca^{2+} and inward currents were preserved, despite inhibition of RyRs (Figure 38B). Conversely, blockade of the NCX prevented inward currents in the presence of increased cytosolic Ca^{2+} (Figure 38C).

To define the role of NCX following activation of IP3Rs, a nickel sensitive current, indicative of NCX activity, was measured (Ozdemir et al. 2008). ATP, ET-1, and dialysis with IP3 induced large inward currents, consistent with enhanced Ca^{2+} extrusion via forward mode NCX (Figure 39).

Additionally, to strengthen the possibility that Ca^{2+} extrusion was enhanced following Ca^{2+} mobilization by IP3Rs, myocytes were voltage-clamped at -70 mV; Ca^{2+} transient was triggered by short depolarizing steps and caffeine puffs to monitor intracellular SR Ca^{2+} stores. In the presence of ATP or ET-1, this protocol resulted in a gradual decrease in Ca^{2+} transients (Figure 40), supporting the notion that Ca^{2+} leak occurs under conditions favoring IP3R function.

To test whether the mobilization of Ca^{2+} from the SR via IP3Rs was implicated in the prolongation of the AP, decreased RMP, and increased EADs, Ca^{2+} from the SR was depleted by inhibition of SERCA and exposure to caffeine (Zaniboni et al. 1998; Zima et al. 2010). By this

approach, ATP and ET-1 showed a markedly reduced effect on RMP, AP duration, and arrhythmia (Figure 41). Additionally, to establish the impact of increased Ca^{2+} load on the electrical instability of cardiomyocytes, these cells were studied under $[Ca^{2+}]_i$ buffered conditions, to prevent changes in cytosolic Ca^{2+} (Song et al. 1998). GPCR agonists had no effects on RMP and AP (Figure 42). Collectively, these observations indicate that Ca^{2+} mobilization from the SR via IP3Rs contributes to the alterations in the electrical properties of cardiomyocytes mediated by GPCR stimulation.

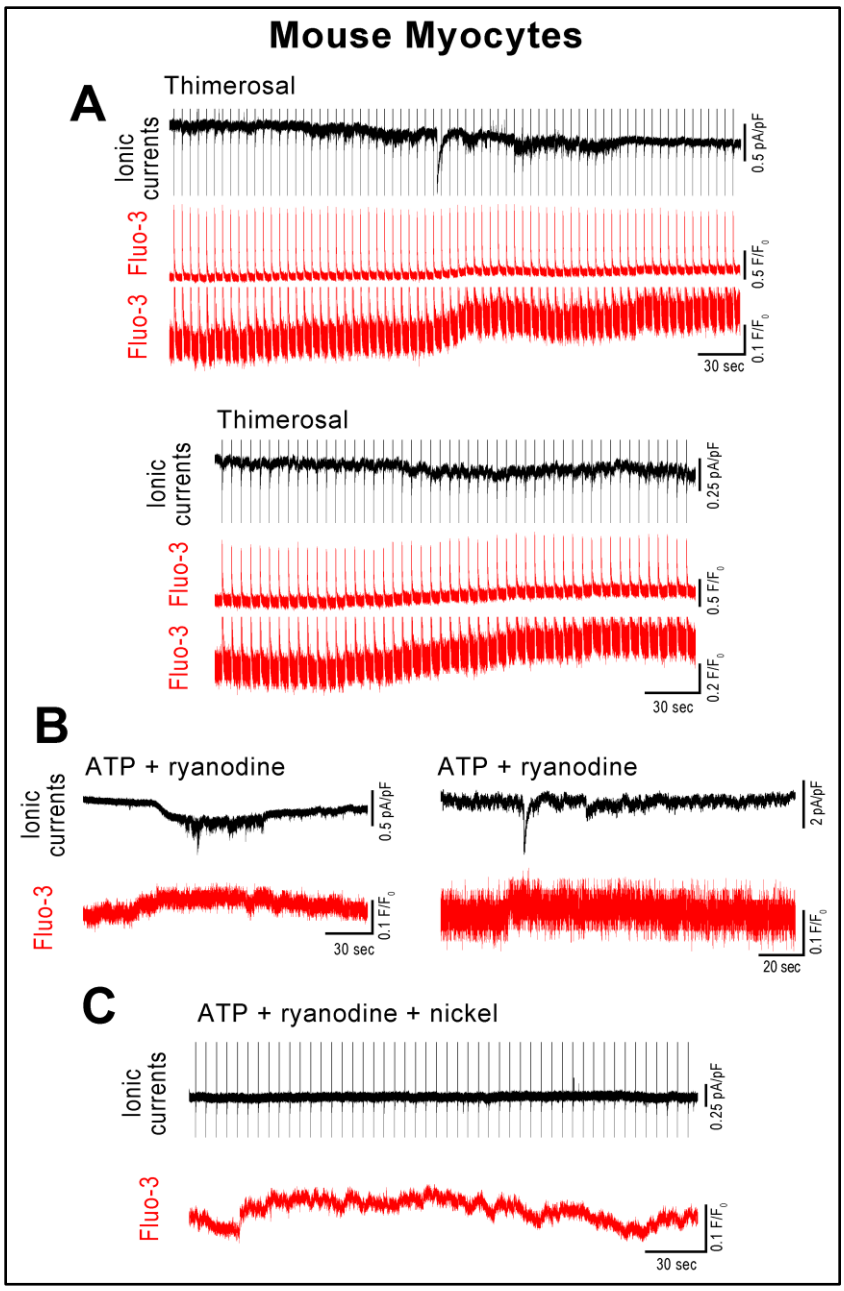

Figure 38. IP3Rs activate the NCX through changes in $[Ca^{2+}]_i$. (See next page) A, Transient and sustained inward currents (black-traces) and slowly developing diastolic $[Ca^{2+}]_i$ elevations (red-traces) in mouse myocytes exposed to thimerosal. Membrane potential was held at -70 mV; short (5 ms) depolarizing steps to 0 mV were used to trigger Ca^{2+} transients. The Ca^{2+} fluorescent signal is reported at higher magnification in the lower traces. **B,** Transient and sustained inward currents (black-traces) and slowly developing $[Ca^{2+}]_i$ elevations (red-traces) in mouse myocytes held at -70 mV following exposure to ATP and ryanodine. **C,** Slowly developing diastolic $[Ca^{2+}]_i$ elevations (red-traces) in a mouse myocytes exposed to ATP and ryanodine in the presence of nickel (2.5 mmol/L), fail to induce transient and sustained inward currents (black-traces). Membrane potential was held at -70 mV; short (5 ms) depolarizing steps to 0 mV were employed.

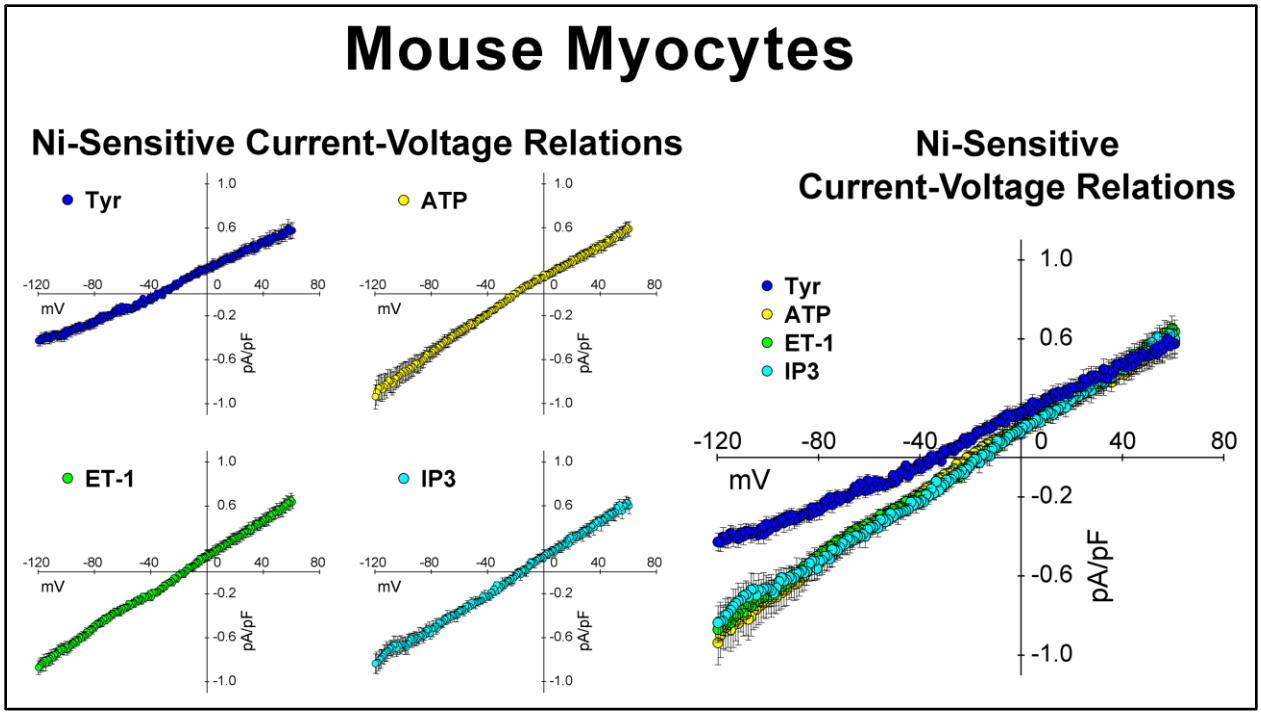

Figure 39. IP3R stimulation and NCX function. Current voltage relations for the nickel (Ni)-sensitive current measured in voltage-clamp in the absence of IP3R stimulation and in the presence of ATP, ET-1, or IP3 dialysis (left). On the right, superimposed curves indicate that the Ni-sensitive current is enhanced following IP3R stimulation. To prevent RyR-Ca^{2+} release, ryanodine was employed.

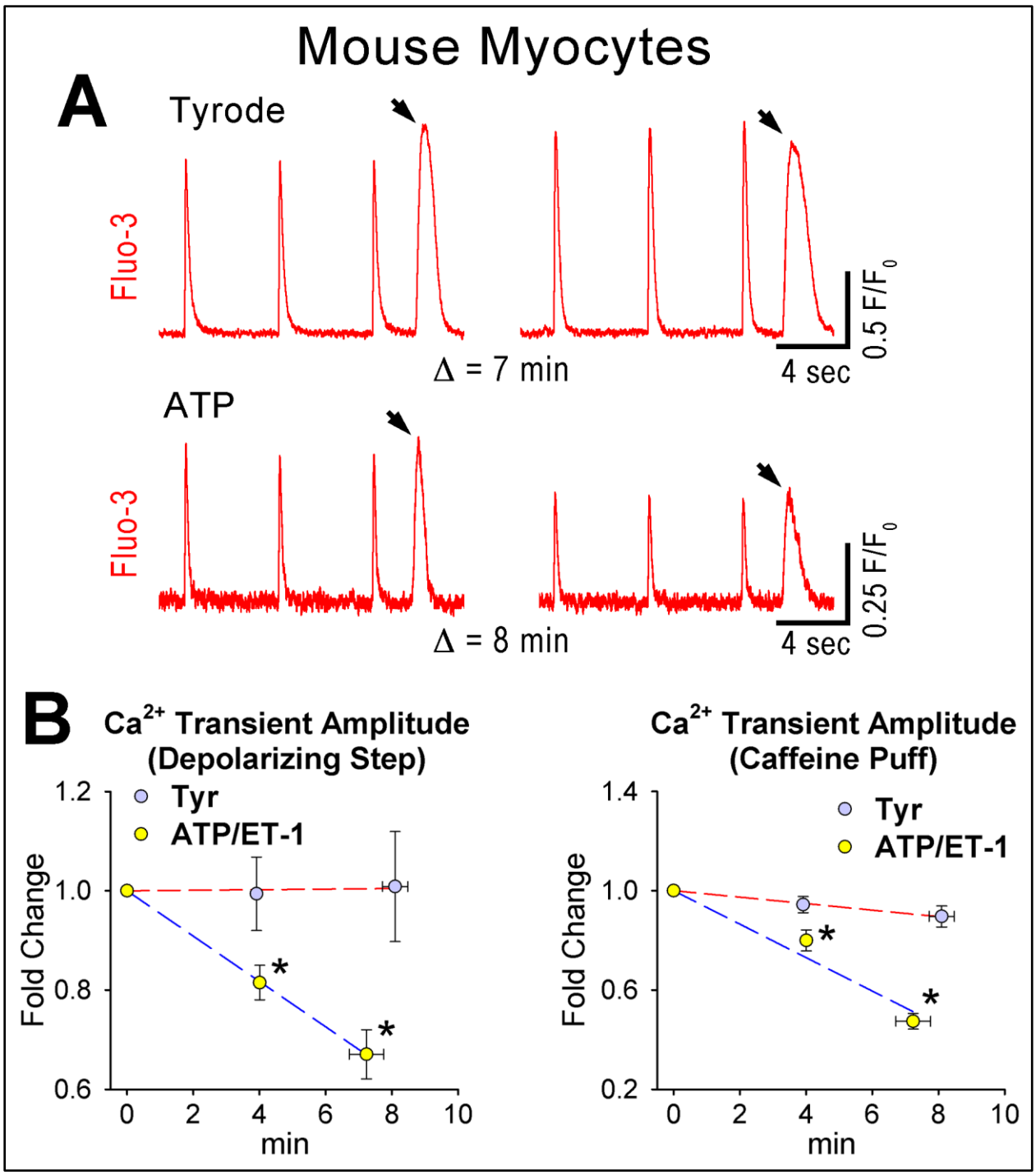

Figure 40. GPCR stimulation and SR Ca^{2+} release in voltage-clamped myocytes. A, Ca^{2+} transients elicited by depolarizing steps from -70 to 0 mV, and by caffeine (20 mmol/L) puffs (arrows) in mouse myocytes in the absence (upper traces) and presence of ATP (lower traces). Δ indicates the time interval between traces displayed on the left and right panel. **B,** Changes in Ca^{2+} transient amplitude over time for myocytes exposed to Tyrode (Tyr) or GPCR agonists (ATP or ET-1). Quantitative data are shown as mean±SEM. **P*<0.05 versus Tyr, using paired *t*-test.

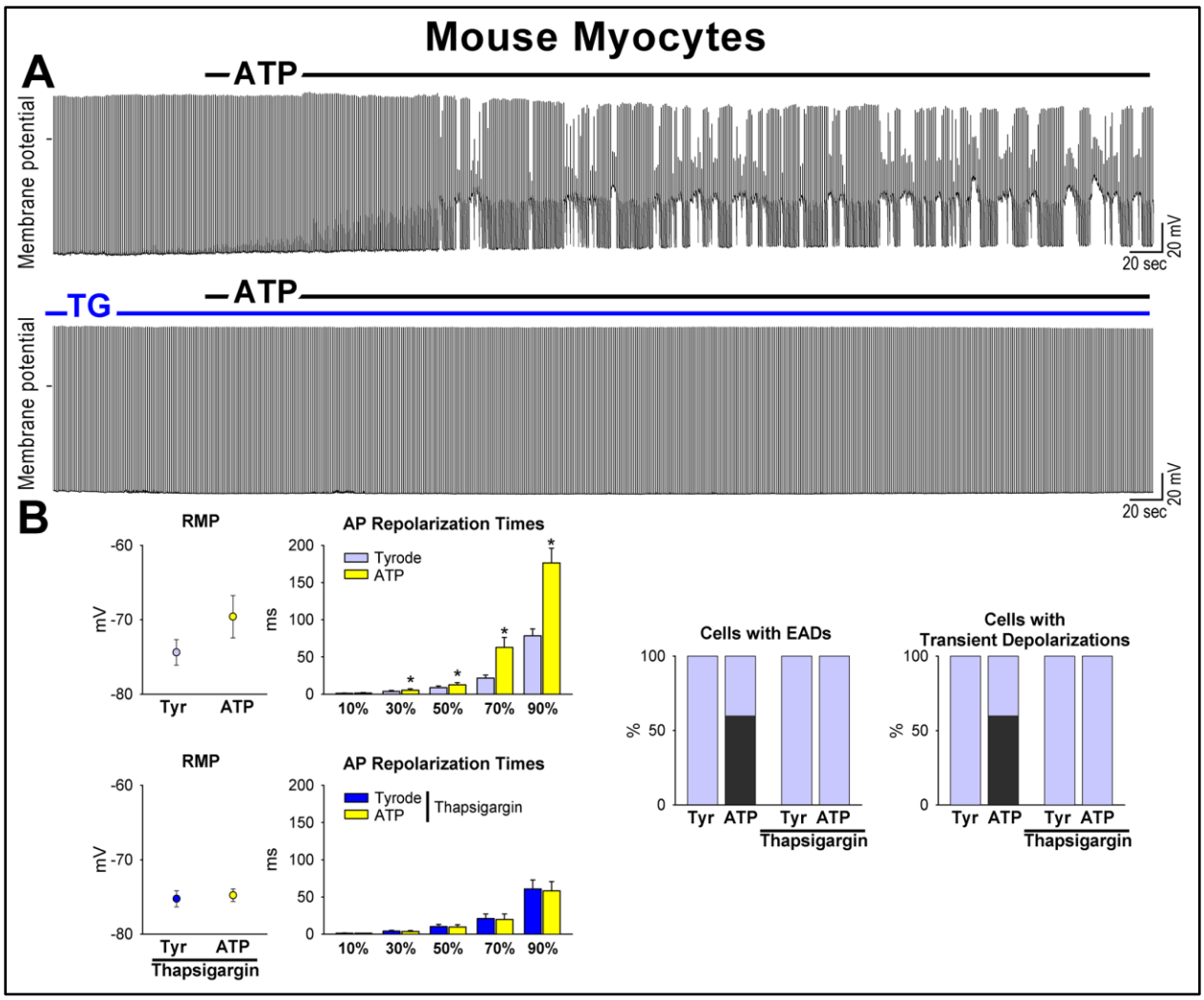

Figure 41. The effects of GPCR activation on mouse myocytes are abolished by depletion of Ca^{2+} from the SR. A, Transmembrane potential in mouse myocytes exposed to ATP in control conditions (upper trace) or following depletion of SR Ca^{2+} (lower trace). Thapsigargin (10 μmol/L), TG. **B,** Quantitative data are shown as mean±SEM. **P*<0.05 versus Tyr.

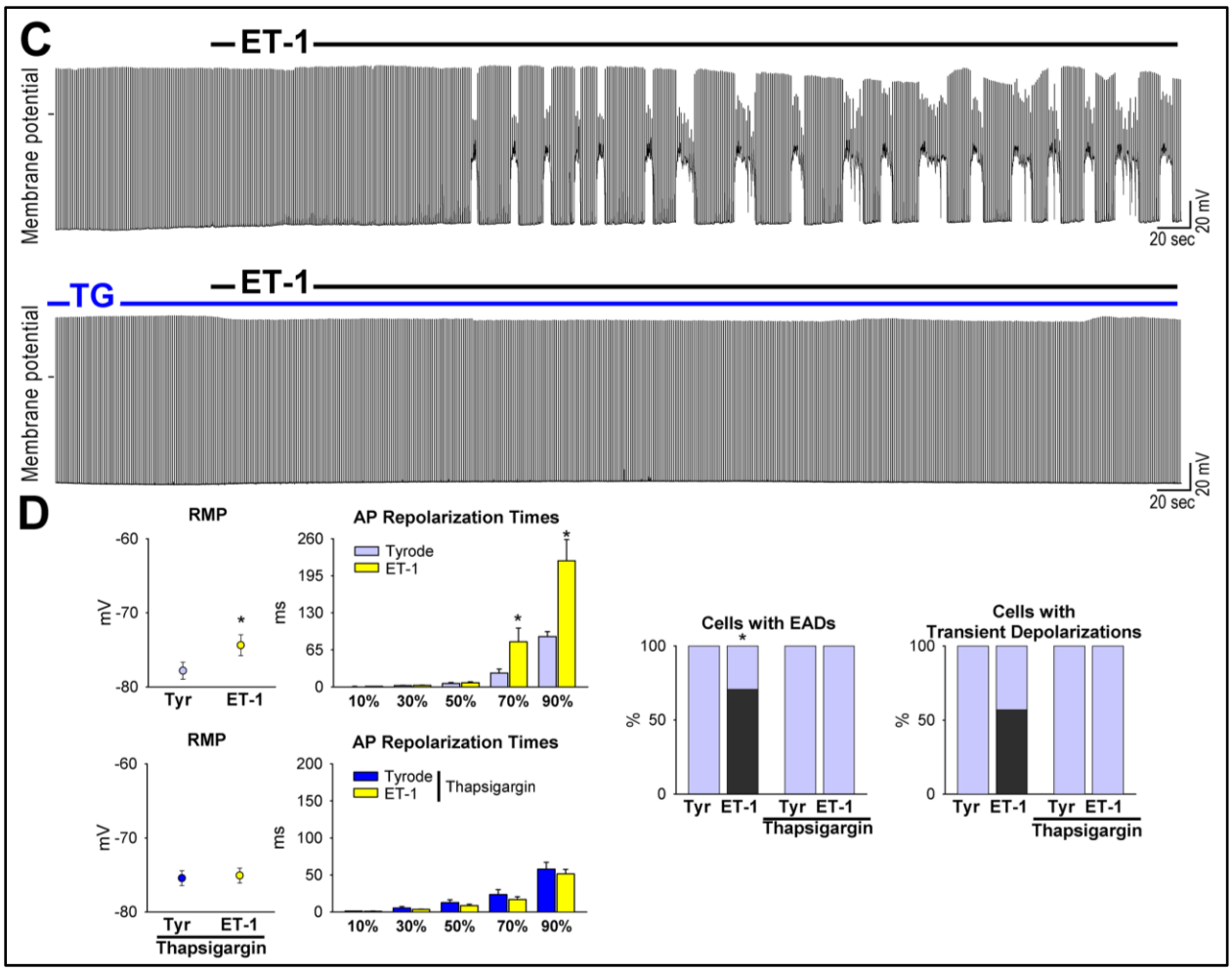

Figure 41. The effects of GPCR activation on mouse myocytes are abolished by depletion of Ca^{2+} from the SR (continued). C, Transmembrane potential in mouse myocytes exposed to ET-1 in control conditions (upper trace) or following depletion of SR Ca^{2+} (lower trace). Thapsigargin, TG. **D,** Quantitative data are shown as mean±SEM. **P*<0.05 versus Tyr

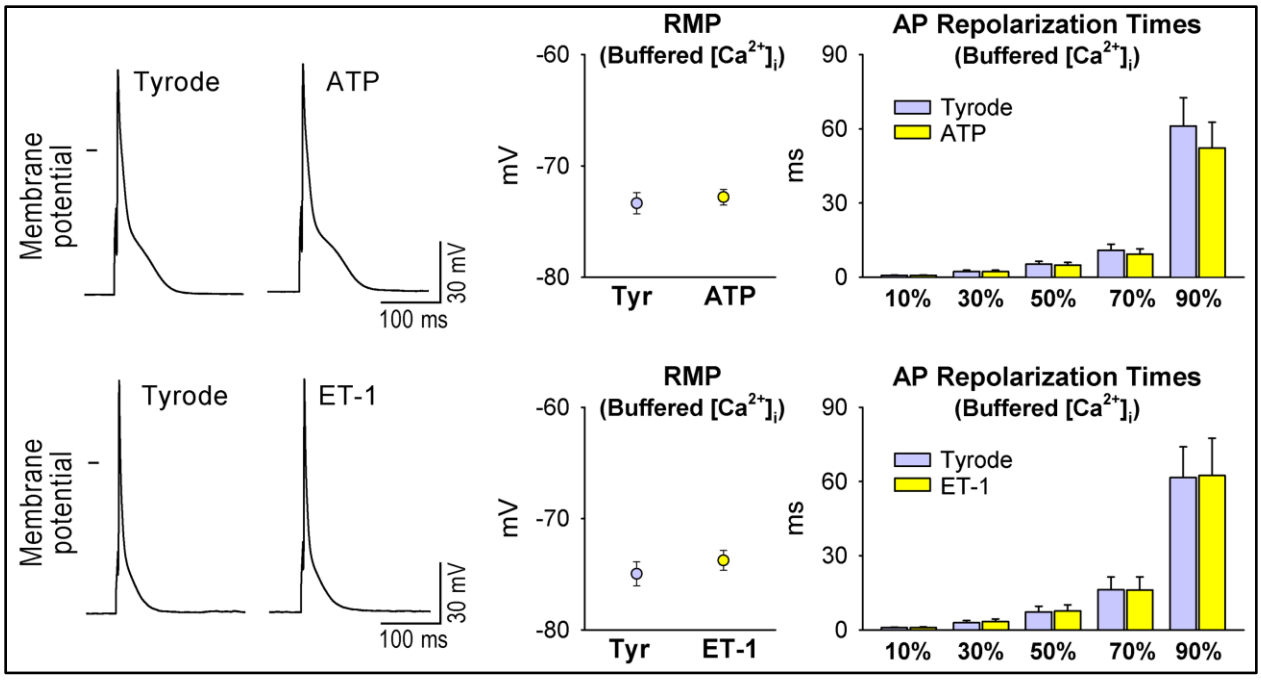

Figure 42. The effects of GPCR activation on mouse myocytes are abolished by intracellular Ca^{2+} buffered condition. In the presence of buffered $[Ca^{2+}]_i$, ATP and ET-1 fail to alter the myocyte AP profile. Quantitative data are shown as mean±SEM.

Discussion

The results of the current study provide a characterization of the electrical and mechanical properties of human LV myocytes and emphasize the critical role that the GPCR/IP3R axis has in regulating Ca^{2+} homeostasis, contractile performance and the electrical stability of the human heart. IP3Rs are expressed and functional in human LV myocytes, and the Ca^{2+} mobilized from the SR by IP3Rs contributes to the decrease in RMP, prolongation of the AP, and to the occurrence of EADs and sustained depolarizations following GPCR stimulation. Ca^{2+} transient amplitude and cell shortening are enhanced, and extra-systolic and dysregulated Ca^{2+} elevations and contractions become apparent. These alterations in the electromechanical behavior of human cardiomyocytes are coupled with increased isometric twitch of the myocardium and arrhythmic events, indicating that the GPCR/IP3R effector pathway offers inotropic reserve, which is hampered by electrical instability and contractile abnormalities.

IP3Rs are present in primitive cells of the fetal and adult heart (Ferreira-Martins et al. 2009, Ferreira-Martins et al. 2012). However, the growth promoting effects of IP3Rs in progenitor cells are lost in post-mitotic human cardiomyocytes (Kockskämper et al. 2008). In both cases, IP3Rs modulate the release of Ca^{2+} from the SR, but its distal effect varies dramatically; the increase in cytosolic Ca^{2+} favors cell cycle reentry and asymmetric division of fetal progenitor cells (Ferreira-Martins et al. 2009), while, as shown here, the release of Ca^{2+} in adult human cardiomyocytes enhances cell contractile performance. Whether a link between these two distinct mechanisms actually exists is currently unknown, although IP3Rs have a critical independent biological function in these two different cell types.

The contribution of IP3Rs to the electromechanical behavior of ventricular myocytes in small and large mammals is controversial (Domeier et al. 2008; Kockskämper et al. 2008). Our findings support the notion that in the human heart IP3Rs represent an important substrate able to increase myocyte contractility and the propensity for electrical instability coupled with GPCR agonists. Increases in the circulating levels of neurohumoral transmitters and cytokines physiologically and pathologically (Francis et al. 1993; Molkentin, 2000) may involve IP3R activation predisposing the heart to arrhythmic events. The increased incidence of arrhythmias and sudden death in patients with chronic heart failure (Huikuri et al. 2001; Rubart & Zipes,

2005) may be related partly to upregulation of IP3Rs in the hypertrophied, dysfunctional cardiomyocytes (Del Monte & Hajjar, 2008; Houser & Margulies, 2003).

The GPCR agonists ATP and ET-1 stimulate IP3Rs in human cardiomyocytes, but other signaling pathways may be upregulated as well. These GPCR agonists activate PLC that generates not only IP3 but also DAG, which activates TRPCs and PKC isoforms (Hardie, 2007; Mohácsi et al. 2004). PKC phosphorylates ion channels and myofilament proteins, affecting the electrical and mechanical properties of cardiomyocytes (Steinberg et al. 1995; Braz et al. 2004; Mohácsi et al. 2004). Additionally, ATP and ET-1 may enhance PLC-independent molecular events (Mohácsi et al. 2001; Vassort, 2001), which may trigger transmembrane ionic fluxes. Importantly, the effects of ATP and ET-1 on myocyte contractility were maintained in the presence of a PKC inhibitor. Similarly, the alterations in the electrical properties of cardiomyocytes were recapitulated by direct stimulation with IP3 or by enhancing IP3R affinity. Conversely, the effects of GPCR agonists were abrogated by: (a) downregulation of IP3Rs; (b) inhibition of IP3R function or reduced IP3 production; (c) depletion of Ca^{2+} from the SR; and (d) buffered intracellular Ca^{2+}. Collectively, our data support the notion that the Ca^{2+} mobilized by IP3Rs is a critical determinant of the electrical abnormalities dictated by stimulation of GPCRs. However, we cannot exclude that DAG-sensitive and PLC-independent signaling pathways may participate in the electromechanical changes initiated by IP3R function. GPCR agonists modulate I_{CaL} and the delayed rectifier K^+ currents, which can alter the AP profile (Mohácsi et al. 2001; Vassort, 2001). Moreover, changes in membrane potential may result from TRPCs and store-operated Ca^{2+} channels activated, respectively, by DAG and SR Ca^{2+} levels (Hardie, 2007; Parekh & Putney, 2005).

A significant issue concerned whether, following GPCR stimulation, Ca^{2+} mobilization from the SR via IP3Rs alters the electrical properties of myocytes directly, or indirectly by Ca^{2+} release from RyR channels (Domeier et al. 2008; Harzheim et al. 2009). The contribution of RyRs to the process was analyzed by combining Ca^{2+} imaging with electrophysiological measurements. Our findings indicate that IP3Rs contribute to the alteration of the AP, independently from an increase in sensitivity of the RyRs. Excitation contraction-coupling gain was preserved in the presence of GPCR agonists, documenting that RyR function was not enhanced by the changes in Ca^{2+}.

Despite inhibition of RyRs, cytosolic Ca^{2+}, NCX forward mode, and electrical abnormalities increased in LV myocytes following stimulation of the GPCR/IP3R axis. Collectively, the cascade of events initiated by GPCR ligands involves promotion of PLC enzymatic activity, IP3 production, opening of IP3R channels, and Ca^{2+} translocation from the SR to the cytoplasm. The latter favors the electrogenic extrusion of this cation via NCX, resulting in depolarization of the RMP and prolonged repolarization of the AP (see catoon in Figure 43).

These electrical changes positively impact on the process of Ca^{2+} induced Ca^{2+} release since the delayed repolarization of the AP sustains Ca^{2+} influx, amplifying Ca^{2+} transients and cell shortening (Sah et al. 2001, Rota et al. 2007). By AP-clamp, remodeled APs, in the absence of GPCR ligands, elicited Ca^{2+} transients comparable to those associated with GPCR agonists. These findings indicate that the altered electrical activity has a critical role in the process, rather than suggesting a direct interaction between IP3R and RyR function. Moreover, the enhanced Ca^{2+} entry by the protracted AP may counteract the excess of Ca^{2+} extruded during diastole via NCX, restoring intracellular SR Ca^{2+} stores. This may account for the prolonged effects of IP3R in the presence of GPCR agonists. Conversely, with stable (time constrained) depolarizations in voltage-clamp, GPCR agonists are coupled with a progressive decrease in Ca^{2+} transient amplitude and SR Ca^{2+} load, emphasizing the importance that the changes in the AP profile have in mediating a sustained positive inotropic effect.

The extra-systolic elevations in Ca^{2+} and after-contractions detected in cardiomyocytes with GPCR agonists appear to be due to EADs, which may be the product of the alteration in the AP (Rubart & Zipes, 2005). In fact, changes in AP profile alone were sufficient to trigger alone extra-systolic Ca^{2+} elevations, pointing to the alterations in the electrical properties of cardiomyocytes as the primary mediator of Ca^{2+} cycling abnormalities. However, the ionic basis for the sustained membrane depolarization, protracted Ca^{2+} increases and myocyte contractures remains to be completely defined. IP3-independent effector pathways may participate in the process, although the cellular alterations were abrogated by attenuating IP3R function.

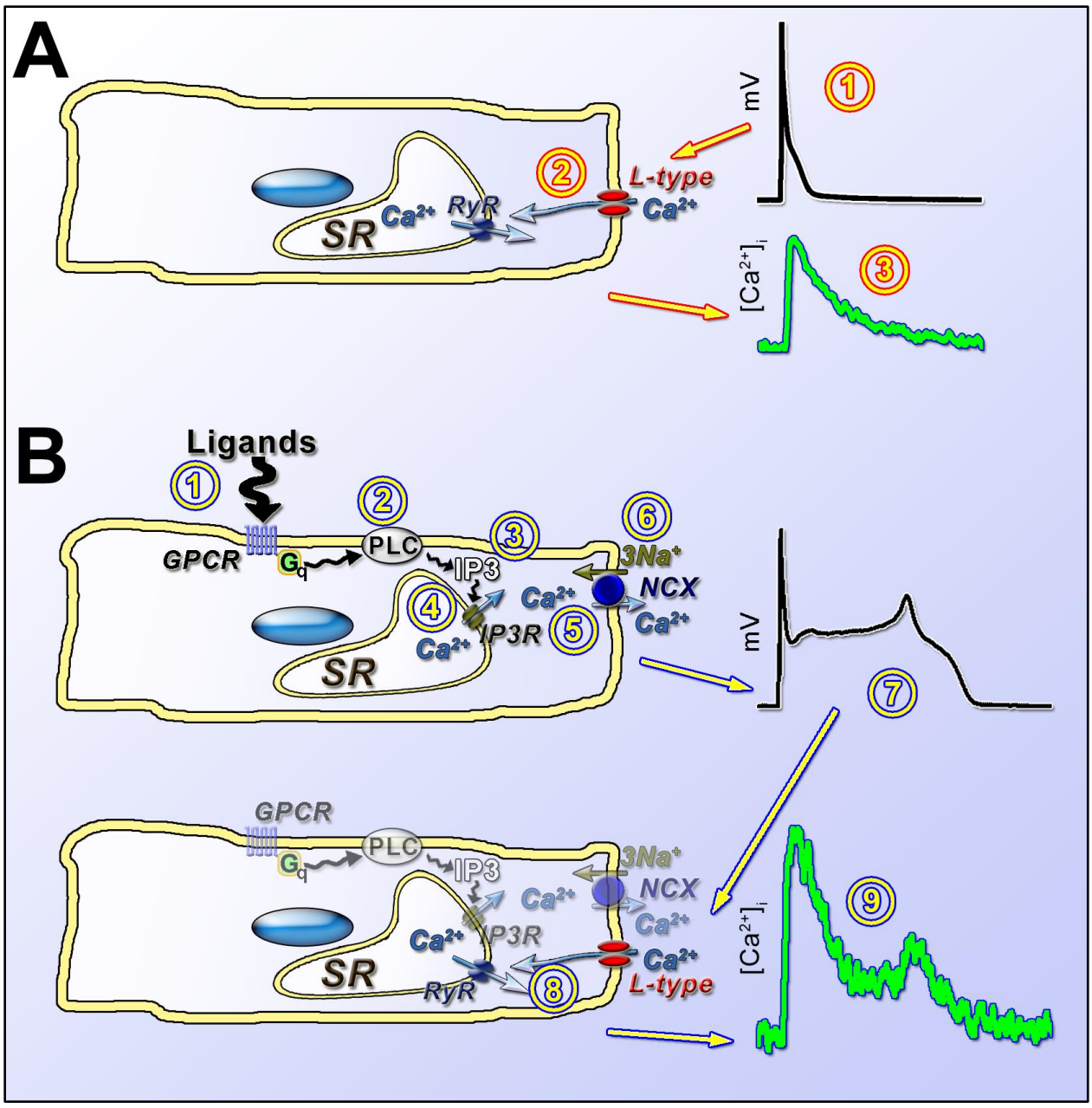

Figure 43. Excitation-contraction coupling and GPCR stimulation in myocytes. A, Schematic representation of the process of Ca^{2+}-induced Ca^{2+} release under physiological conditions. During the AP (1), Ca^{2+} enters the cell via L-type channels, triggering the opening of RyRs and release of Ca^{2+} from the SR (2), which originates a cytosolic Ca^{2+} transient (3). **B,** Signaling cascade initiated by GPCR activation. Ligand-GPCR interaction (1) promotes PLC enzymatic activity (2), leading to the formation of soluble IP3 (3). The latter triggers the opening of IP3Rs and Ca^{2+} translocation from the SR to the cytoplasm (4). The increased cytoplasmic Ca^{2+} load (5) induces the electrogenic extrusion of this cation (6); this phenomenon results in depolarization of the RMP, protracted repolarization of the AP, and the occurrence of EADs (7). The remodeled profile of the AP leads to a sustained Ca^{2+} influx and potentiated Ca^{2+} release via RyRs (8), enhancing Ca^{2+} transients (9). Extra-systolic Ca^{2+} elevations are coupled with EADs.

The spatiotemporal dynamics of Ca^{2+} mobilized by IP3Rs is dictated by the hierarchical recruitment of elementary Ca^{2+} release when $[IP3]_i$ is increased; this condition originates Ca^{2+} blips, puffs, and global regenerative waves (Berridge et al. 2000). In the absence of GPCR agonists, blockade of IP3R channels has little or no impact on the mechanical and electrical behavior of cardiomyocytes, indicating that extracellular activators of PLC are needed to increase $[IP3]_i$ and trigger an IP3R response. As in other cell types (Ferreira-Martins et al. 2009; Berridge et al. 2000; Ferreira-Martins et al. 2012), IP3R activation results in a time-dependent increase in cytosolic Ca^{2+} of cardiomyocytes that develops slowly over a number of seconds. With GPCR agonists, the temporal dynamic of IP3R-mediated Ca^{2+} release provides the basis for the sustained changes in the AP, cellular contractility, and incidence of electrical disorders. A similar sequence of events appears to be operative in failing human cardiomyocytes, in which IP3R transcripts (Go et al. 1995) and proteins are up-regulated, providing a potential etiology for arrhythmias and sudden death in this patient population.

Ca^{2+} release channels are differentially expressed during cardiac development and postnatally (Kockskämper et al. 2008; Gorza et al. 1997; Janowski et al. 2010); in cardiomyocytes, the contribution of the ubiquitous IP3R to intracellular Ca^{2+} mobilization is progressively attenuated from the fetal to the neonatal and adult life, in favor of the more specialized function of RyRs (Kockskämper et al. 2008; Janowski et al. 2010). Thus, the up-regulation of IP3Rs may be viewed as a component of a larger fetal reprogramming in the failing myocardium, together with the multiple pathological changes that characterize the progression of the disease state.

Acknoledgements

Findings presented in this thesis have been publised in Circulation (Wolters Kluwer Health Lippincott Williams & Wilkins). Unless otherwise specified, images were reproduced from the published article.

Signore S, Sorrentino A, Ferreira-Martins J, Kannappan R, Shafaie M, Del Ben F, Isobe K, Arranto C, Wybieralska E, Webster A, Sanada F, Ogórek B, Zheng H, Liu X, Del Monte F, D'Alessandro DA, Wunimenghe O, Michler RE, Hosoda T, Goichberg P, Leri A, Kajstura J, Anversa P, Rota M. Inositol 1, 4, 5-trisphosphate receptors and human left ventricular myocytes. Circulation. 2013 Sep 17;128(12):1286-97. doi: 10.1161/CIRCULATIONAHA.113.002764. Epub 2013 Aug 27. PubMed PMID: 23983250; PubMed Central PMCID: PMC3873649. Wolters Kluwer Health Lippincott Williams & Wilkins© No modifications will be permitted.

References

Armoundas AA, Hobai IA, Tomaselli GF, Winslow RL, O'Rourke B. Role of sodium-calcium exchanger in modulating the action potential of ventricular myocytes from normal and failing hearts. Circ Res. 2003;93:46-53.

Berenson ML, Levine DM, Rindskopf D, eds. Applied statistics. Englewood Cliffs, New Jersey: Prentice-Hal; 1988.

Berne & Levy. Physiology - Sixth Edition, 2010.

Berridge MJ, Lipp P, Bootman MD. The versatility and universality of calcium signalling. Nat Rev Mol Cell Biol. 2000;1:11-21.

Bers DM. Calcium cycling and signaling in cardiac myocytes. Annu Rev Physiol. 2008;70:23-49.

Bers DM. Cardiac excitation-contraction coupling. Nature. 2002;415:198-205.

Bootman MD, Taylor CW, Berridge MJ. The thiol reagent, thimerosal, evokes Ca2+ spikes in HeLa cells by sensitizing the inositol 1,4,5-trisphosphate receptor. J. Biol. Chem. 1992;267:25113–25119.

Braz JC, Gregory K, Pathak A, Zhao W, Sahin B, Klevitsky R, Kimball TF, Lorenz JN, Nairn AC, Liggett SB, Bodi I, Wang S, Schwartz A, Lakatta EG, DePaoli-Roach AA, Robbins J, Hewett TE, Bibb JA, Westfall MV, Kranias EG, Molkentin JD. PKC-alpha regulates cardiac contractility and propensity toward heart failure. Nat Med. 2004;10:248-254.

Del Monte F, Hajjar RJ. Intracellular devastation in heart failure. Heart Fail Rev. 2008;13:151-162

Dobson JG Jr, Shea LG, Fenton RA. Adenosine A2A and beta-adrenergic calcium transient and contractile responses in rat ventricular myocytes. Am J Physiol Heart Circ Physiol. 2008;295:H2364-H2372.

Domeier TL, Zima AV, Maxwell JT, Huke S, Mignery GA, Blatter LA. IP3 receptor-dependent Ca2+ release modulates excitation-contraction coupling in rabbit ventricular myocytes. Am J Physiol Heart Circ Physiol. 2008;294:H596-H604.

Fabiato A. Calcium-induced release of calcium from the cardiac sarcoplasmic reticulum. Am. J. Physiol. 1983;245:C1-14.

Ferreira-Martins J, Ogórek B, Cappetta D, Matsuda A, Signore S, D'Amario D, Kostyla J, Steadman E, Ide-Iwata N, Sanada F, Iaffaldano G, Ottolenghi S, Hosoda T, Leri A, Kajstura J, Anversa P, Rota M. Cardiomyogenesis in the developing heart is regulated by C-kit-positive cardiac stem cells. Circ Res. 2012;110:701-715.

Ferreira-Martins J, Rondon-Clavo C, Tugal D, Korn JA, Rizzi R, Padin-Iruegas ME, Ottolenghi S, De Angelis A, Urbanek K, Ide-Iwata N, D'Amario D, Hosoda T, Leri A, Kajstura J, Anversa P, Rota M. Spontaneous calcium oscillations regulate human cardiac progenitor cell growth. Circ Res. 2009;105:764-774.

Francis GS, McDonald KM, Cohn JN. Neurohumoral activation in preclinical heart failure. Remodeling and the potential for intervention. Circulation. 1993;87:IV90-IV96.

Gambassi G, Spurgeon HA, Ziman BD, Lakatta EG, Capogrossi MC. Opposing effects of alpha 1-adrenergic receptor subtypes on Ca2+ and pH homeostasis in rat cardiac myocytes. Am J Physiol. 1998;274:H1152-H1162.

Gergs U, Boknik P, Schmitz W, Simm A, Silber RE, Neumann J. A positive inotropic effect of ATP in the human cardiac atrium. Am J Physiol Heart Circ Physiol. 2008;294:H1716-H1723.

Goichberg P, Bai Y, D'Amario D, Ferreira-Martins J, Fiorini C, Zheng H, Signore S, del Monte F, Ottolenghi S, D'Alessandro DA, Michler RE, Hosoda T, Anversa P, Kajstura J, Rota M, Leri A. The ephrin A1-EphA2 system promotes cardiac stem cell migration after infarction. Circ Res. 2011;108:1071-1083.

Go LO MM, Watras J, Handa KK, Fyfe BS, Marks AR. Differential regulation of two types of intracellular calcium release channels during end-stage heart failure. J Clin Invest. 1995;95:888–894.

Gomez AM, Guatimosim S, Dilly KW, Vassort G, Lederer WJ. Heart failure after myocardial infarction: altered excitation-contraction coupling. Circulation. 2001;104:688-93.

Gonzalez A, Rota M, Nurzynska D, Misao Y, Tillmanns J, Ojaimi C, Padin-Iruegas ME, Müller P, Esposito G, Bearzi C, Vitale S, Dawn B, Sanganalmath SK, Baker M, Hintze TH, Bolli R,

Urbanek K, Hosoda T, Anversa P, Kajstura J, Leri A. Activation of cardiac progenitor cells reverses the failing heart senescent phenotype and prolongs lifespan. Circ Res. 2008;102:597-606.

Gorza L, Vettore S, Tessaro A, Sorrentino V, Vitadello M. Regional and age-related differences in mRNA composition of intracellular Ca(2+)-release channels of rat cardiac myocytes. J Mol Cell Cardiol. 1997;29:1023-1036.

Hardie RC. TRP channels and lipids: from Drosophila to mammalian physiology. J Physiol. 2007;578:9-24.

Harzheim D, Movassagh M, Foo RS, Ritter O, Tashfeen A, Conway SJ, Bootman MD, Roderick HL. Increased InsP3Rs in the junctional sarcoplasmic reticulum augment Ca2+ transients and arrhythmias associated with cardiac hypertrophy. Proc Natl Acad Sci USA. 2009;106:11406-11411.

Herron TJ, Milstein ML, Anumonwo J, Priori SG, Jalife J. Purkinje cell calcium dysregulation is the cellular mechanism that underlies catecholaminergic polymorphic ventricular tachycardia. Heart Rhythm. 2010;7:1122-1128.

Higazi DR, Fearnley CJ, Drawnel FM, Talasila A, Corps EM, Ritter O, McDonald F, Mikoshiba K, Bootman MD, Roderick HL. Endothelin-1-stimulated InsP3-induced Ca2+ release is a nexus for hypertrophic signaling in cardiac myocytes. Mol Cell. 2009;33:472-482.

Hoesch RE, Weinreich D, Kao JP. Localized IP3-evoked Ca2+ release activates a K+ current in primary vagal sensory neurons. J Neurophysiol. 2004;91:2344-2352.

Holzem KM, Efimov IR. Arrhythmogenic remodelling of activation and repolarization in the failing human heart. Europace. 2012;14 Suppl 5:v50–v57.

Houser SR. When does spontaneous sarcoplasmic reticulum Ca2+ release cause a triggered arrhythmia? Cellular versus tissue requirements. Circ Res. 2000;87:725-727.

Houser SR, Margulies KB. Is depressed myocyte contractility centrally involved in heart failure? Circ Res. 2003;92:350-358.

Houser SR, Piacentino V, Mattiello J, Weisser J, Gaughan JP. Functional properties of failing human ventricular myocytes. Trends Cardiovasc. Med. 2000;10:101-107.

Huikuri HV, Castellanos A, Myerburg RJ. Sudden death due to cardiac arrhythmias. N Engl J Med. 2001;345:1473-1482.

Janowski E, Berríos M, Cleemann L, Morad M. Developmental aspects of cardiac Ca(2+) signaling: interplay between RyR- and IP(3)R-gated Ca(2+) stores. Am J Physiol Heart Circ Physiol. 2010;298:H1939-H1950.

Janse MJ. Electrophysiological changes in heart failure and their relationship to arrhythmogenesis. Cardiovasc. Res. 2004;61:208–217.

Joyner RW, Picone J, Veenstra R, Rawling D. Propagation through electrically coupled cells. Effects of regional changes in membrane properties. Circ Res. 1983;53:526-534.

Kockskämper J, Zima AV, Roderick HL, Pieske B, Blatter LA, Bootman MD. Emerging roles of inositol 1,4,5-trisphosphate signaling in cardiac myocytes. J Mol Cell Cardiol. 2008;45:128-147.

Knollmann BC, Chopra N, Hlaing T, Akin B, Yang T, Ettensohn K, Knollmann BE, Horton KD, Weissman NJ, Holinstat I, Zhang W, Roden DM, Jones LR, Franzini-Armstrong C, Pfeifer K. Casq2 deletion causes sarcoplasmic reticulum volume increase, premature Ca2+ release, and catecholaminergic polymorphic ventricular tachycardia. J Clin Invest. 2006;116:2510-2520.

Liang J, Wang YJ, Tang Y, Cao N, Wang J, Yang HT. Type 3 inositol 1,4,5-trisphosphate receptor negatively regulates apoptosis during mouse embryonic stem cell differentiation. Cell Death Differ. 2010;17:1141-1154.

Li G-R, Lau C-P, Ducharme A, Tardif J-C, Nattel S. Transmural action potential and ionic current remodeling in ventricles of failing canine hearts. Am J Physiol Heart Circ Physiol. 2002;283:H1031-H1041.

Maltsev VA, Lakatta EG. Normal heart rhythm is initiated and regulated by an intracellular calcium clock within pacemaker cells. Heart Lung Circ. 2007;16:335–348.

Mohácsi A, Magyar J, Tamás B, Nánási PP. Effects of endothelins on cardiac and vascular cells: new therapeutic target for the future? Curr Vasc Pharmacol. 2004;2:53-63.

Molkentin JD. Calcineurin and beyond: cardiac hypertrophic signaling. Circ Res. 2000;87:731-738.

Nakayama H, Bodi I, Maillet M, DeSantiago J, Domeier TL, Mikoshiba K, Lorenz JN, Blatter LA, Bers DM, Molkentin JD. The IP3 receptor regulates cardiac hypertrophy in response to select stimuli. Circ Res. 2010;107:659-666.

Nett MP, Vassalle M. Obligatory role of diastolic voltage oscillations in sino-atrial node discharge. J Mol Cell Cardiol. 2003;35:1257-1276.

Ozdemir S, Bito V, Holemans P, Vinet L, Mercadier JJ, Varro A, Sipido KR. Pharmacological inhibition of na/ca exchange results in increased cellular Ca2+ load attributable to the predominance of forward mode block. Circ Res. 2008;102:1398-1405.

Pandit SV, Kaur K, Zlochiver S, Noujaim SF, Furspan P, Mironov S, Shibayama J, Anumonwo J, Jalife J. Left-to-right ventricular differences in I(KATP) underlie epicardial repolarization gradient during global ischemia. Heart Rhythm. 2011;8:1732-1739.

Parekh AB, Putney JW Jr. Store-operated calcium channels. Physiol Rev. 2005;85:757-810.

Piacentino V 3rd, Weber CR, Chen X, Weisser-Thomas J, Margulies KB, Bers DM, Houser SR. Cellular basis of abnormal calcium transients of failing human ventricular myocytes. Circ Res. 2003;92:651-658.

Pieske B, Beyermann B, Breu V, Löffler BM, Schlotthauer K, Maier LS, Schmidt-Schweda S, Just H, Hasenfuss G. Functional effects of endothelin and regulation of endothelin receptors in isolated human nonfailing and failing myocardium. Circulation. 1999;99:1802-1809.

Pott C, Philipson KD, Goldhaber JI. Excitation-contraction coupling in Na+-Ca2+ exchanger knockout mice: reduced transsarcolemmal Ca2+ flux. Circ Res. 2005; 97:1288-1295.

Remus TP, Zima AV, Bossuyt J, Bare DJ, Martin JL, Blatter LA, Bers DM, Mignery GA. Biosensors to measure inositol 1,4,5-trisphosphate concentration in living cells with spatiotemporal resolution. J Biol Chem. 2006;281:608-616.

Roell W, Lewalter T, Sasse P, Tallini YN, Choi BR, Breitbach M, Doran R, Becher UM, Hwang SM, Bostani T, von Maltzahn J, Hofmann A, Reining S, Eiberger B, Gabris B, Pfeifer A, Welz A, Willecke K, Salama G, Schrickel JW, Kotlikoff MI, Fleischmann BK. Engraftment of connexin 43-expressing cells prevents post-infarct arrhythmia. Nature. 2007;450:819-824.

Rota M, Boni A, Urbanek K, Padin-Iruegas ME, Kajstura TJ, Fiore G, Kubo H, Sonnenblick EH, Musso E, Houser SR, Leri A, Sussman MA, Anversa P. Nuclear targeting of Akt enhances ventricular function and myocyte contractility. Circ Res. 2005;97:1332-1341.

Rota M, Hosoda T, De Angelis A, Arcarese ML, Esposito G, Rizzi R, Tillmanns J, Tugal D, Musso E, Rimoldi O, Bearzi C, Urbanek K, Anversa P, Leri A, Kajstura J. The young mouse heart is composed of myocytes heterogeneous in age and function. Circ Res. 2007;101:387-399.

Rota M, Kajstura J, Hosoda T, Bearzi C, Vitale S, Esposito G, Iaffaldano G, Padin-Iruegas ME, Gonzalez A, Rizzi R, Small N, Muraski J, Alvarez R, Chen X, Urbanek K, Bolli R, Houser SR, Leri A, Sussman MA, Anversa P. Bone marrow cells adopt the cardiomyogenic fate in vivo. Proc Natl Acad Sci USA. 2007;104:17783-17788.

Rota M, Vassalle M. Patch-clamp analysis in canine cardiac Purkinje cells of a novel sodium component in the pacemaker range. J Physiol. 2003;548:147-165.

Rubart M, Zipes DP. Mechanisms of sudden cardiac death. J Clin Invest. 2005;115:2305-2315.

Sah R, Ramirez RJ, Kaprielian R, Backx PH. Alterations in action potential profile enhance excitation-contraction coupling in rat cardiac myocytes. J Physiol. 2001;533:201-214.

Song LS, Sham JS, Stern MD, Lakatta EG, Cheng H. Direct measurement of SR release flux by tracking 'Ca2+ spikes' in rat cardiac myocytes. J Physiol. 1998;512:677-691.

Spencer CI, Sham JS. Effects of Na+/Ca2+ exchange induced by SR Ca2+ release on action potentials and afterdepolarizations in guinea pig ventricular myocytes. Am J Physiol Heart Circ Physiol. 2003;285:H2552–H2562.

Steadman E, Ferreira-Martins J, Signore S, Korn JA, Sanada F, Zheng H, Cappetta F, Hosoda T, Fiorini C, Leri A, Anversa P, Kajstura J, Rota M. Electrophysiological Properties of the Infarcted Rodent Myocardium. J Card Fail. 2011;17:S16.

Steinberg SF, Goldberg M, Rybin VO. Protein kinase C isoform diversity in the heart. J Mol Cell Cardiol. 1995;27:141-153.

ter Keurs HEDJ, Boyden PA. Calcium and arrhythmogenesis. Physiol Rev. 2007;87:457-506.

Uchida K, Aramaki M, Nakazawa M, Yamagishi C, Makino S, Fukuda K, Nakamura T, Takahashi T, Mikoshiba K, Yamagishi H. Gene knock-outs of inositol 1,4,5-trisphosphate receptors types 1 and 2 result in perturbation of cardiogenesis. PLoS One. 2010;5.pii:e12500.

Vassort G. Adenosine 5'-triphosphate: a P2-purinergic agonist in the myocardium. Physiol Rev. 2001;81:767-806.

Wehrens XH, Lehnart SE, Marks AR. Intracellular calcium release and cardiac disease. Annu Rev Physiol. 2005;67:69-98.

Zaniboni M, Cacciani F, Lux RL. Beat-to-Beat Cycle Length Variability of Spontaneously Beating Guinea Pig Sinoatrial Cells: Relative Contributions of the Membrane and Calcium Clocks. PLoS ONE. 2014;9:e100242.

Zaniboni M, Yao A, Barry WH, Musso E, Spitzer KW. Complications associated with rapid caffeine application to cardiac myocytes that are not voltage clamped. J Mol Cell Cardiol. 1998;30:2229-2235.

ZhuGe R, Tuft RA, Fogarty KE, Bellve K, Fay FS, Walsh JV Jr. The influence of sarcoplasmic reticulum Ca2+ concentration on Ca2+ sparks and spontaneous transient outward currents in single smooth muscle cells. J Gen Physiol. 1999;113:215-228.

Zima AV, Bovo E, Bers DM, Blatter LA. Ca^{2}+ spark-dependent and –independent sarcoplasmic reticulum Ca^{2+} leak in normal and failing rabbit ventricular myocytes. J Physiol. 2010;588:4743-4757.

Zygmunt AC, Eddlestone GT, Thomas GP, Nesterenko VV, Antzelevitch C. Larger late sodium conductance in M cells contributes to electrical heterogeneity in canine ventricle. Am J Physiol Heart Circ Physiol. 2001;281:H689-H697.

Zygmunt AC, Goodrow RJ, Antzelevitch C. $I_{(NaCa)}$ contributes to electrical heterogeneity within the canine ventricle. Am J Physiol Heart Circ Physiol. 2000;278:H1671-H1678.

Appendix

Magnitude of Sampling

	Parameter	Experimental Condition	n	Figure
Mouse myocytes	Sarcomere shortening	Non-loaded myocytes	27	Fig 4
		Fluo-loaded myocytes	13	
Mouse myocytes	Ca^{2+} transients	Rhod-2	69	Fig 5
		Fluo-4	62	
Human tissue	Myocyte apoptosis	Control Hearts (Autopsy)	3	Fig 6
		Donor Hearts	3	
Human myocytes	Sample Composition	FACS	5	Fig 7
Mouse myocytes	Sample Composition	FACS	5	Fig 7
Human myocytes	Ca^{2+} transients, sarcomere shortening	Tyrode (Tyr)	23	Fig 12-B, Fig 13-B
		ATP	9	
		ET-1	6	
		XeC	9	
		ET-1+XeC	3	
Human LV trabecuale	Isometric force (paired analysis)	ATP	18	Fig 14-B
		ET-1	14	
		ATP+XeC	4	
Human myocytes	Current-clamp, Ca^{2+} transients (paired analysis)	ATP	11, 8	Fig 15-D
		ET-1	6, 4	
		Thimerosal	6, 4	
Perfused human LV	Monophasic action	ATP	7	Fig 16-B

myocardium (paired analysis)	potential (MAP), EKG	ET-1	4	
		Glibenclamide	2	Fig 17
Human myocytes	Western blotting, IP3R-2 expression	Normal Hearts	5	Fig 18-A
		Failing Hearts	5	
Failing human myocytes	Current-clamp	ATP	4	Fig 18-B
Human LV trabecuale	Isometric force (paired analysis)	Isoproterenol, Normal Hearts	10	Fig 19-A
		Isoproterenol, Failing Hearts	6	
Failing human LV trabecuale	Isometric force (paired analysis)	ATP	12	Fig 19-B
		ET-1	10	
Mouse myocytes	Ca^{2+} transients, sarcomere shortening (paired analysis)	ATP	8	Fig 20-E
		ET-1	8	
		AngII	9	
		Phenylephrine (Phe)	10	
		Thimerosal	14	
		ATP in the presence of XeC	7	
		ET-1 in the presence of XeC	7	
		ET-1 in the presence of U-73122	8	
	Ca^{2+} transients, sarcomere	Tyrode (Tyr)	144	Fig 20-F
		ATP	21	

	shortening	ET-1	29	
		AngII	15	
		phenylephrine (Phe)	21	
		Thimerosal (Thi)	14	
		ATP in the presence of XeC	49	
		ATP in the presence of U-73122	46	
		ET-1 in the presence of XeC	13	
		ET-1 in the presence of U-73122	45	
Mouse myocytes	Cell shortening	ATP	7	Fig 22
		ET-1	9	
		ATP in the presence of chelerythrine	9	
		ET-1 in the presence of chelerythrine	8	
LV mouse myocardium	qRT-PCR	Control	7	Fig 23
		shRNA-IP3R2	7	
shRNA-IP3R2-EGFP negative mouse myocytes	Ca^{2+} transients (Rhod-2)	Tyrode	21	Fig 24-C
		ATP	43	
		ET-1	20	

shRNA-IP3R2-EGFP positive mouse myocytes		Tyrode	5	
		ATP	9	
		ET-1	9	
Mouse myocytes	Current-clamp, Ca^{2+} transients (paired analysis)	ATP	12	Fig 26-B,C and 27-B
		ET-1	10	
		Thimerosal	12	
Mouse myocytes	Current-clamp, Ca^{2+} transients (paired analysis)	D-myo-Inositol 1,4,5-trisphosphate potassium salt (IP3) dyalisis	5	Fig 28-B
Mouse myocytes	Current-clamp, Ca^{2+} transients (paired analysis)	2-APB	11	Fig 29-B
Mouse myocytes	Cell shortening (paired analysis)	2-APB	11	Fig 29-C
Perfused mouse heart	Monophasic action potential (MAP)	Control (Ctrl)	25	Fig 31-B
		ET-1	9	
		Thimerosal (Thimer)	6	
	Monophasic action potential (MAP) PES protocol	Control (Ctrl)	14	
		ET-1	5	
		Thimerosal (Thimer)	4	
Mouse myocytes	Voltage-clamp, Ca^{2+} transients (ECC gain)	Tyrode	15	Fig 35-B
		ATP	9	
		ET-1	11	
Mouse myocytes	Current-clamp,	ATP in the presence of	8	Fig 37-B

	Ca^{2+} transients (paired analysis)	ryanodine		
Mouse myocytes	Voltage-clamp (Ni-sensitive Current)	Tyr in the presence of ryanodine	10	Fig 39
		ATP in the presence of ryanodine	12	
		ET-1 in the presence of ryanodine	16	
		D-myo-Inositol 1,4,5-trisphosphate potassium salt (IP3) dialysis	6	
Mouse myocytes	Voltage-clamp, Ca^{2+} transients (steps and caffeine puffs)	Tyrode, t=0	8	Fig 40-B
		Tyrode, t=3-5 min	8	
		Tyrode, t=7-10 min	8	
		ATP/ET-1, t=0	11	
		ATP/ET-1, t=3-5 min	11	
		ATP/ET-1, t=7-10 min	5	
Mouse myocytes	Current-clamp (paired analysis)	ATP	5	Fig 41-B
		ATP in the presence of thapsigargin	5	
		ET-1	7	Fig 41-D
		ET-1 in the presence of thapsigargin	7	
Mouse myocytes	Current-clamp, (buffered $[Ca^{2+}]_i$,	ATP	10	Fig 42
		ET-1	7	

	paired analysis			